Oregon State University | College of Forestry

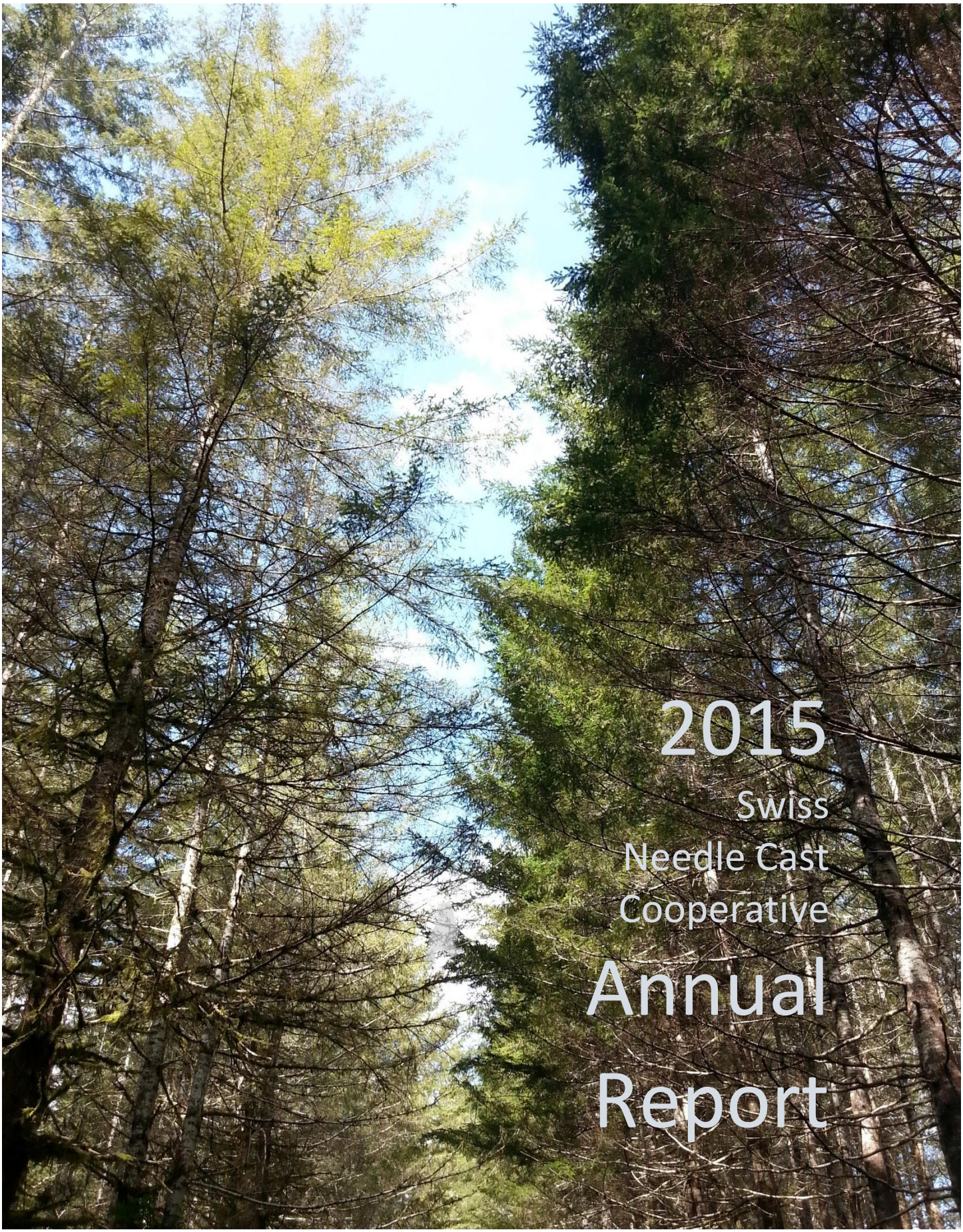

2015 Swiss Needle Cast Cooperative Annual Report

Swiss Needle Cast Cooperative Staff

Dave Shaw – Director and Associate Professor of Forest Health

Gabriela Ritóková – Assistant Director

Members of the Swiss Needle Cast Cooperative

Bureau of Land Management

Oregon Department of Forestry

USDA Forest Service

Starker Forests

Stimson Lumber

Weyerhaeuser Corporation

Edited by Gabriela Ritóková and Dave Shaw
Cover photo by Gabriela Ritóková

Table of Contents

SNCC Background and Organization

A major challenge to intensive management of Douglas-fir in Oregon and Washington is the current Swiss needle cast (SNC) epidemic. Efforts to understand the epidemiology, symptoms, and growth losses from SNC have highlighted gaps in our knowledge of basic Douglas-fir physiology, growth, and silviculture. The original mission of the Swiss Needle Cast Cooperative (SNCC), formed in 1997, was broadened in 2004 to include research aiming to ensure that Douglas-fir remains a productive component of the Coast Range forests. The SNCC is located in the Department of Forest Engineering, Resources and Management within the College of Forestry at Oregon State University. The Membership is comprised of private, state, and federal organizations. Private membership dues are set at a fixed rate. An annual report, project reports, and newsletters are distributed to members each year. Our objective is to carry out projects in cooperation with members on their land holdings.

SNCC Mission

To conduct research on enhancing Douglas-fir productivity and forest health in the presence of Swiss needle cast and other diseases in coastal forests of Oregon and Washington.

SNCC Objectives

(1) Understand the epidemiology of Swiss needle cast and the basic biology of the causal fungus, *Phaeocryptopus gaeumannii*.

(2) Design silvicultural treatments and regimes to maximize Douglas-fir productivity and ameliorate disease problems in the Coast Range of Oregon and Washington.

(3) Understand the growth, structure, and morphology of Douglas-fir trees and stands as a foundation for enhancing productivity and detecting and combating various diseases of Douglas-fir in the Coast Range of Oregon and Washington.

Department of Forest Engineering, Resources and Management
Oregon State University, 204 Peavy Hall, Corvallis, Oregon 97331
T 541-737-4952 | **F** 541-737-4316 | http://ferm.forestry.oregonstate.edu/

January 26, 2016

To: Swiss Needle Cast Cooperative Members and Friends

From: David Shaw, Director, and Gabriela Ritóková, Assistant Director,
Swiss Needle Cast Cooperative, College or Forestry, Oregon State University

SNCC Members and Friends,

In this Annual Report we provide updates on the annual aerial detection survey, other important on-going research, and new SNC-related journal publications. We are excited because the cooperative will complete initial measurement of the SNCC Research and Monitoring Plot Network this year, and pseudothecial occlusion data will be finalized by late fall, so that analyses and testing of many of our assumptions about *Phaeocryptopus gaeumannii* will be made over then next year or two. The network extends from the California border north into SW Washington and 35 miles inland. More than 100 plots are stratified throughout the region (See report from Gabriela Ritóková). Thanks to all the landowners in western Oregon and Washington who have allowed us to use their lands for this key network in 10 to 30-year old plantations.

In addition, we are collaborating with SNCC members and other partners to establish research and monitoring plots in older forest stands in the Oregon Coast Range and the western Oregon Cascade Mountains. Sky Lan, a Ph.D. student, is investigating the relationship of forest/crown structure, microclimate, and foliage nutrition to needle retention and disease severity in older stands. In addition, she and the SNCC are collaborating with Jeff Hatten, Soil Scientist at the College of Forestry, to interpret soil and foliar nutrition across the SNCC Research and Monitoring Plot Network.

We hope this Annual Report is informative and provides insight into the direction of the SNCC in the next decade. The focus of the cooperative will be:

- SNCC Research and Monitoring Plot Network
    - 10-year plan (ending in 2026) to monitor and better understand the relationship of disease severity to tree growth at the landscape scale. This network will provide opportunities for further epidemiological studies.

- Monitoring
    - Disease distribution using aerial detection survey, with hopes of collaborations in Washington and British Columbia.
    - Ground based plots linking disease severity, tree growth, needle retention and nutrition.
- Research
    - Epidemiology, Molecular Ecology (lineages)
    - Models linking growth to landscape severity of disease
    - SNC in older stands and trees
    - SNC and soils
    - SNC and landscape leaf wetness dynamics
- Management Applications
    - Silviculture and SNC
    - Integrated Pest Management for SNC
    - Models for improved growth and yield estimates under variable SNC severity
- Collaborations:
    - Tree improvement programs; PNW Tree Improvement Cooperative
    - Center for Intensive Planted Silviculture
- Awareness of emerging insect, disease, and climate related impacts to Douglas-fir forest plantation management other than SNCC

Thank you for your continued support of the SNCC. This is an important and relevant research cooperative that seeks to support Douglas-fir management in the Douglas-fir Region, the timber basket of the Northwest!

The winter of 2016 begins with the drought abating, and snowpack returning to the mountains. Hopefully we've dodged the bullet and won't see increased mortality due to drought this year.

Sincerely,

David Shaw Gabriela Ritóková

2015 Swiss Needle Cast Aerial Survey

Alan Kanaskie and Danny Norlander
Oregon Department of Forestry

Survey procedures

The observation plane flew at 1,500 to 2,000 feet above the terrain, following north-south lines separated by 2 miles. Observers looked for areas of Douglas-fir forest with obvious yellow to yellow-brown foliage, a symptom of Swiss needle cast (SNC). Patches of forest with these symptoms (patches are referred to as polygons) were sketched onto computer touch-screens displaying topographic maps or ortho-photos and the position of the aircraft. Each polygon was classified for degree of discoloration as either "S" (severe) or "M" (moderate). Polygons classified as "S" had very sparse crowns and brownish foliage, while those classified as "M" were predominantly yellow to yellow-brown foliage with slightly denser crowns than those classified as "S". The survey area extended from the Columbia River in Oregon south to the California border, and from the coastline eastward until obvious symptoms were no longer visible. We also surveyed a portion of the west slope of the Cascade Range in 2015, from Lane County north through Clackamas County.

Results

The survey was flown on May 18, 20, 27, 28, 29 and June 3 & 4, 2015, and covered 3,692,653 acres in the Coast Range and 638,000 acres in the Cascade Range (figure 1). Bud break was earlier than normal because of unusually warm weather, but the survey was delayed until much later than planned because of technical and administrative difficulties related to the aircraft. Despite this, symptoms remained visible to observers well after bud-break and into June. The delay may have been fortuitous because symptom development earlier in the year was poor, probably related to the unusually mild weather of early 2015 (although we don't understand the relationship).

The survey showed an increase in the area of forest with symptoms of Swiss needle cast compared to the previous 5 years, reaching an all-time high for the sixth year in a row. In the Coast Range we mapped 589,851 acres of Douglas-fir forest with obvious symptoms of Swiss needle cast (figure 2). As has been the case for the past several years, the easternmost area with obvious SNC symptoms was approximately 28 miles inland from the coast in the Highway 20 corridor, but most of the area with symptoms occurred within 18 miles of the coast. Figures 3 and 4 show the trend in damage from 1996 through 2015.

In 2015, as in 2014, we extended the survey south through Curry County to the California border even though few symptoms typically are observed south of Port-Orford. In Curry County we mapped only 80 polygons representing 4,319 acres with symptoms, most of them in the Port-Orford area.

In the partial survey of the Cascades Range (Lane, Linn, Marion, and Clackamas Counties), we mapped 3,186 acres with moderate Swiss needle cast symptoms. Limited ground truthing suggested that in some cases the symptoms may have been caused by something other than SNC.

The Swiss needle cast aerial survey provides a conservative estimate of damage because observers can map only those areas where disease symptoms have developed enough to be visible from the air. We know Swiss needle cast occurs throughout the survey area, but discoloration often is not severe enough to enable aerial detection. The total area of forest affected by Swiss needle cast is far greater than indicated by the aerial survey. The aerial survey does, however, provide a reasonable depiction of the extent of moderate and severe damage, and coarsely documents trends in damage over time.

Acknowledgements

The survey was conducted by the Oregon Department of Forestry Forest Health and Air Operations sections, and was funded by the Oregon State University Swiss Needle Cast Cooperative, the USDA Forest Service Forest, and the Oregon Department of Forestry. Steve Larsen (ODF) and Dan McCarron piloted the plane. Danny Norlander (ODF) is the survey coordinator and primary observer. Other aerial observers were Bob Schroeter (USFS Region 6 FHP), Zack Heath (USFS), Wyatt Williams (ODF) and Christine Buhl (ODF).

Additional Notes

We appreciate any information regarding the accuracy or usefulness of the maps. If you have a chance to look at some of the mapped areas on the ground, please let us know what you observe. Please call Alan Kanaskie (503-945-7397) or Danny Norlander (503-945-7395) if you have questions, suggestions, or comments.

The GIS data and a .pdf file can be accessed via the ODF web page at:

http://www.oregon.gov/ODF/privateforests/fhMaps.shtml

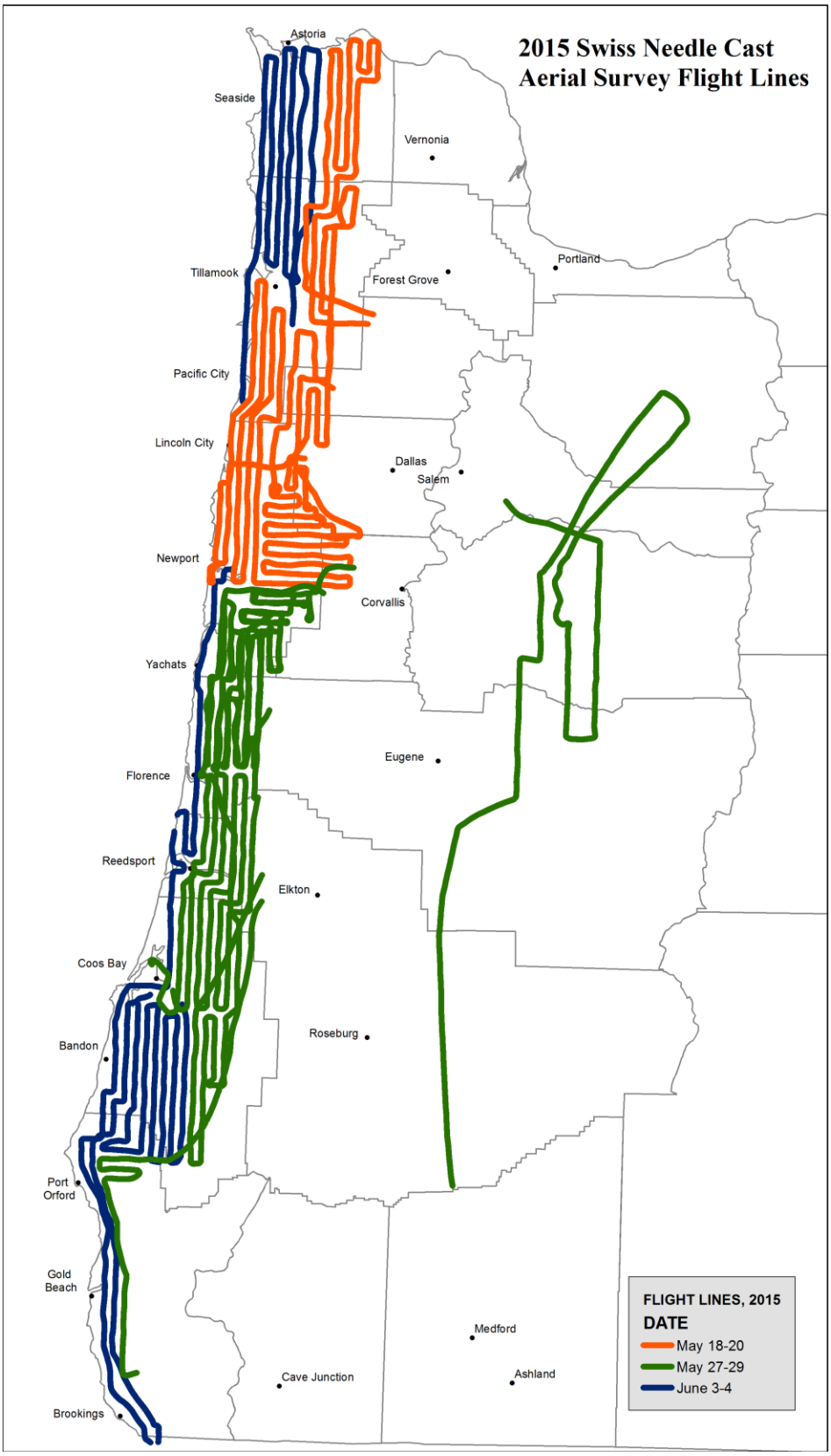

Figure 1. Area surveyed for Swiss needle cast symptoms, 2015. Flight lines are two miles apart.

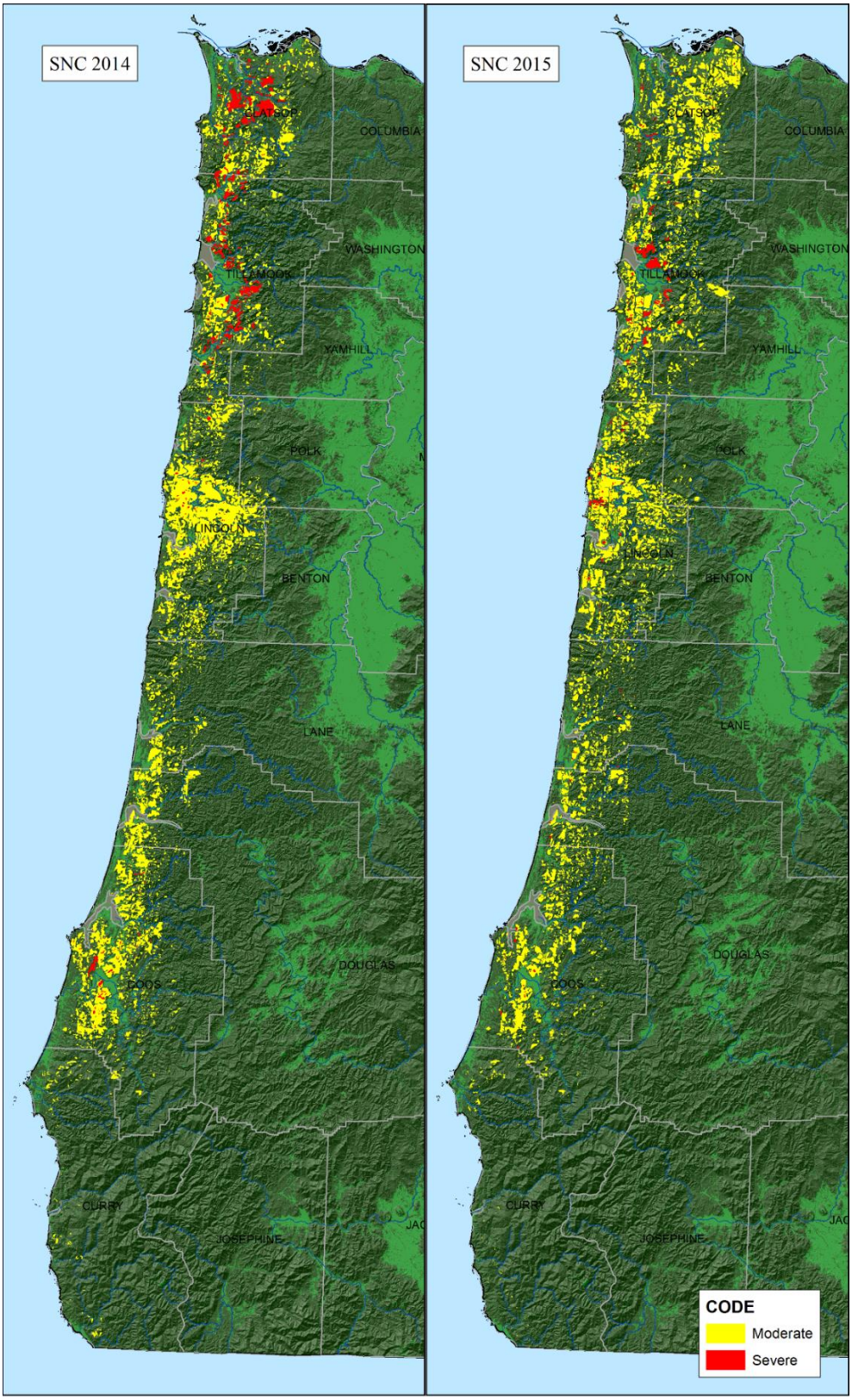

Figure 2. Areas of Douglas-fir forest with symptoms of Swiss Needle Cast detected in the 2014 and 2015 aerial surveys, Coast Range, Oregon.

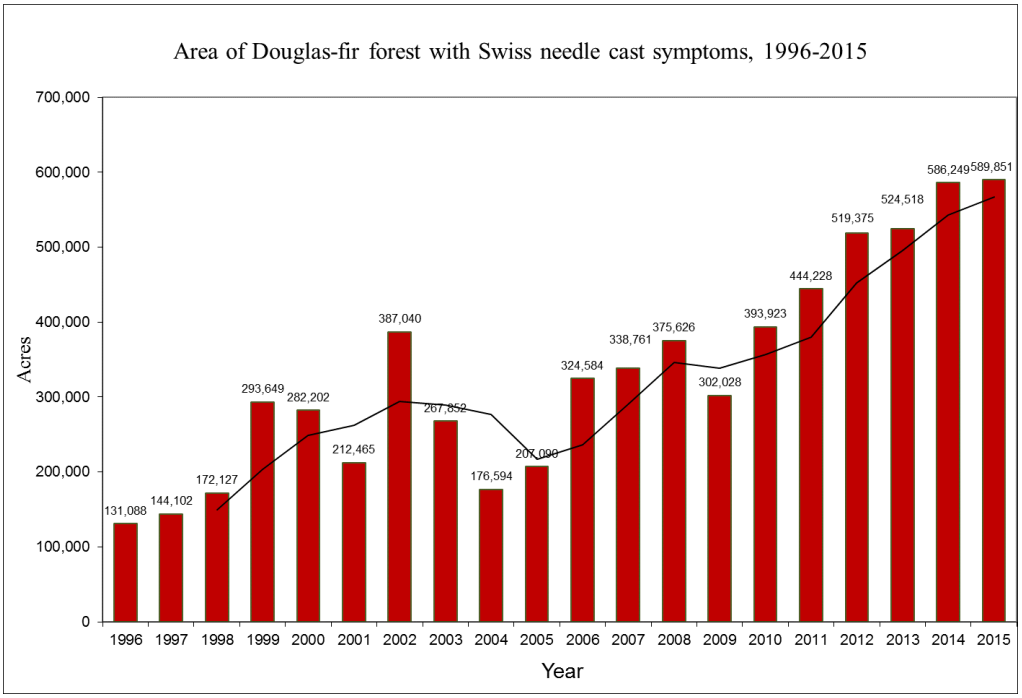

Figure 3. Area of Douglas-fir forest in western Oregon with symptoms of Swiss needle cast detected during aerial surveys conducted in April-June, 1996-2015 (2008 area estimated from partial survey consisting of 3 sample blocks). Trend line is 3-year rolling average. Coast Range, Oregon

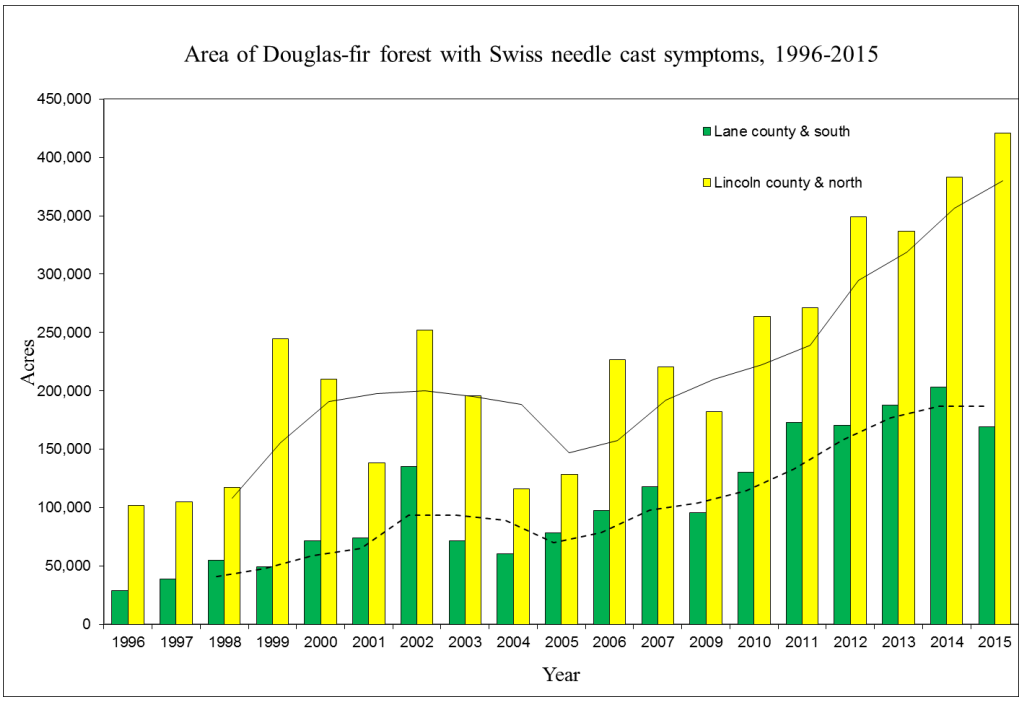

Figure 4. Area of Douglas-fir forest in western Oregon with symptoms of Swiss needle cast detected during aerial surveys conducted in April-June, 1996-2015; north and south halves of survey area (2008 area estimated from partial survey consisting of 3 sample blocks). Trend line is 3-year rolling average. Coast Range, Oregon.

Swiss Needle Cast Aerial and Ground Survey Coastal Washington, 2015

Amy Ramsey[1], Dan Omdal[1], Aleksandar Dozic[1], Glenn Kohler[1], and Michele Boderck[2]
[1]Washington Department of Natural Resources, Forest Health Program, Olympia, WA, [2]The Evergreen State College, Master of Environmental Studies, Olympia, WA

Abstract

In late April and May, an aerial survey, covering 2.6 million acres, was flown to detect and map the distribution of Swiss Needle Cast (SNC) symptoms in coastal Washington. Nearly 350,000 acres of symptomatic Douglas-fir were mapped, which is an increase from the 230,000 acres mapped in the 2012 aerial survey. Forty-seven ground sites across the range of the aerial survey were surveyed for Douglas-fir needle retention and SNC incidence and severity, determined by pseudothecial counts. An average of 2.3 years of foliage were on the trees across all sites. The average percentage of occluded stomata on all sites was 5.4% for 2014 (1-year-old) foliage and 22.5% for 2013 foliage (2-years-old).

Introduction

The fungus that causes SNC, *Phaeocryptopus gaeumannii* (T.Rohde) Petrak is found throughout the range of its only host, Douglas-fir (Shaw et al. 2011). The disease is most damaging near the coast due to the fungi-favorable climatic (mild winters and wet springs and summers) and topographic conditions. Swiss Needle Cast can reduce growth of host trees, alter wood properties, and affect stand structure and development (Johnson et al. 2005, Maguire et al. 2011, Weiskittel et al. 2006).

An aerial survey for SNC has been conducted in the Oregon Coast Range since 1996, with over 300,000 acres of SNC symptomatic Douglas-fir mapped since 2006 and over 400,000 acres mapped since 2011 (Kanaskie and Norlander 2014). Oregon has noted that even though land managers have been altering their land management practices to try and reduce the impacts of SNC, SNC disease continues at very high levels.

The 2015 SNC aerial survey in Washington was coupled with a ground survey. Ground surveys have been conducted annually in Washington since 1997, with aerial surveys occurring in 1998-2000, 2012 and 2015. The objective of the ground surveys was to validate the aerial survey results and to monitor changes in incidence and severity of the disease over time.

Methods

The observation plane flew at 1,500 to 2,000 feet above the terrain, following north-south lines separated by 3 miles. Observers looked for areas of Douglas-fir forest with obvious yellow-brown foliage, a symptom of SNC. Patches (referred to as polygons) of forest with these symptoms were sketched onto computer touch-screens displaying topographic maps or ortho-photos and the position of the aircraft. Each polygon was classified for degree of discoloration as either “S” (severe) or “M” (moderate). Polygons classified as “S” (CODE, SNC-S) had very

sparse crowns and brownish foliage, while those classified as "M" (CODE, SNC-M) were predominantly yellow-brown foliage with slightly denser crowns than those classified as "S".

The 2015 Washington SNC aerial survey was flown on April 27, May 7, 8 18 and 20 and covered 2,588,000 acres of forest. The survey is timed to occur when the crown color symptoms have developed, but before the new foliage has emerged (bud break) in late spring. While bud break commenced earlier than normal because of unusually warm weather, and the survey was delayed until later than planned because of inclement weather, SNC symptoms remained visible to observers well after bud-break and into May. The survey area extended from the Columbia River in Washington north to the Strait of Juan de Fuca, and from the coastline eastward.

Forty-seven ground sites were included in the SNC survey. Stand color, landscape position, elevation, aspect and average tree age were recorded for each site. Needle retention, diameter at breast height and crown color were recorded for ten trees at each site. Foliage from 2014 and 2013 were collected from the upper third of each of the ten trees at each site and taken back to the lab for microscopic examination of *P. gaeumannii* pseudothecial, or reproductive structure, density. Three hundred stomata on each of ten needles from each foliage cohort were microscopically examined for pseudothecial occurrence.

Results and Discussion

The aerial surveyors flew and made observations on 2,588,000 acres of forest land in coastal Washington and mapped 350,000 of Douglas-fir with obvious symptoms of SNC (Figure 1a-b). This is an increase from the 229,000 acres mapped during the 2012 SNC aerial survey (Figure 2). The survey boundaries were similar to those in the 2012 survey. The easternmost area with obvious SNC symptoms was approximately 45 miles inland in central coastal western Washington. However, symptoms varied based on geographic location, ranging up to 34 miles on the Olympic Peninsula and 40 miles in southwest Washington. In Grays Harbor County symptoms were visible for almost entire county area except on elevations that are higher than 1,500 feet.

More specifically, SNC symptoms were detected on 14% of the total acres surveyed (8.5% in 2012), with 1% (19,000 acres) of the total area surveyed mapped as severe and 13% (332,000 acres) mapped as moderate. Severely symptomatic stands were generally located near the coast and the Grays Harbor area, which is near Ocean Shores and Westport, in the 2015 survey. The cause of the dramatic increase in acreage mapped from 2012 to 2015 remains uncertain, in part due to our ground plot network not extending as far east as the mapped aerial survey polygons and the unclear impacts of an unusually dry and warm winter and spring in 2015. Figure 3 shows how the 2015 SNC aerial survey compares to the 1998, 1999, 2000 and 2012 SNC aerial surveys in Washington.

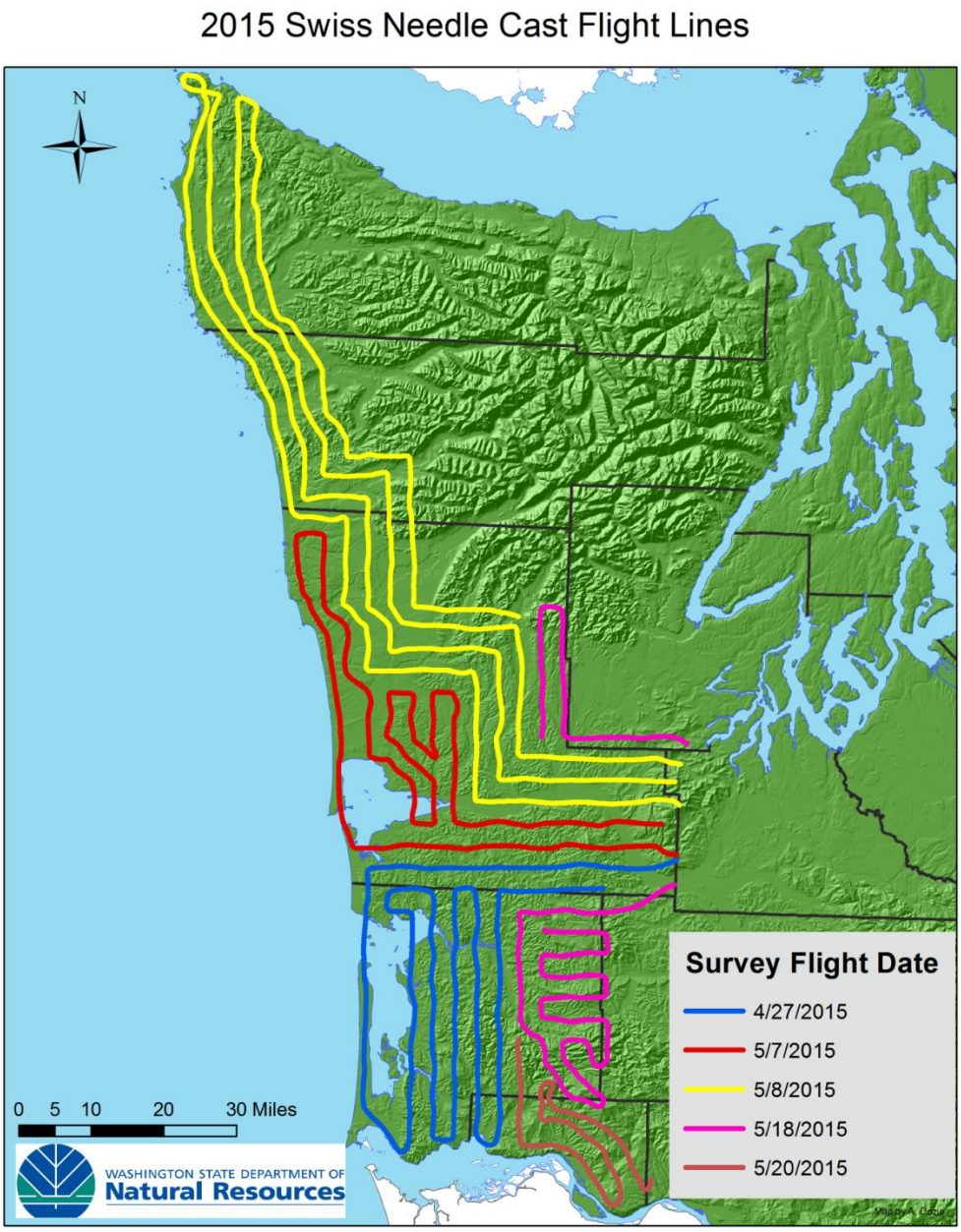

Figure 1a. Washington 2015 Swiss needle cast (SNC) aerial survey map showing flight lines and dates of aerial survey.

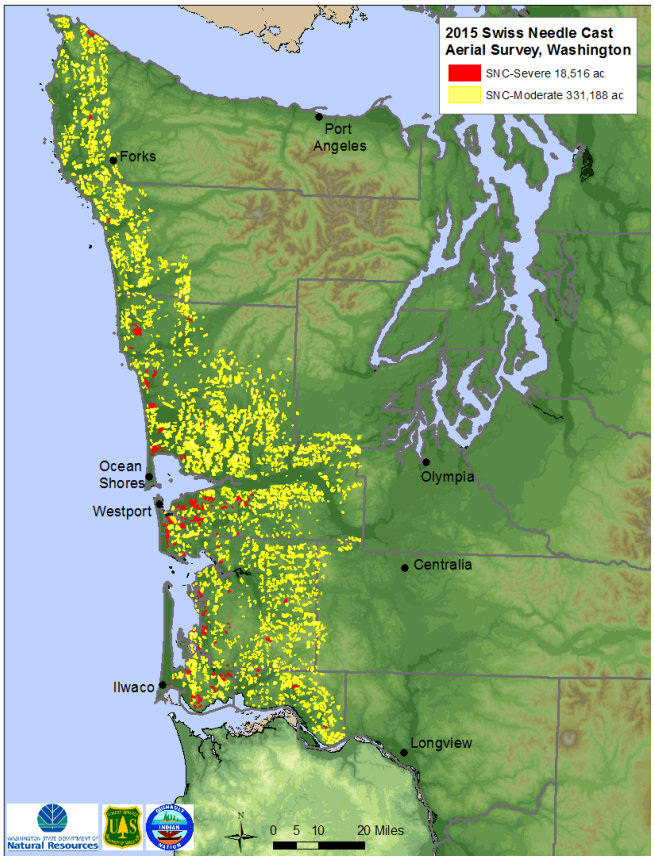

Figure 1b. Washington 2015 SNC aerial survey map showing severe and moderate SNC symptom mapped polygons.

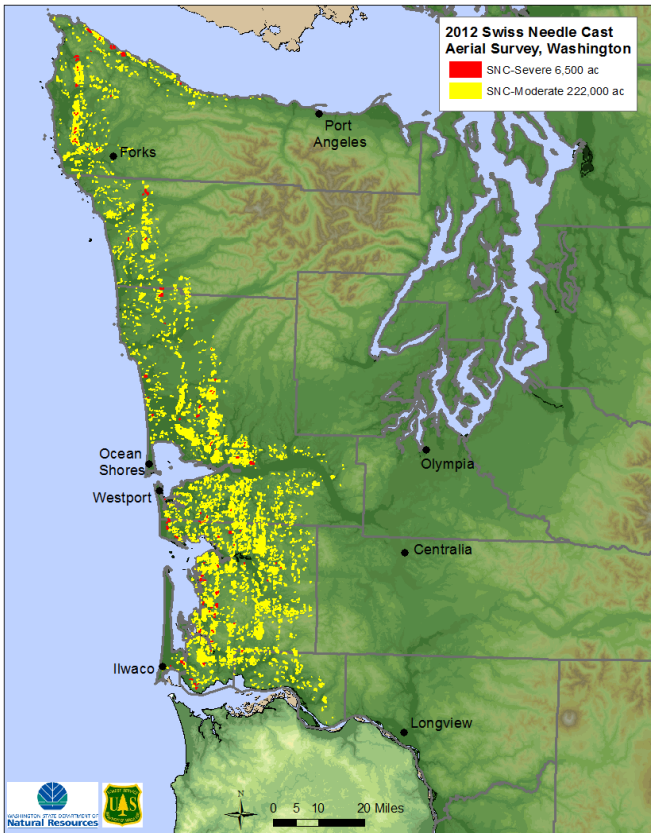

Figure 2. Washington 2012 Swiss needle cast aerial survey map.

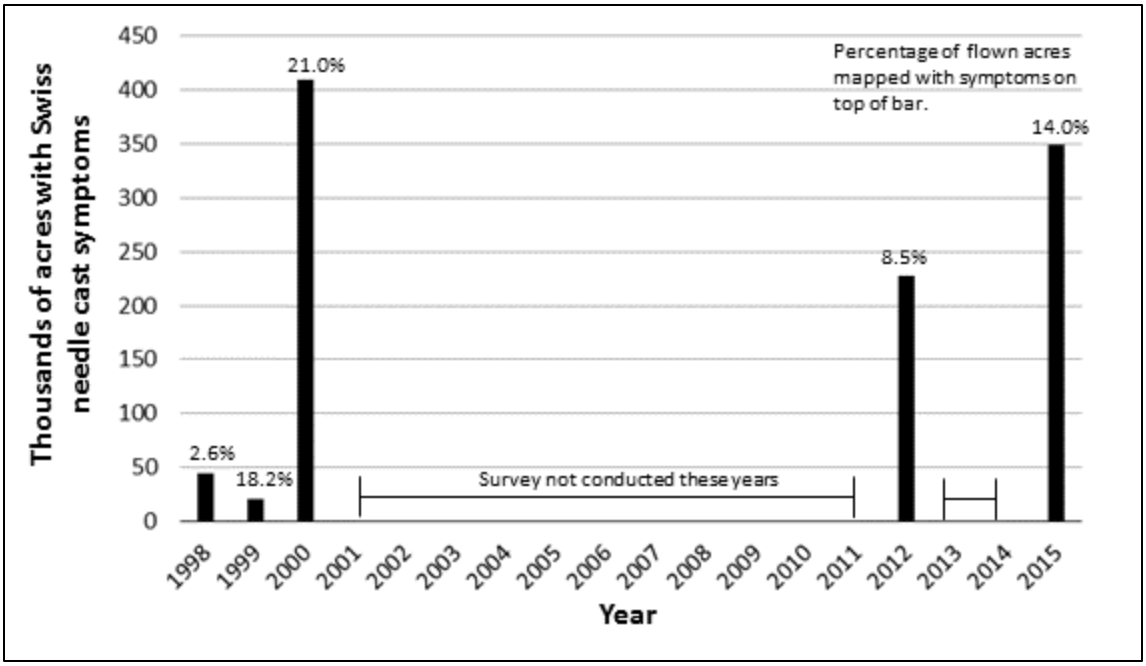

Figure 3. Area of Douglas-fir forest with Swiss needle cast symptoms detected by aerial surveys in Washington, 1998-2015.

Phaeocryptopus gaeumannii was found in Douglas-fir needles on all ground survey sites. Needle retention varied across the area surveyed with an average of 2.3 years across all sites. Across the 47 ground survey sites, average needle retention ranged from 1.2 to 3.3 years (Figure 4). Based on these values, growth losses of Douglas-fir are estimated to range from 0 to 40%, depending on the average needle retention at each site (Figure 4) (Maguire et al. 2011). Needle retention values are higher than those reported in the 2012 SNC survey, when the average needle retention across 75 sites was 2.2 years and ranged from 0.9 to 2.7 years.

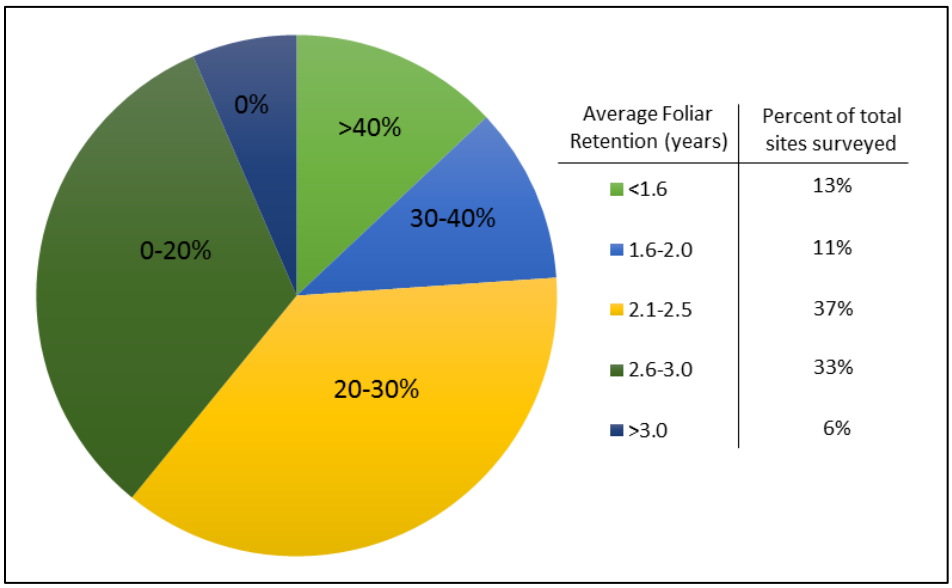

Figure 4. Estimated percent of Douglas-fir growth loss based on average yearly foliar retention in western Washington in 2015. Estimated growth losses of Douglas-fir are within each associated section of the chart and are based on needle retention values and adapted from Maguire et al. 2011.

Douglas-fir needles from the 2014 cohort, which were assessed in 2015 and represent the one year old needles, had an average of 5.4% stomata occluded by *P. gaeumannii* and from the 2013 cohort had an average of 22.5% stomatal occlusion (Figure 5). This is an increase in the occluded stomata reported in the 2012 SNC ground survey, which was an average of 2.8% in the one year old needles and 15.5% in the two year old needles.

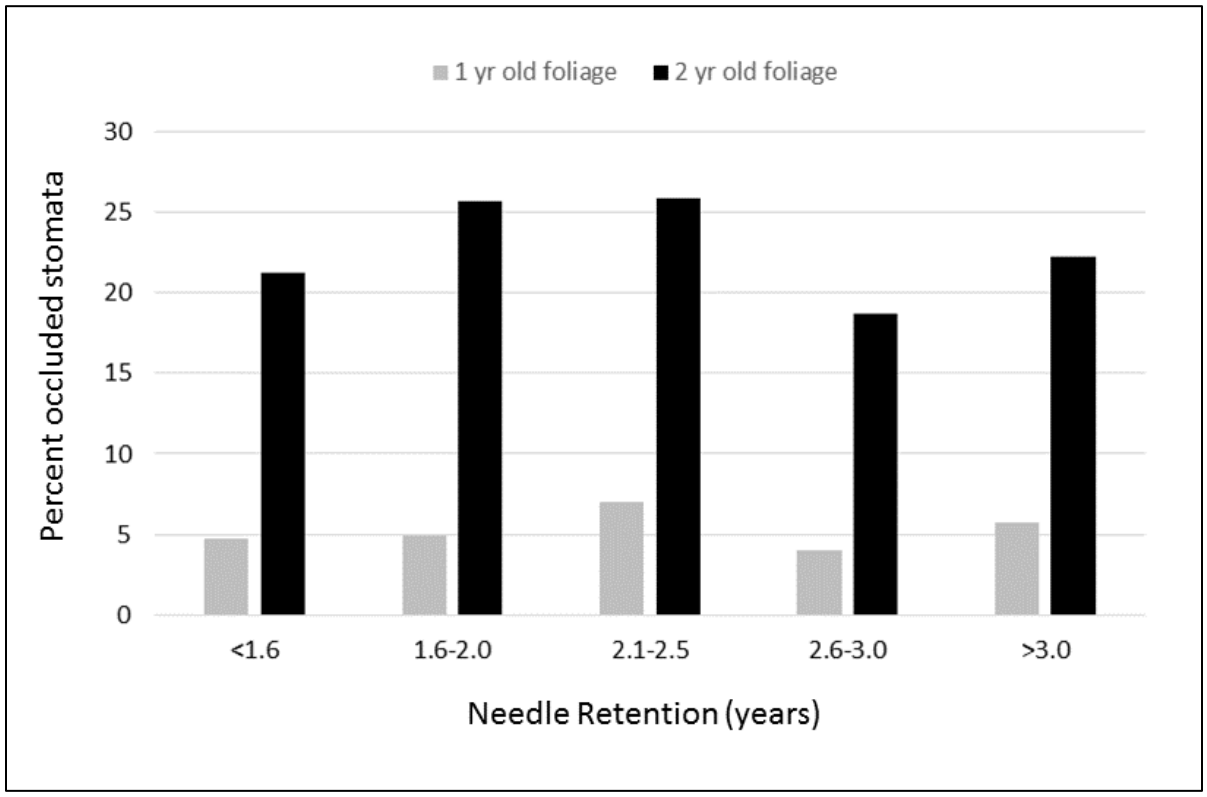

Figure 5. Percentage of *Phaeocryptopus gaeumannii* caused stomatal occlusion in one and two year old Douglas-fir foliage in western Washington in 2015. Data are sorted by 2015 needle retention age classes.

Caution should be advised when interpreting aerial survey data. The SNC survey should be considered a conservative estimate of the acreage affected by SNC because aerial observers can only map areas where disease symptoms have developed enough to be visible from the air. SNC aerial survey can be used to coarsely document trends in damage over time. The ground data shows that SNC is present in areas that were not mapped during the aerial survey. While the aerial survey can be used as a guide for identifying areas impacted by SNC, on the ground surveys should be conducted in stands of interest before SNC mitigating management decisions are made.

Douglas-fir is the only host of this disease, therefore forest managers can grow non-host species such as red alder, western red cedar, western hemlock and Sitka spruce in efforts to reduce damage from SNC. However, it should be noted that if a Douglas-fir has more than three years of foliage on its branches, then damage in the form of growth loss impacts are likely minimal to none.

Acknowledgements

The survey was conducted by the Washington Department of Natural Resources (WDNR) forest health program and the Washington Department of Fish and Wildlife (WDFW) aviation section. Marty Kimbrel (WDFW) and Steve Lindberg piloted the plane. Funding for the survey was provided by the Quinault Indian Nation and the USDA Forest Service, an equal opportunity employer.

Additional Notes

We appreciate any information regarding the accuracy or usefulness of the maps and ground survey data. Please contact Amy Ramsey (amy.ramsey@dnr.wa.gov or 360-902-1309) if you have questions, comments or suggestions.

References

Johnson, G.R., A.T. Grotta, B.L. Gartner and G. Downes. 2005. Impact of the foliar pathogen Swiss needle cast on wood quality of Douglas-fir. Can. J. For. Res. 35: 331–339.

Kanaskie, A. and D. Norlander. 2014. 2014 Swiss Needle Cast Aerial Survey. Oregon Dept. of Forestry, Office report, Salem, OR. Aerial survey data available online at http://www.oregon.gov/ODF/ForestBenefits/Pages/ForestHealth.aspx, under Maps & Data, Swiss Needle Cast. Last accessed December 21, 2015.

Maguire, DA, Mainwaring DB, Kanaskie A. 2011. Ten-year growth and mortality in young Douglas-fir stands experiencing a range in Swiss needle cast severity. Can. J. For. Res. 41: 2064-2076.

Shaw, D.C., G.M. Filip, A. Kanaskie, D.A. Maguire, and W.A. Littke. 2011. Managing an epidemic of Swiss needle cast in the Douglas-fir region of Oregon; the role of the Swiss Needle Cast Cooperative. *J. of For.* 109(2): 109-119.

Weiskittel, A.R., D.A. Maguire, S.M. Garber and A. Kanaskie. 2006. Influence of Swiss needle cast on foliage age-class structure and vertical foliage distribution in Douglas-fir plantations in north coastal Oregon. Can. J. For. Res. 36: 1497–1508.

Detecting Swiss Needle Cast in Coast Douglas-fir using a Low-cost Unmanned Aerial System equipped with a Consumer-grade Digital Camera

Jonathan D. Burnett, Michael G. Wing and Dave Shaw

Introduction

Swiss needle cast (SNC) is a foliar disease in Douglas-fir caused by the native fungus *Phaeocryptopus gaeumannii* (Hansen et al. 2000). SNC has been intensifying in Oregon's Coast Range since the 1980's (Black 2010). The disease is of special concern to the Pacific Northwest region (PNW) because Douglas-fir (*Pseudotsuga menziesii)* is the major lumber producing species of Oregon (Brandt 2006) and contributes heavily to the State's $12.7 billion annual industrial forest output (OFRI 2013). SNC causes premature leaf abscission, which reduces annual growth increment that can accumulate to end-of-rotation volume losses as high as 50% (Manter et al. 2000; Maguire 2002). These projected volume losses lead to significant reductions in stand net present value (Kimberley et al. 2011). Accurate identification and mapping of SNC infection in Douglas-fir stands are critical for employing economically sound loss-mitigation strategies such as stand conversion or thinning treatments that favor non-susceptible tree species (Shaw et al. 2011; Zhao et al. 2014).

The conventional method of mapping SNC is aerial detection survey (ADS), which uses trained observers in an aircraft who visually identify and manually map disease severity across western Oregon (MacLean et al. 1996; Kanaskie et al. 2007; Johnson and Dwittwer 2008). A major advantage to ADS is the ability to immediately apply expert knowledge across a broad area and the survey results require minimal post-processing to create actionable maps of disease extent and severity. However, ADS is not without limitation. A number of trees must be affected by SNC for the observer to detect presence from thousands of feet above the ground while moving at a speed of 100+ mph. Also, the spatial accuracy of results is at the acre level and is not sufficient for individual tree assessments that are better suited for stand-level decision making. Furthermore, the spring phenology of the disease signature aligns with Oregon's rainy season, which can limit the number of flying days and create poor canopy illumination for SNC detection. The use of Unmanned Aircraft Systems (UAS) offers a potential solution to these limitations with the added benefit of removing the risk of human injury inherent to manned low elevation aerial surveys.

Objectives

This study examines the accuracy of detecting visible SNC presence and absence in coastal Douglas-fir trees using a small low-cost UAS equipped with a color digital camera. Given the possible cost implications of SNC presence on management decisions, the SNC detection model will be considered useful if positive predicted value and negative predicted value are both at least 85%. This study will also examine whether classification models can be generally applied to all sites or if site specificity limits generalization. The scope of inference for this study is restricted to the five Douglas-fir stands surveyed in May 2015 in western Oregon. If

successful, the results of this study build the foundation for deeper inquiry into detection methods that can be used with broader area studies

Methods

A UAS equipped with a digital camera and flying lower than 400' above ground level (AGL) can produce images with ~ 1" ground sampling distance (GSD) (Wing et al. 2013). The images can be used individually for conventional photo interpretation and if there are enough overlapping images, they can be compiled into a single georeferenced orthomosaic and digital surface model using structure from motion (SFM) (Verhoeven 2011; Gross 2015). Orthomosaics, especially when produced from linear sensors calibrated to surface reflectance, can be used in conventional remote sensing workflows that look for quantitative patterns in the data such as object based image analysis, maximum likelihood classification, classification and regression trees, and logistic regression (Laliberte and Rango 2009; Lillesand and Kiefer 2008).

Four study sites were selected from within the Swiss Needle Cast Cooperative's plot network (SNCC 2014) in western Oregon. Criteria for stand selection was based on prior knowledge of SNC presence, coverage from an existing Federal Aviation Administration Certificate of Authorization (COA), and the ability to maintain line of sight to an unmanned aircraft flying 200' above ground level (AGL). A fifth site was added due to close proximity to Corvallis, Oregon, known SNC infection and the availability of a high point to maintain line of sight to the UAS. Sites ranged from 5 to 20 acres in size with Douglas-fir cohorts ranging between 25 and 60 years of age and terrain relief of 0 to 250 feet. The survey was conducted in May 2015, which corresponded to the phenological response of Douglas-fir to SNC infection (Manter et al. 2000).

The UAS used for this study was a TurboAce Matrix quadcopter UAS equipped with a GPS controlled 3DR Pixhawk autopilot and a commercial-off-the shelf Sony Nex 5T digital camera. Total cost of the UAS was about $6000 USD including man hours for assembly and testing. The five sites were flown with the UAS and imaged in intervals that ensured ~80% overlap and 80% sidelap of all images. Images were mosaicked using Agisoft Photoscan ver. 2.1. This produced a color orthomosaic at 2 cm resolution and a digital surface model (DSM) at 5 cm resolution for each of the five sites. Tree populations on an individual tree basis for each site were automatically extracted from the DSM using FUSION CanopyMaxima. Color information from the orthomosaic was averaged over the crown area of each of the trees at each site to produce tree level color reflectance metrics. One-hundred thirty trees were randomly selected from the tree population at each site for visual evaluation of SNC infection status.

The 130 selected trees for each site were evaluated in the corresponding 2 cm orthomosaic (Figure 1) as diseased or not diseased, with the assistance of an aerial observer trained specifically for forest insect and disease detection. Thirty trees were randomly selected from each site to be withheld for classification validation. Logistic regression was performed in

R to classify tree disease (diseased / non diseased) status of the 100 randomly selected trees as a function of each tree's crown color reflectance in terms of red, green, and blue. The classification scheme was applied to the 30 validation trees at each site and the results were evaluated for accuracy and certainty. Accuracy is the percentage of trees assigned the proper designation (diseased/not diseased) relative to what the observer determined. Uncertainty is assessed through two metrics: positive predictive value (PPV) and negative predictive value (NPV). PPV is the probability that a tree classified as being diseased is truly diseased and NPV is the probability that a tree classified as being not-diseased is truly not diseased.

Preliminary Results and Conclusions

Evaluation of one site in Tillamook county suggests detection of SNC presence/absence can be assessed with a high degree of accuracy (>90%) and certainty (NPV > 0.85, PPV > 0.85). Complete analysis on the remaining four sites is required before inference can be made to any degree of confidence. If classification performance on the remaining sites is similar and the model is generalizable across the study sites, this study may set the stage for further research that will eventually lead to an automated wide area survey for SNC using a large landscape scale UAS such a civilianized MQ-9 Reaper.

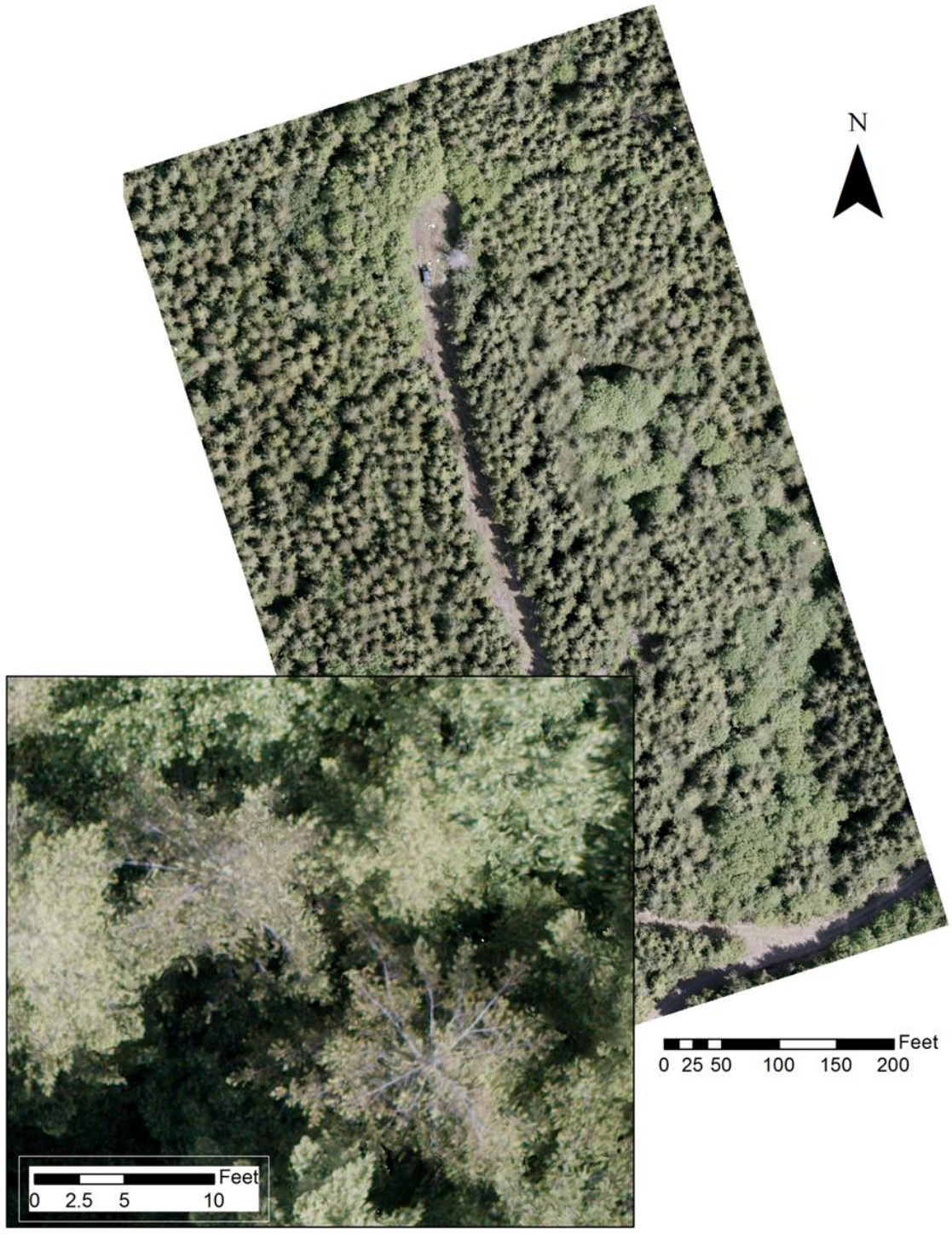

Figure 1 – Site T01 Orthomosaic: Orthomosaic produced from May 2015 UAS aerial survey of Site T01 on Stimson Timber property. Resolution is 2 cm. The larger image is the entire 9.5-acre survey area. The smaller image in the lower left corner is zoomed in on a select portion of the mosaic to demonstrate infected Douglas-fir with lower leaf area relative to adjacent non-symptomatic Douglas-fir.

Berni, J., P.J. Zarco-Tejada, L. Suarez, and E. Fereres. 2009. “Thermal and Narrowband Multispectral Remote Sensing for Vegetation Monitoring From an Unmanned Aerial Vehicle.” *IEEE Transactions on Geoscience and Remote Sensing* 47 (3): 722–38.

Black, Bryan A., David C. Shaw, and Jeffrey K. Stone. 2010. "Impacts of Swiss needle cast on overstory Douglas-fir forests of the western Oregon Coast Range." *Forest Ecology and Management* 259, no. 8: 1673-1680.

Brandt, Jason P.; Morgan, Todd A.; Dillon, Thale; Lettman, Gary J.; Keegan, Charles E.; Azuma, David L. 2006. “Oregon's forest products industry and timber harvest, 2003.” Gen. Tech. Rep. PNW-GTR-681. Portland, OR: U.S. Department of Agriculture, Forest Service, Pacific Northwest Research Station. 53p.

Gross, John W. 2015. “A Comparison of Orthomosaic Software for Use with Ultra High Resolution Imagery of a Wetland Environment.” Accessed 12/10/2015: http://www.imagin.org/awards/sppc/2015/papers/john_gross_paper.pdf.

Hansen, E. M., J. K. Stone, B. R. Capitano, P. Rosso, W. Sutton, L. Winton, A. Kanaskie, and M. G. McWilliams. 2000. “Incidence and Impact of Swiss Needle Cast in Forest Plantations of Douglas-Fir in Coastal Oregon.” *Plant Disease* 84 (7): 773–78.

Kanaskie, A., M. McWilliams, K. Sprengel, D. Overhulser. 2007. “Swiss Needle Cast Aerial Surveys, 1996 – 2007”. Swiss Needle Cast Cooperative 2007 Annual Report.

Kimberley, M. O., I. A. Hood, and R. L. Knowles. 2011. “Impact of Swiss Needle-Cast on Growth of Douglas-Fir.” *Phytopathology* 101 (5): 583–93.

Johnson, E. W., and D. Wittwer. 2008. “Aerial Detection Surveys in the United States.” Australian Forestry 71 (3): 212–15.

MacLean, David A., and Wayne E. MacKinnon. 1996. “Accuracy of Aerial Sketch-Mapping Estimates of Spruce Budworm Defoliation in New Brunswick.” Canadian Journal of Forest Research 26 (12): 2099–2108. doi:10.1139/x26-238.

Laliberte, A.S., and A. Rango. 2009. “Texture and Scale in Object-Based Analysis of Subdecimeter Resolution Unmanned Aerial Vehicle (UAV) Imagery.” Geoscience and Remote Sensing, IEEE Transactions on 47 (3): 761–70. doi:10.1109/TGRS.2008.2009355.

Lillesand, T.M., Kiefer, R.W. and Chipman, J.W., 2008. Remote sensing and image interpretation.

Maguire, Douglas A., Alan Kanaskie, William Voelker, Randy Johnson, and Greg Johnson. 2002. "Growth of young Douglas-fir plantations across a gradient in Swiss needle cast severity." Western Journal of Applied Forestry 17, no. 2: 86-95.

Manter, Daniel K., Barbara J. Bond, Kathleen L. Kavanagh, Pablo H. Rosso, and Gregory M. Filip. 2000. “Pseudothecia of Swiss Needle Cast Fungus, Phaeocryptopus Gaeumannii,

Physically Block Stomata of Douglas Fir, Reducing CO2 Assimilation." *New Phytologist* 148 (3): 481–91.

Oregon Forest Resources Institute (OFRI) 2012. "2012 Forest Report: An Economic Snapshot of Oregon's Forest Sector". Accessed 03/16/2016: http://library.state.or.us/repository/2013/201301171606454/index.pdf

Shaw, David C., Gregory M. Filip, Alan Kanaskie, Douglas A. Maguire, and Will A. Littke. 2011. "Managing an Epidemic of Swiss Needle Cast in the Douglas-Fir Region of Oregon: The Role of the Swiss Needle Cast Cooperative."

Verhoeven, Geert. 2011. "Taking computer vision aloft–archaeological three-dimensional reconstructions from aerial photographs with photoscan."*Archaeological Prospection* 18, no. 1: 67-73.

Wing, Michael G., Jonathan Burnett, John Sessions, Josh Brungardt, Vic Cordell, Dave Dobler, and David Wilson. 2013. "Eyes in the Sky: Remote Sensing Technology Development Using Small Unmanned Aircraft Systems." Journal of Forestry 111 (5): 341–47. doi:10.5849/jof.12-117.

Zarco-Tejada, P.J., V. González-Dugo, and J.A.J. Berni. 2012. "Fluorescence, Temperature and Narrow-Band Indices Acquired from a UAV Platform for Water Stress Detection Using a Micro-Hyperspectral Imager and a Thermal Camera." Remote Sensing of Environment 117 (February): 322–37. doi:10.1016/j.rse.2011.10.007.

Zhao, J, Maguire DA, Mainwaring DB, Wehage J, Kanaskie A. 2014. Thinning Mixed-Species Stands of Douglas-Fir and Western Hemlock in the Presence of Swiss Needle Cast: Guidelines Based on Relative Basal Area Growth of Individual Trees. Forest Science. 60(1)

Swiss Needle Cast Cooperative Research and Monitoring Plot Network

Gabriela Ritóková[1], Dave Shaw[1], Doug Maguire[1], Doug Mainwaring[1], John Browning[2], Mark Gourley[3], Greg Filip[4], Alan Kanaskie[5]

[1]Forest Engineering, Resource, and Management, Oregon State University, [2]Weyerhaeuser Corporation, [3]Starker Forests, [4]US Forest Service, [5]Oregon Department of Forestry

Introduction

Among the long term objectives of the SNCC is a constant monitoring of disease conditions. While this can be accomplished qualitatively with the results of the annual aerial survey, quantitative assessment of the tree growth loss resulting from Swiss needle cast requires periodic measurements. This has been accomplished up until now with the Growth Impact Study (GIS) plot network (Maguire et al. 2011).

During the final remeasurement of the GIS plots (2008), it was decided that their utility had become limited. The original sample of 10-30 year old GIS stands is now 25-45, which is considered outside the age range of those stands for which information is especially valuable. Furthermore, ground observation of foliage retention, the original methodology for determining disease severity, has become difficult to impossible as a result of crown recession and canopy closure. In addition, these plots were distributed only between Newport and Astoria, thereby providing inference only to the northern Oregon Coast Range.

In order to address these limitations, the decision was made to install a new monitoring plot network, which is foreseen to provide disease condition and growth loss information for at least 10 years. These plots have been installed in 10-20 year stands, thereby addressing the shortcomings of the aged GIS network. In addition, these plots will be distributed as far south as the California border, and as far north as southern Washington.

These plots will not only provide periodic information about disease severity, growth loss and its geographic distribution, but will also offer sites to be used for other SNC research, be it epidemiological, climatological, or other forms.

Methods

Criteria for selection

Candidate stands should not be treated by fertilization or disturbed (thinned, cleared) for ten years. The selected one-fifth acre plots with a 0.5 chain buffer (0.58 ac) should have not been pre-commercially thinned or fertilized in the past 5 years. The targeted basal area composition is 80% Douglas-fir, targeted age between 10 and 30-years old of Douglas-fir. Ideally dense understory should be avoided and density aimed to 300-400 trees per acre.

At each plot, a 1/5 acre plot has been laid out, and all trees tagged. Field methods have followed Kanaskie and Maguire, March 30, 2002 Field Specifications and Manual for Rating

Swiss Needle Cast in Douglas-fir. The following is adapted from that document but specific to the 1/5 acre plot and needle retention will be estimated in years.

Sampling matrix

We identified four zones based on distance from coast (in miles): 0-5, 5-15, 15-25, and 25-35. Each of these zones was equally divided (north-south), following township lines as closely as possible. Each block spans approximately 58 miles north-south. This resulted in 20 sampling blocks. In addition to the 20 cell matrix in coastal Oregon, 4 sampling blocks were established in SW Washington. Attached Google Earth image shows these blocks (Fig.1.)

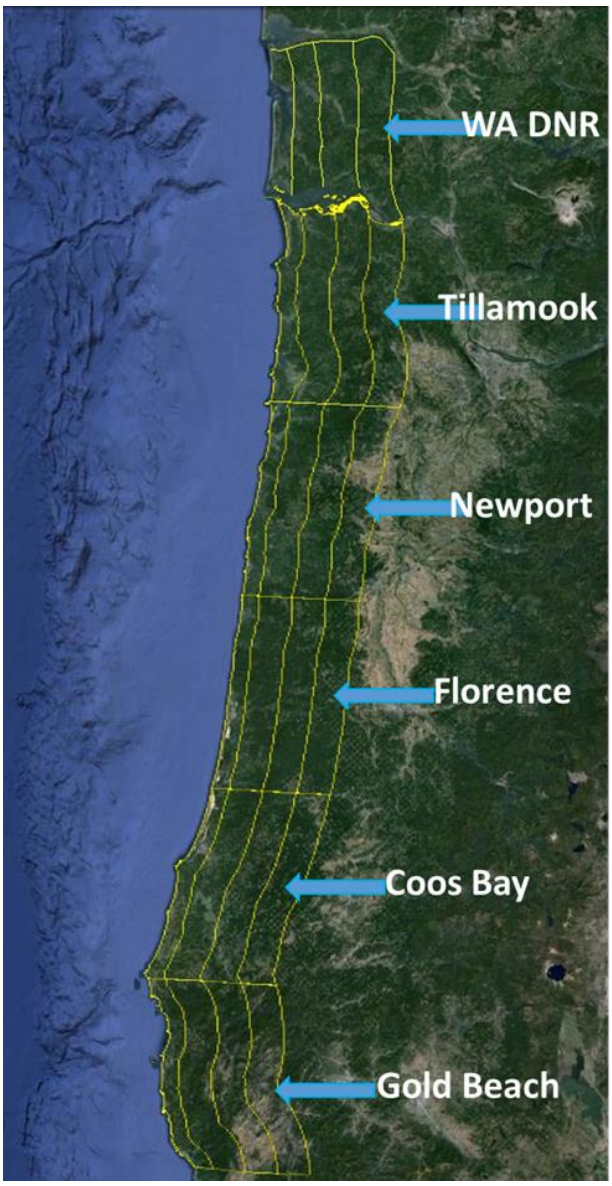

Figure 1. Research plot network matrix.

Sites

In addition to the 69 plots established in 2013 and 2014, thus far for 2015 we selected, installed and measured 38 sites. All of the 2015 sites are located in Oregon on property owned by Weyerhaeuser, South Coast Lumber, Oregon Department of Forestry, Bureau of Land Management, and Roseburg Resources, bringing the overall number of sites to 107. Plots within the stands were chosen subjectively.

Measurements

Following the establishment and marking of plot boundaries, all trees were given a unique numbered tag. Following the conclusion of the 2015 growing season, all trees were measured for dbh and species was recorded. A forty tree height sample was collected, such that it included the 10 largest trees by dbh, the four smallest by dbh, and the final 26 were ranged across the diameter distribution. In the spring, the 10 largest trees will be assessed for foliage retention, and needles will be sampled for pseudothecial occlusion, and foliar nutrition. In addition, soil samples were collected for Jeff Hatten's soil study.

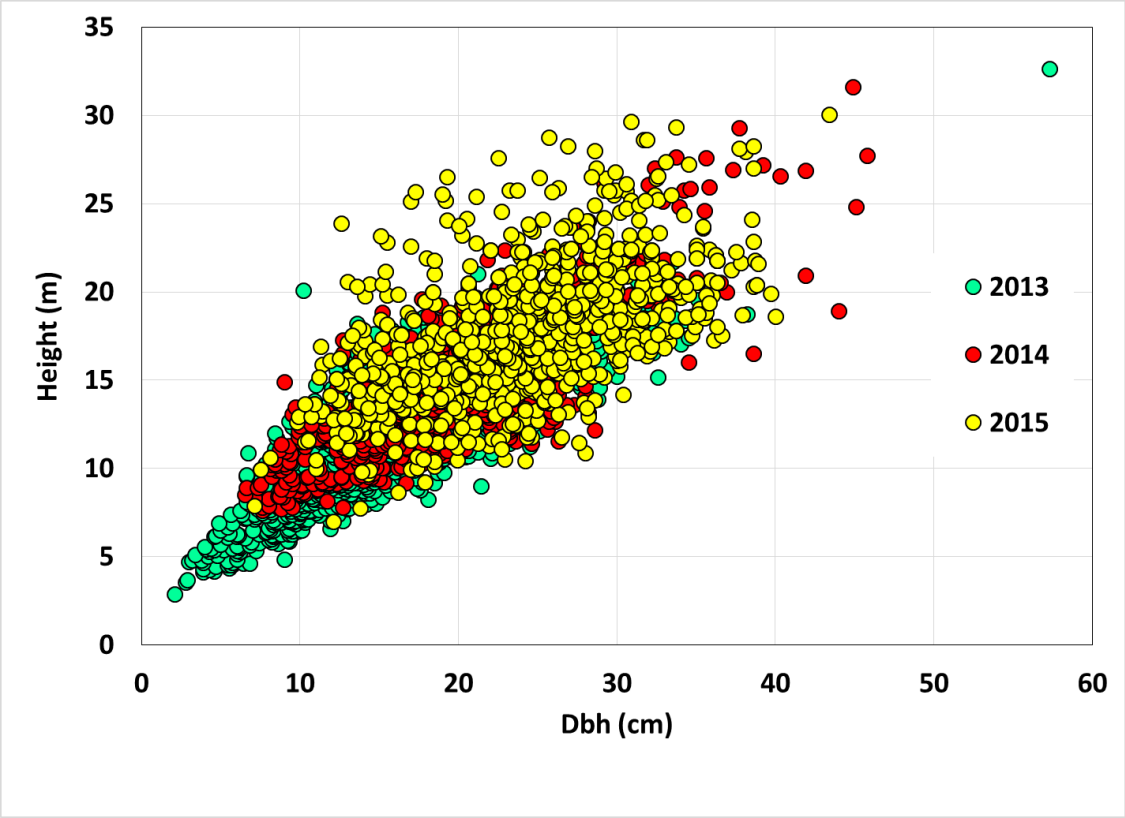

Figure 2. Height-diameter relationships for plots established in 2013, 2014 and 2015

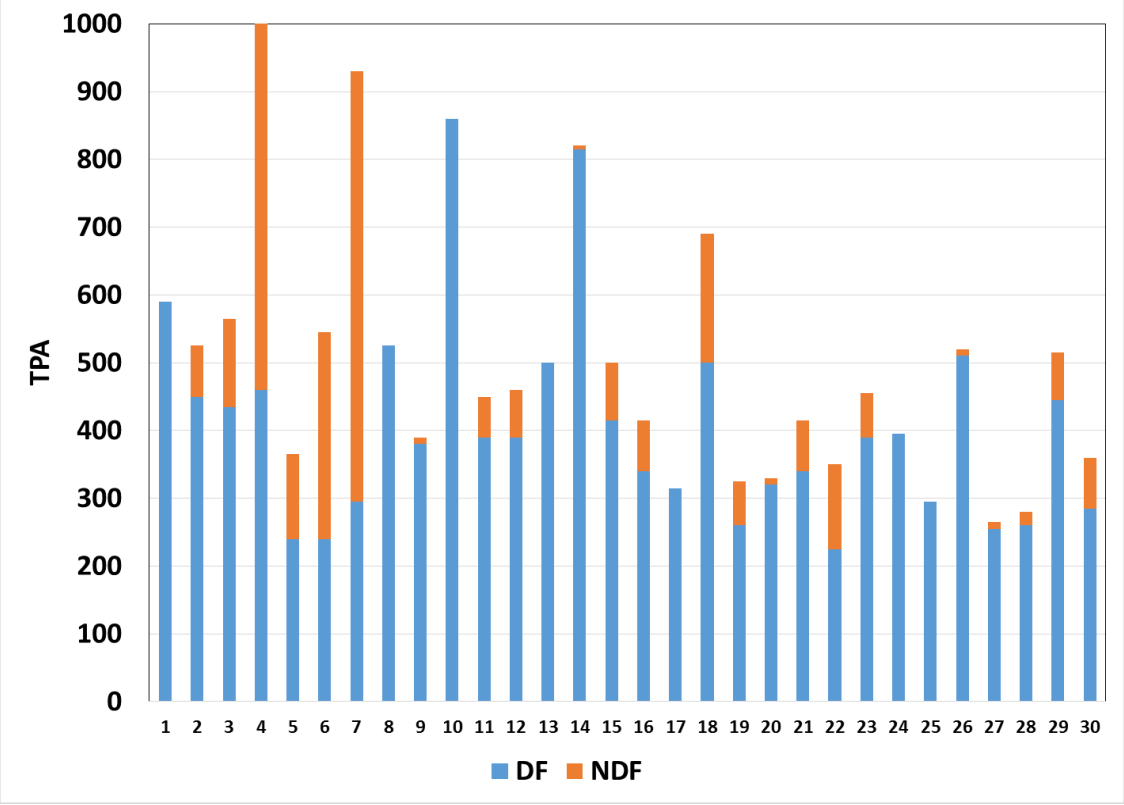

Figure 3a. Proportion of Douglas-fir and non-Douglas-fir in plots established in 2013.

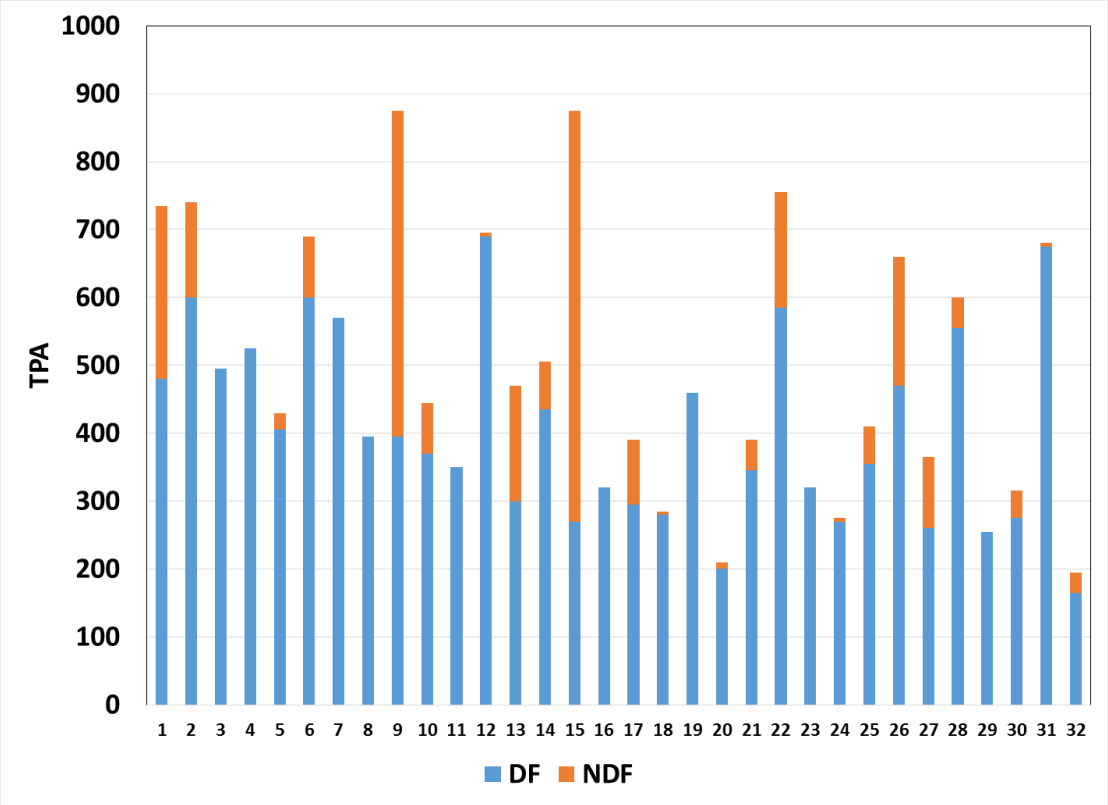

Figure 3b. Proportion of Douglas-fir and non-Douglas-fir in plots established in 2014.

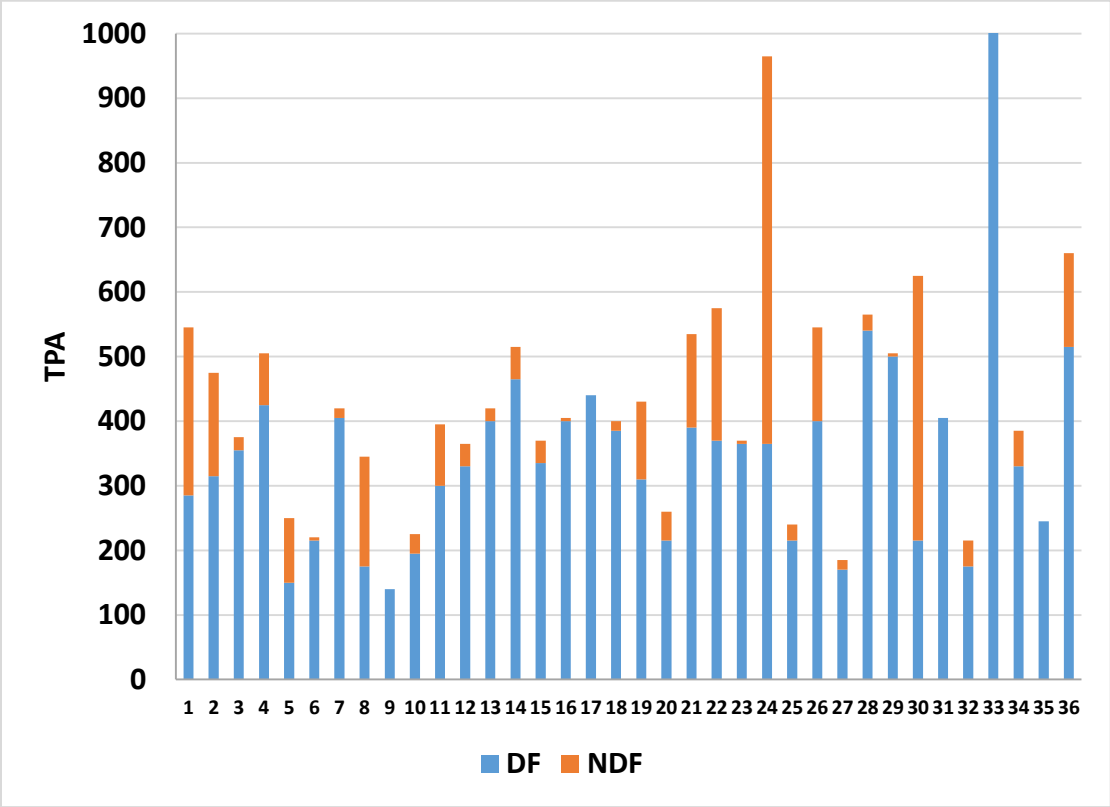

Figure 3c. Proportion of Douglas-fir and non-Douglas-fir in plots established in 2015.

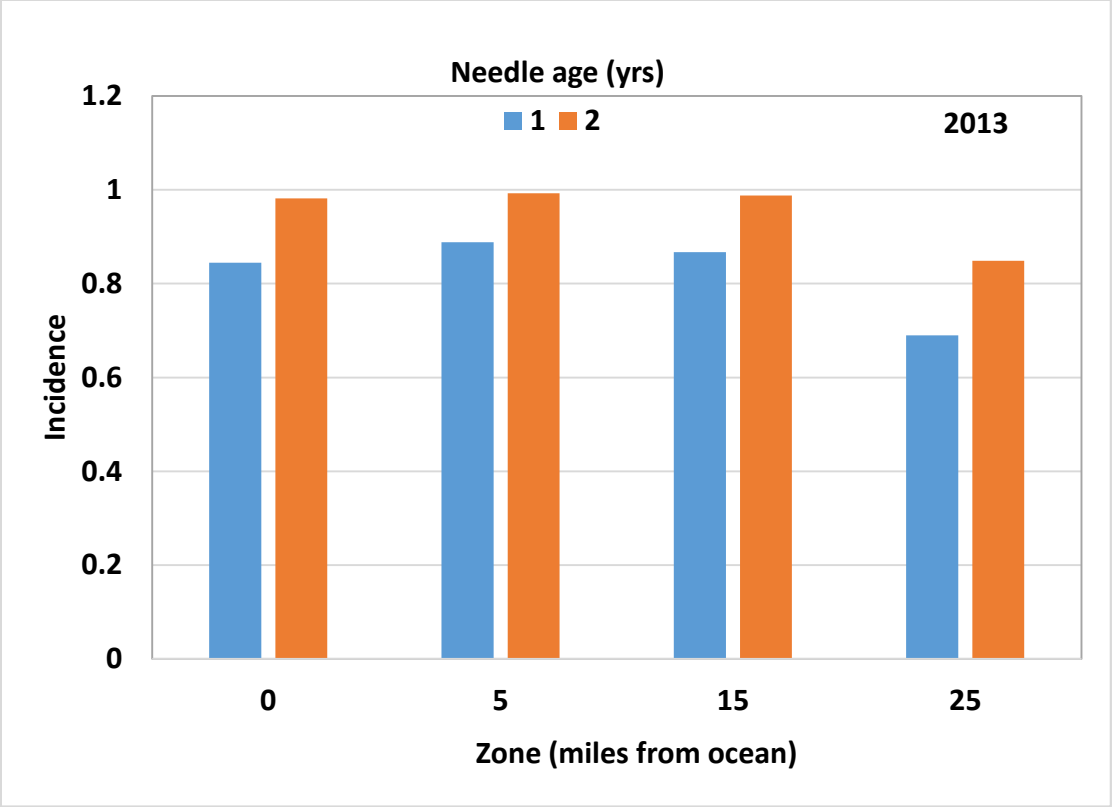

Figure 4. Incidence (pseudothecial presence) on 1- and 2-year old needles from plots established in **a)** 2013 (above), and **b)** 2014 (below).

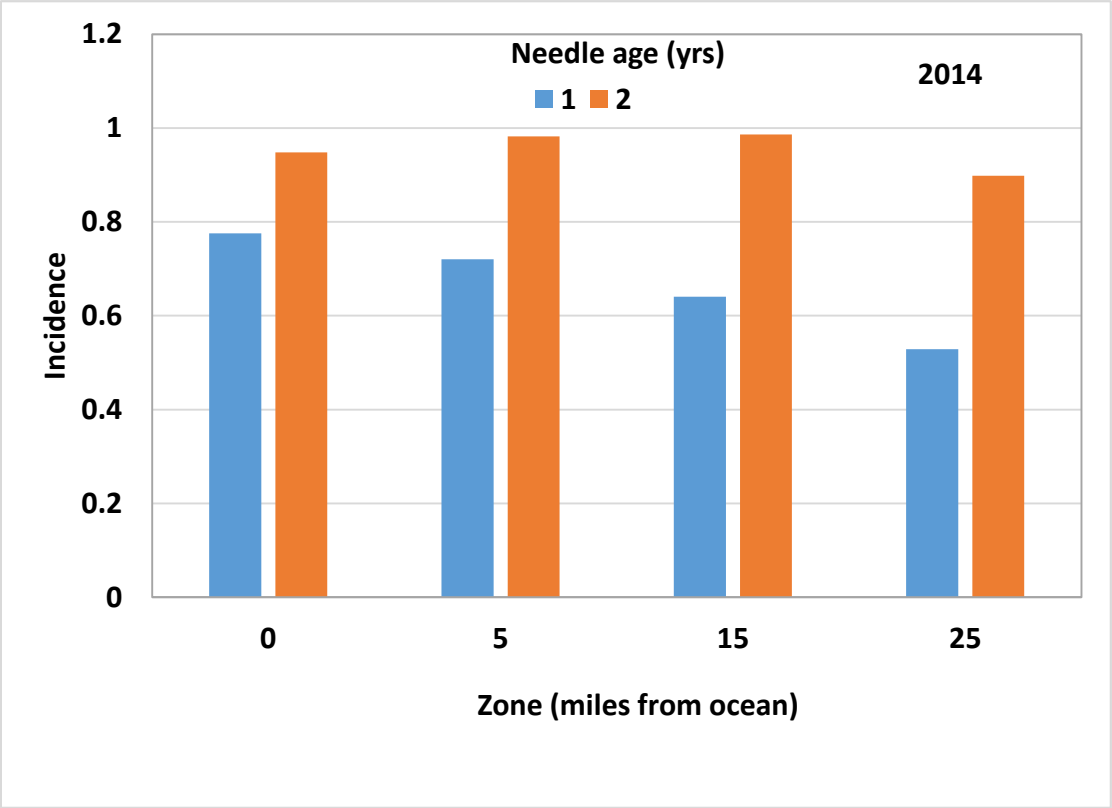

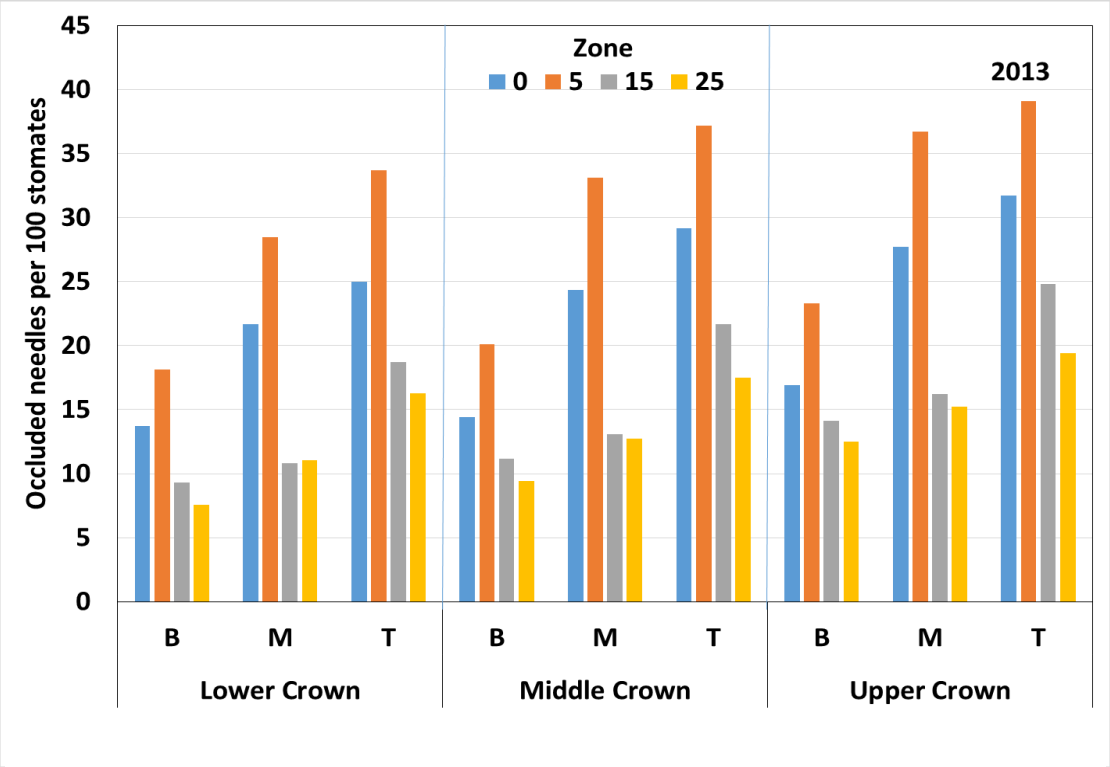

Figure 5. Percentage of occluded needles by zone, crown position and needle position for **a)** 2013 plots (above), and **b)** 2014 plots (below).

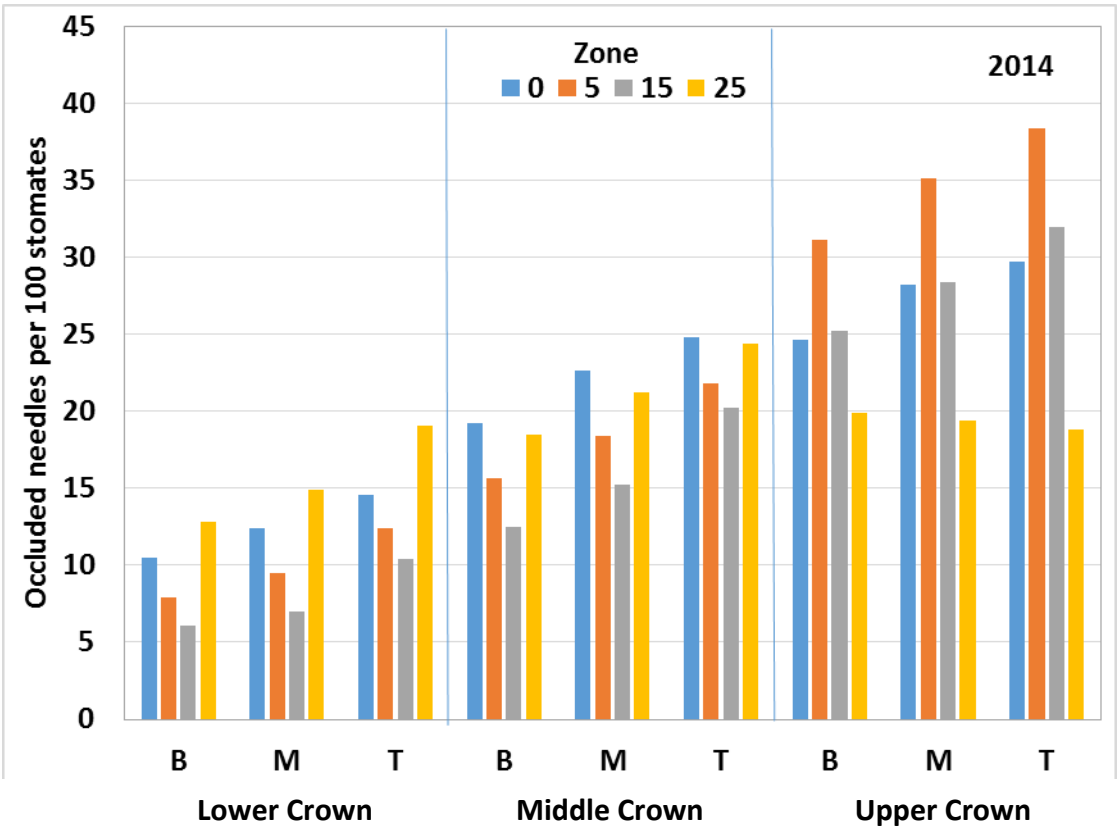

Do Soils Play a Role in the Current Swiss Needle Cast Epidemic?

Jeff Hatten, Gabriela Ritóková, Dave Shaw, Yvan Alleau, Sky Lan
Forest Engineering, Resources, and Management, Oregon State University

Introduction

The severity of Swiss Needle Cast (SNC) has been shown to vary as a function of climate (Zhao et al., 2011; Zhao et al., 2012), and generally the disease is more severe with proximity to the coast and the climate characteristics that brings. There has been some work showing that high foliar and soil nitrogen, low soil calcium, and low soil pHs are significantly correlated with SNC severity (Waring et al., 2000). This suggests soils influence the disease. However, these studies have not covered the full latitudinal gradient of SNC and soil N (Perakis et al., 2006; Perakis et al., 2013). Most perplexing is the correlation between soil characteristics, climate, and SNC severity and occurrence. Therefore, it has been very difficult to separate the influence of soil from that of climate over the range of SNC in the coastal ranges of Oregon and Washington. We hypothesize that there is an interaction of climate and soil along a latitudinal gradient that affects SNC occurrence and severity.

The results presented in this report are a preliminary examination of the soils and foliar data we have collected to compliment the suite of SNC disease severity and Douglas-fir growth data currently being collected.

Methods

Soils and foliage were sampled from the SNC monitoring plots currently being established by the Swiss Needle Cast Cooperative (SNCC). From each 0.08 ha square plot, soils were collected from O-horizons, 0-10, 10-20, and 20-30cm. Soils were collected from 5 different locations within each plot; one sample was collected from approximated plot center and the other four were collected 4.5m from the corners toward plot center (this was approximately 2/3 the distance from the plot center towards the corners). O-horizons were sampled at the plot center by removing material from a known area using a 10cm x 10cm cutting template 1m north of plot center. All material within the template was collected except live vascular plants and mineral soil. Depths of the O-horizon were recorded along 4 sides of the template in order to calculate bulk density. Mineral soils were collected at 0-10, 10-20, and 20-30cm using a push probe form an area devoid of O-horizon. Mineral soils from each depth were composited across the 5 locations from each plot (i.e. one sample per plot per depth).

One-year old needles were collected from three branch tips of one branch from mid-crown section, mostly from 5th whorl of the south side of the tree. Since 10 trees are being sampled in each plot we collected 25-30 needles from each tree and composited this material prior to drying. Approximately 1 g of material was collected (200-250 needles). Foliage, O-horizon, and mineral soil samples were stored in a refrigerator (<4 °C) for less than 4 weeks

prior to being oven dried at 40 °C until a constant weight achieved. Mineral soil samples were weighed, sieved to 2mm and the fine fraction weighed to determine coarse content.

Mineral soil pH was determined in deionized water using the 2:1 method (Thomas, 1996). C and N were determined on dried and ground O-horizon, mineral soil, and foliar material using dry combustion on a Thermo FlashEA 1112. Mineral soils were extracted using 1M NH_4Cl to extract the exchangeable pools of cations, while O-horizons and foliar samples were digested using 30% H_2O_2 and a 1:10 nitric-hydrochloric (HNO_3-HCL) acid digestion of organic matter in conjunction with external heating (EPA method 3050; Benton and Wolf, 1997). Digests and extracts were analyzed for Ca, K, Na, Mg, B, Al, Cu, Fe, Mn, Mo, P, S, and Zn on an inductively coupled plasma atomic emission spectrometry (ICP-AES) using a Thermo Scientific ICP-OES 61E.

Ortho-phosphate was extracted using a Bray 1 solution (0.03 M NH_4F and 0.025 N HCl) at a ratio of 7:1 (solution to soil) and filtered using a VWR 494 quantitative filter paper (Olsen and Sommers, 1982). The filtrate was analyzed for total extractable P using the previously described ICP-AES.

Results/Discussion

We analyzed soil and foliar samples from 69 plots collected during the SNCC 2014 and 2015 sampling field campaigns. The remaining SNC monitoring plots are planned to be sampled in April and May 2016, therefore we plan to complete the analyses of soils and foliage from these plots in the coming year (2016-17), barring severe disruption from the Peavy Hall demolition and rebuild.

Figure 1 shows some preliminary data we have collected so far. Perakis et al (2013) suggested that total nitrogen concentrations in the surface mineral soil horizon ("tn.g_Soil_0to10" in Figure 1) greater than 0.35% would result in high levels of Ca leaching and potential ecosystem level Ca limitations. That threshold is represented by the maroon vertical line. Points falling to the right are plots that may be experiencing high levels of Ca leaching. Foliar Ca concentrations ("ca.ugg_Plant_Foliar" in Figure 1) lower than 2500 ug/g may be a sign of a Ca limitation in Douglas-fir (Ballard and Carter, 1985). This threshold is represented as the horizontal green line in Figure 1. Points falling below the green line may be plots with Douglas-fir tree growth limited by Ca availability.

There appears to be a negative relationship between soil N content and foliar Ca, which is consistent with recent findings on Ca cycling in the Oregon Coast Range (Perakis et al., 2006 and 2013).

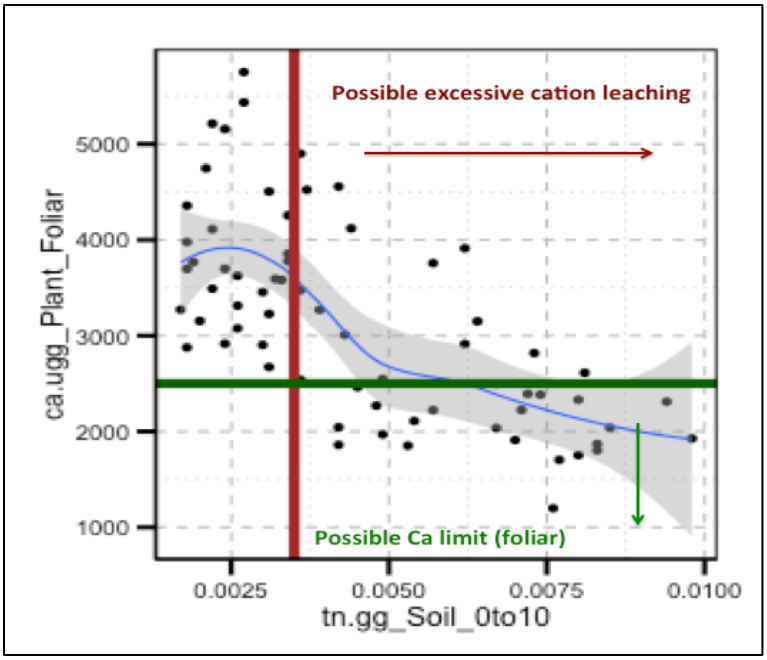

Figure 1 shows a good coverage across a range in soil N, a key predictor in the availability of cations such as Ca. This coverage will improve with the additional samples collected in the coming year suggesting that we will have good ability to examine the interactive effects of climate and soils on SNC severity.

References

Ballard, T. M., and R. E. Carter. 1985. Evaluating Forest Stand Nutrient Status. British Columbia Ministry of Forests, Vancouver, BC.

Benton, J. and Wolf, B., 1997. Plant analysis handbook II: a practical sampling, preparation, analysis, and interpretation guide. Micro-Macro Publishing, Incorporated, Athens, GA.

Perakis, S.S., Maguire, D.A., Bullen, T.D., Cromack, K., Waring, R.H., Boyle, J.R., 2006. Coupled Nitrogen and Calcium Cycles in Forests of the Oregon Coast Range. Ecosystems 9, 63-74.

Olsen, S., Sommers, L., 1982. Phosphorus. In: Page, A.L. (Ed.), Methods of Soils Analysis. Part II. Agron, Monograph 9. 2nd ed. ASA/SSA, Madison, WI.

Perakis, S.S., Sinkhorn, E.R., Catricala, C.E., Bullen, T.D., Fitzpatrick, J., Hynicka, J.D., Cromack Jr, K., 2013. Forest calcium depletion and biotic retention along a soil nitrogen gradient. Ecol. Appl. 23, 1947-1961.

Thomas, G.W. 1996. Soil pH and Soil Acidity. pp 475-490. *In:* Sparks, D.L., A.L. Page, P.A. Helmke, R.H. Loeppert, P.N. Soltanpour, M.A. Tabatabai, C.T. Johnston, M.E. Sumner, eds. Methods of Soil Analysis; Part 3 Chemical Methods. Soil Science Society of America and America Society of Agronomy, Madison, WI 53711.

Waring, R., Boyle, J., Cromack, K., Maguire, D., Kanaskie, A., 2000. Researchers offer new insights into Swiss needle cast. Western Forester 45, 10-11.

Zhao, J., Maguire, D.A., Mainwaring, D.B., Kanaskie, A., 2012. Climatic influences on needle cohort survival mediated by Swiss needle cast in coastal Douglas-fir. Trees 26, 1361-1371.

Zhao, J., Mainwaring, D.B., Maguire, D.A., Kanaskie, A., 2011. Regional and annual trends in Douglas-fir foliage retention: Correlations with climatic variables. Forest Ecology and Management 262, 1872-1886.

The effect of Swiss needle cast on stem taper within merchantable Douglas-fir plantations

Doug Mainwaring[1], Doug Maguire[1], Gabriela Ritóková[1],
Dave Shaw[1], Mark Gourley[2], George McFadden[3]
[1] Department of Forest Engineering, Resources, and Management, Oregon State University,
[2]Starker Forests, [3] Bureau of Land Management

Introduction

The distribution of diameter increment throughout the height of a tree is strongly dependent upon crown size and condition (Forward and Nolan 1961, Larsen 1963, Fajvan et al. 2008, Goudiaby et al.). The deleterious effects of Swiss needle cast (SNC) on total foliage mass and its alteration of foliage distribution throughout the tree crown (Weiskittel et al. 2006) has produced interest in investigating SNC effects on stem diameter increment and taper (Weiskittel and Maguire 2004). Stem dissection indicated that the greater the intensity of SNC (lower the foliage retention), the more narrow the upper stem for a given dbh, height, and live crown length. This result agrees with numerous studies that have established that the cross-sectional increment at any given height on the stem is proportional to the amount of foliage above that height.

The dataset used for the previous SNCC study (Weiskittel and Maguire 2004) included 105 trees from age 11 to 62, and thus much of the stem growth within the older trees was produced before the onset of the current SNC epidemic, generally recognized as starting sometime in the mid to late 1980s. Reported observations made in Swiss needle cast infected stands since that study suggest that stems may now be narrower for a given dbh, height, and live crown length than observed at the time of the 2004 study. Because SNC seems to change stem form, and because the trees have been subjected to the disease for 10 more years, it is likely that changes imposed by SNC may have increased.

Last year's winter ice storm, and the observed top breakage within Coast Range Douglas-fir stands, raised questions about whether SNC-infected stands are more prone to breakage than healthy stands. Changes in both stem form and wood density of the upper stem caused by SNC would potentially increase the risk of top breakage. Past research has demonstrated that infected trees produce a higher percentage of latewood (Johnson et al. 2003), which is of greater density than earlywood. Because of the positive correlation between density and modulus of elasticity (MOE) (Vikram et al. 2011), it is hypothesized that greater density for a given diameter in tree tops would result in diminished flexibility, and a greater likelihood of breakage under the force applied by ice or wet snow loading. Disks sampled during the course of taper sampling can be measured for density in an attempt to test for differences.

Production of a new taper equation that accounts for the effects of SNC would be of more general practical value as well. Early and viable commercial entries into young stands depend on

the availability of sawlogs, and this requires predicting the volume of wood that meets a minimum scaling diameter to make the entry profitable. Fortunately, retirement of the SNCC growth impact plots (GIS, Maguire et al. 2011) provides a source of numerous stands of approximately commercial age that have had previous measurements of tree dimensions and ratings of SNC intensity. This existing information would significantly enhance an assessment of current stem form by destructively sampling a strategically selected set of the plots and trees for analysis. The objectives of proposed work are to: 1) produce a stem taper equation that accounts for the intensity of SNC on various taper function parameters; and 2) test the hypothesis that the effect of SNC on stem form has intensified during the 17 years over which these permanent plots have been measured; and 3) test the hypothesis that stemwood density in the tops of SNC-infected trees (stem diameter < 5-10 cm) is greater than that of healthy trees.

Methods

Field

Twenty stands were chosen from among former SNCC GIS plots, distributed across the range of foliage retentions (FR) estimated in 2008. The sample included four plots with the greatest FR, the four with the lowest FR, and the others were distributed across the FR distribution.

In each stand, 5 undamaged and unforked trees were or will be selected for stem form analysis. This sample will include the two largest dbh SNC rating trees, a tree approximately equal to quadratic mean diameter, and two other trees (larger than QMD) distributed across the diameter distribution (if any of the other previous SNC rating trees qualifies for this subset of the sample, it should be used).

Chosen trees were measured for dbh, height, and height to lowest live branch. In addition, old heights were measured on sampled trees to match previous growing seasons for which tree measurements are available (8, 12, 14, 16 and 18 years back). In addition to a stump disk (at 0.15 m of height), and a dbh disk (at tree tag or 1.37 m of height), disk height and diameter outside bark (dob) were recorded for approximately 15-20 disks per tree (the middle of approximately every other interwhorl segment). Above stem diameters <10 cm, disks were cut from the middle of every interwhorl segment.

Lab

Disks were measured for diameter inside bark (dib), heartwood diameter, and diameters 8, 12, 14, 16, and 18 years prior to sampling along two perpendicular axes. In addition, counts of rings within the sapwood were made along the each of the four measurement axes. Density of the small diameter disks (<10 cm dob) were determined using volumetric water displacement, followed by oven drying and weighing.

Statistical Analysis

The effect of SNC on taper was tested by accounting for foliage retention within multiple alternative model forms: 1) a variable exponent taper equation (Kozak 1988); and 2) segmented polynomial equations (Walters and Hann 1986). The effect of duration of SNC impacts on taper will be tested by comparing parameter estimates among different measurement periods.

Results and Discussion

The results reported here are preliminary stem form estimates for trees felled during the winter of 2015-16. The 2015 dib measurements from forty trees were available for analysis. Furthermore, because not all disks have been measured for dib, dib was estimated from dob using the following equation, fit from the data of those disks already measured:

$$[1]\ dib = (0.8216 \cdot dob^{1.0466}) \cdot (RHT^{0.0211}), \text{ where}$$

RHT is relative height of the disk (disk height/total height) and dib and dob are defined above.

Diameter, height and foliage retentions of the sampled trees are shown in Figure 1.

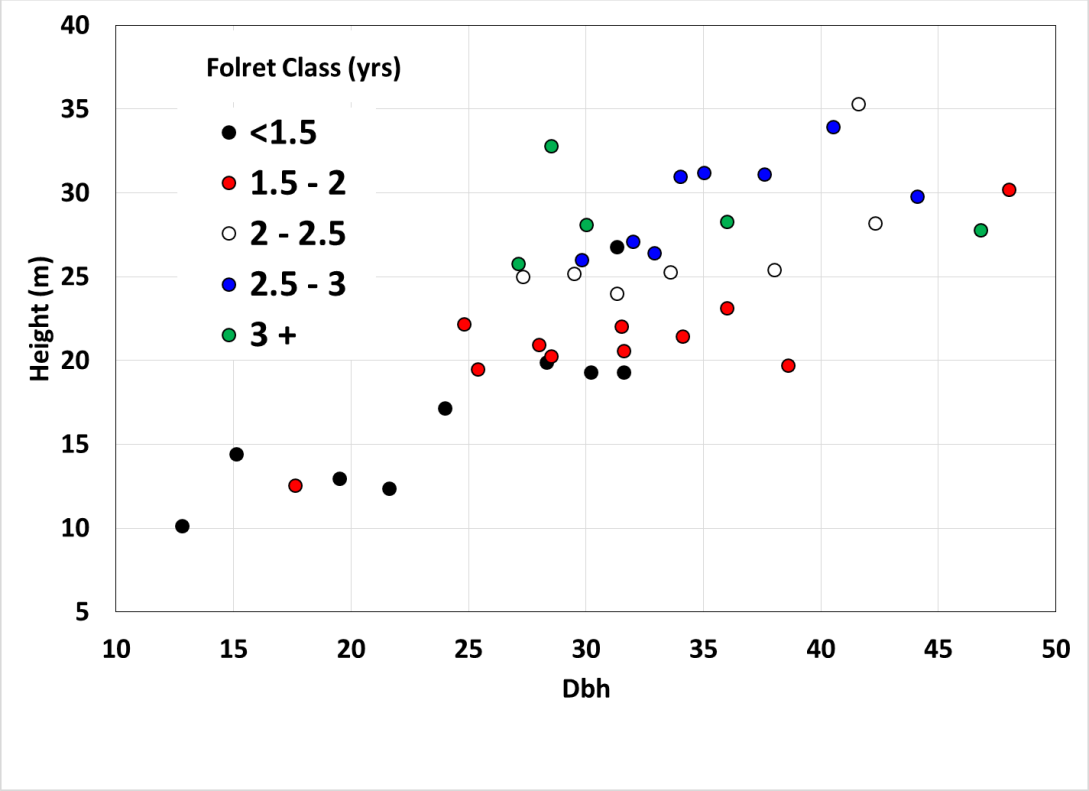

Figure 1. Height and diameter of current sampling dataset by foliage retention class.

A segmented polynomial taper model was found to provide the best fit to the data:

[2] $dib/DIB=(z1+b_1 \cdot z2+b_2 \cdot z3+b_3 \cdot z4+b_4 \cdot FR+b_5 \cdot FR \cdot z1+b_6 \cdot FR \cdot z3+b_7 \cdot FR \cdot z4+1)$, where

dib	= upper stem diameter inside bark for disk *k* (cm)
DIB	= diameter inside bark at BH (cm)
z1	$= i \cdot (a \cdot (1+b)-1)$
z2	$= x+i \cdot (a \cdot (x+j \cdot b)-x)$
z3	$= x^2+i \cdot (j \cdot a \cdot (2 \cdot x-j+j \cdot b)-x^2)$
z4	$= x^3+i \cdot ((j \cdot \cdot^2) \cdot a \cdot (3 \cdot x-2 \cdot j+j \cdot b)-x^3)$
FR	= Foliage retention (yrs)
i	= 0; if x>j then i=1
x	= (dht-1.37)/(ht-1.37)
j	= (0.01·(hllb-1.37)/(ht-1.37))
a	= ((x-1)/(j-1))
b	= ((j-x)/(j-1))
dht	= stem height of disk *k* (m)
Hllb	= Height to lowest live branch (m)
Ht	= total tree height (m)
b_1-b_7	=parameters estimated from the data.

The influence of foliage retention depended on the tree segment, as shown by the significant interactions by segment. Figure 2 indicates that SNC infection results in a smaller diameter for a given relative height, with the biggest proportional difference being near the base of the live crown. Figure 3 indicates that the implied differences in stem dib are not large, with the scaling diameter of a 17' butt log decreased by about 0.1 inches for 6 inch dbh tree and 0.2 inches for a 10 inch dbh tree (ht = 20 m, hllb=10 m).

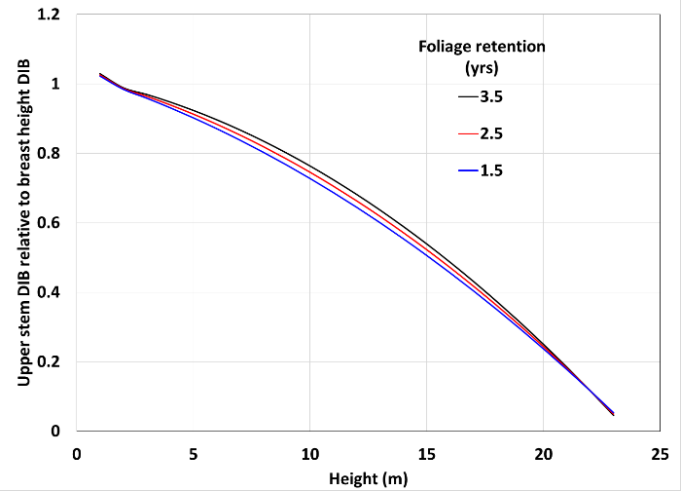

Figure 2. Ratio of upper stem dib to BH DIB for tree with 35 cm dbh, 34 m height, and 12 m height to lowest live branch.

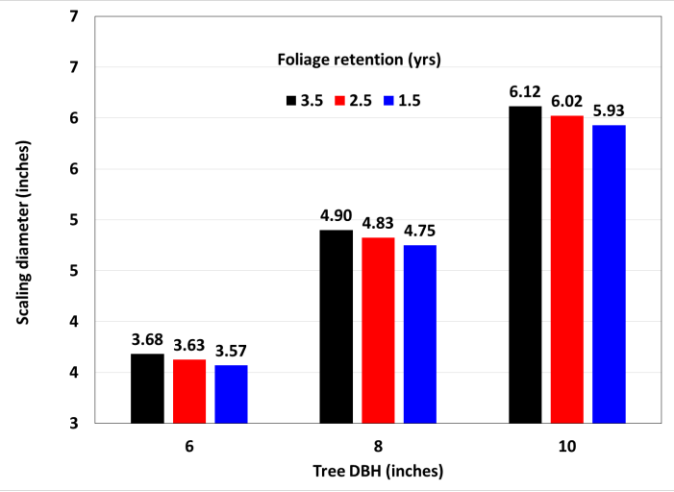

Figure 3. Scaling diameters at the top of a 17' log for trees of varying dbh (height = 20 m, hllb= 10 m).

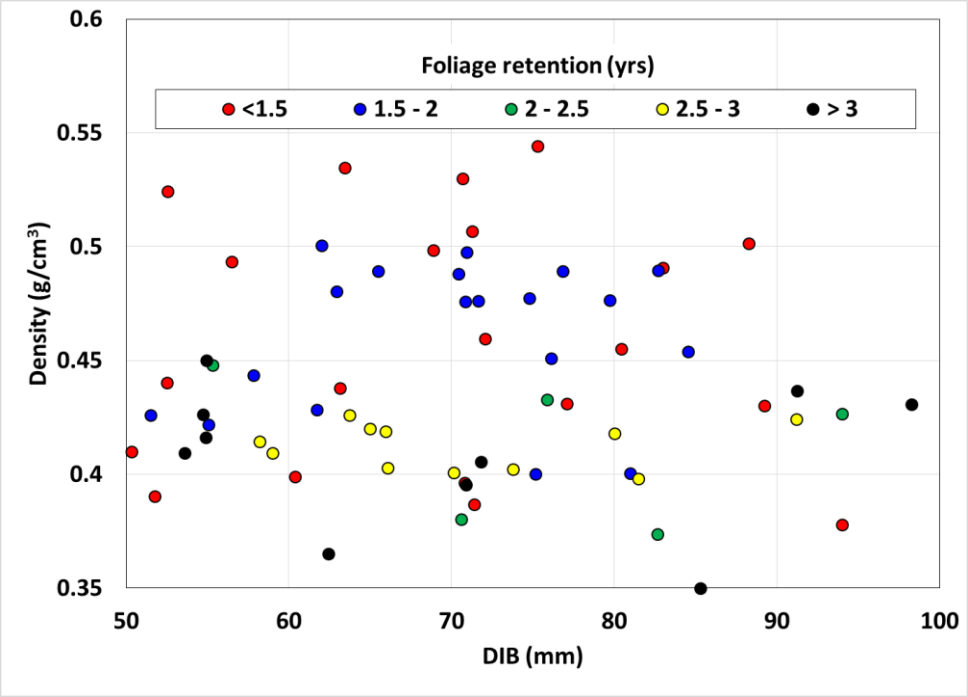

Figure 4. Relationship between density and dib by foliage retention class for upper stem disks.

The difference in scaling diameter exhibited in Figure 3 is much smaller than that implied by the previous taper equation fit for SNC-infected stands. Given the same trees, the previous equation (Weiskittel and Maguire 2004) implies differences of 0.55 inches for the 6 inch tree and 0.95 inches for the 10 inch tree. The source of these large differences between equations is unknown, but none of the trees sampled thus far in the current study produce anything similar to the relatively high dib/DIB values implied for healthy trees by the Weiskittel equation. The earlier work was based on a much larger range in age and size (age: 11-62 yrs; dbh: 12-67 cm; ht: 12-46 m), and presumably included a wider range of crown classes. The sampling for the current study, being focused on the dominant/co-dominant crown classes, will provide a more focused look at the trees making up the bulk of the volume (and value) within a stand. Nevertheless, based on the data collected thus far, it cannot be concluded that form of SNC-infected trees is significantly different from their form when sampling was conducted more than 10 years ago.

Small diameter disks (5-10 cm dob) from the tops of infected trees had a greater average density than disks from healthy trees (Figure 4). This relationship is described quantitatively as follows (see Figure 5):

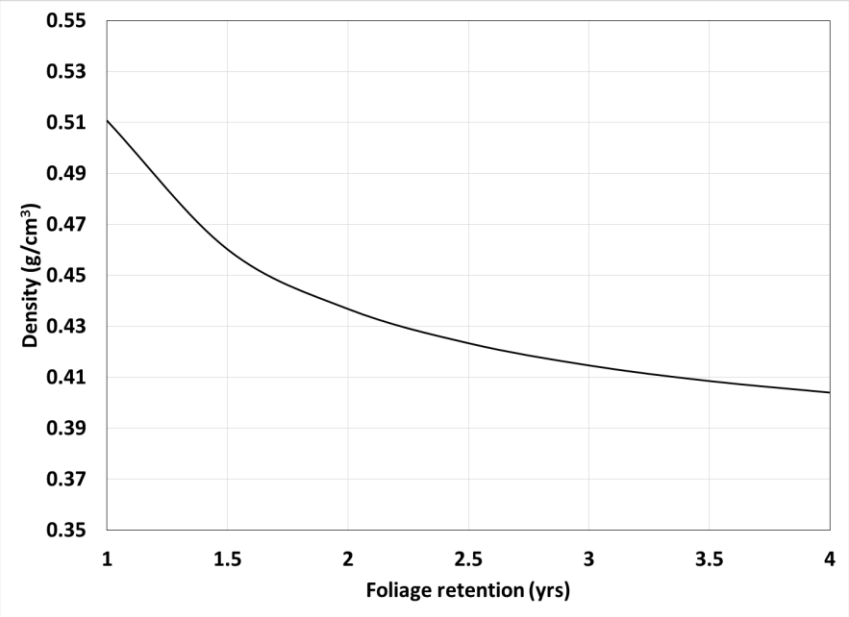

Figure 5. Relationship between density and foliage retention as described by equation [3]

Density

[3] Density=exp(-0.9845+0.3125/folret)

The positive relationship between density and MOE (Vikram et al. 2011) would indicate that SNC-infected tree tops are stiffer than those of healthy trees. An important factor when considering the impact of this stiffness on breakage is the fact that SNC-infected trees have less foliar density and mass, meaning that they would probably hold less snow and ice, and provide less of a "sail" for catching wind.

References

Fajvan, M.A., J., Rentch, and K. Gottschalk. 2008. The effects of thinning and gypsy moth defoliation on wood volume growth in oaks. Trees 22:257-268.

Forward, D.F. and N.J. Nolan. 1961. Growth and morphogenesis in the Canadian forest species: IV. Radial growth in branches and main axis of *Pinus resinosa* under conditions of open growth suppression, and release. Can. J. Bot. 39:385-409.

Goudiaby, V., R. Schneider, S. Brais, and F Berninger. 2012. Vertical patterns in specific volume increment along stems of dominant jack pine (*Pinus banksiana*) and black spruce (*Picea mariana*) after thinning. Can. J. For. Res. 42:733-748.

Johnson, G.R., Gartner, B.L., Maguire, D., and Kanaskie, A. Influence of Bravo fungicide applications on wood density and moisture content of Swiss needle cast affected Douglas-fir trees. For. Ecol. Man. 186: 339-348.

Kozak. A. 1988. A variable exponent taper equation. Can. J. For. Res. 18:1363-1368.

Larson, P.R. 1963. Stem form development of forest trees. For. Sci. Monogr. 5:1–42.

Maguire, D.A., Mainwaring, D.B., and Kanaskie, A. 2011. Ten-year growth and mortality in young Douglas-fir stands experiencing a range in Swiss needle cast severity. Can. J. For.

Res. 41**:** 2064-2076.

Vikram, V., Cherry, M.L., Briggs, D., Cress, D.W., Evans, R. and Howe, G.T. 2011. Stiffness of Douglas-fir lumber: effects of wood properties and genetics. Can. J. For. Res. 41: 1160-1173.

Walters, D.K. and Hann, D.W. 1986. Taper equations for six conifer species in southwest Oregon. Oregon State University, Forest Research Laboratory, Corvallis, Oregon. Research Bulletin 56. 36p

Weiskittel, A.R., and Maguire, D.A. 2004. Influence of Swiss needle cast on Douglas-fir stem properties. P. 91–97 in *Swiss Needle Cast Cooperative annual report*, Mainwaring, D. (ed.). College of Forestry, Oregon State Univ., Corvallis, OR.

Weiskittel, A.R., Maguire, D.A., Garber, S.M., and Kanaskie, A. 2006. Influence of Swiss needle cast on foliage age class structure and vertical distribution in Douglas-fir plantations of north coastal Oregon. Can. J. For. Res., 36: 1497–1508.

The Effects of Seed Source and Planting Environment on Douglas-fir Foliage Diseases

Nicholas Wilhelmi[1], Dave Shaw[1], Connie Harrington[3], Brad St. Clair[3], Lisa Ganio[2]
[1] Forest Engineering, Resource, and Management, Oregon State University, [2] Forest Ecosystems and Society, Oregon State University, [3] PNW Forest Service Research Station

Introduction

Douglas-fir (*Pseudotsuga menziesii*) is an important commercial and ecological tree species in western North America. The current rates of climate change are predicted to have serious impacts on successful regeneration of Douglas-fir forests and may render many of the current Douglas-fir seed zones obsolete. This will result in trees being maladapted to their current geographic locations. Strategies such as assisted migration and the revision of current seed zones may become very important management strategies in the mitigation of these negative impacts on Douglas-fir forests. However, the mechanisms that influence the successful movement of Douglas-fir seed to new locations are not well understood.

Severe impacts of pathogens and insects are commonly associated with maladapted Douglas-fir populations. The foliar pathogens *Phaeocryptopus gaeumannii (P.gaeumannii),* the causal agent of Swiss Needle Cast, and *Rhabdocline* species, the causal agents of Rhabdocline needle cast, are two important Douglas-fir pathogens. These pathogens have been shown to disproportionately affect genetically maladapted seed sources, causing serious growth impacts and sometimes mortality. The relationship between the levels of susceptibility/tolerance to these foliar pathogens and climate of the seed source is a key component in the identification of proper seed sources for reforestation. Understanding the variation in susceptibility/tolerance to Swiss needle cast and Rhabdocline needle cast will be influential in the modification of current seed zones and the successful movement of seeds to new locations.

Objectives

1.) Identify variation in the incidence and impact of these pathogens among these different seed sources 2.) Compare climactic variables between locations of seed sources and test sites to identify patterns in susceptibility/tolerance related to climate

Methods and Preliminary Findings

This study is part of the Douglas-fir Seed Source Movement Trials (SSMT), a large common garden, reciprocal transplant study. Twelve diverse west side Douglas-fir (*Pseudotsuga menziesii var. menziesii*) seed sources, ranging from northern California to southern Washington were evaluated. These seed sources represent 12 regions. Each region is represented by 60 different populations (Figure 1). These seed sources were planted in nine diverse planting environments ranging from southern Oregon to southern Washington, from the high elevation to the coast (Figure 2). Experimental sites and seed sources were selected to represent the range in

temperature and precipitation of western Oregon and Washington, and provide an opportunity to observe seed source – pathogen interactions.

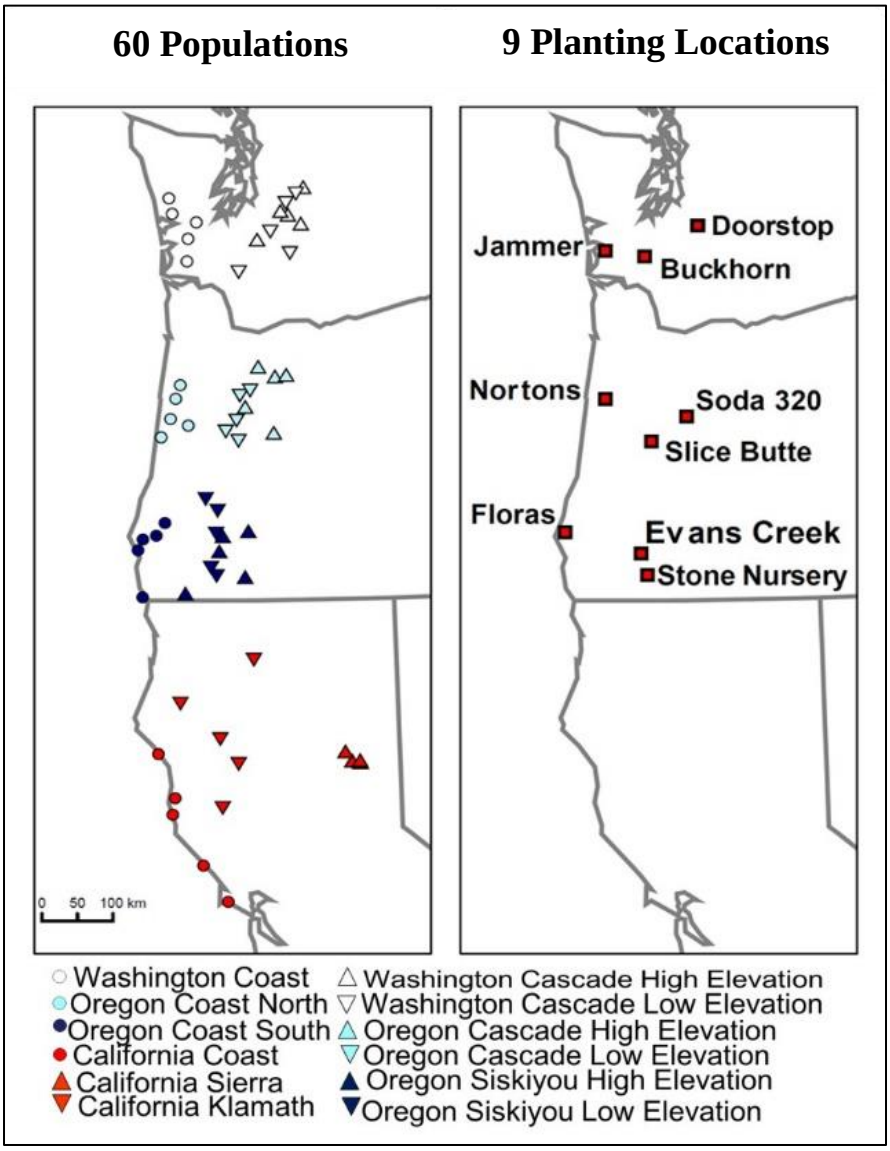

Figure 1. Locations of seed sources (left) and the test sites (right).

Each tree was assessed for the presence of *P.gaeumannii*, *Rhabdocline spp*. and the symptoms associated with SNC and Rhabdocline needle cast. The symptoms include low crown density, chlorotic crown color, and low needle retention. Crown density was rated on a scale ranging from 1 to 4; 1 being low density (unhealthy) and 4 being high density (healthy). Crown color was rated on a scale from 1 to 3; 1 being green (healthy), 3 being yellow (unhealthy). Needle retention was rated on a secondary lateral branch of the fourth whorl on the south side of the tree. Needle retention was estimated as the proportion of needles retained in each year of growth. Growth data, including diameter at breast height and tree height, has been collected previously as a part of the SSMT. Level of infection by *P.gaeumannii* was rated on the north and

south side of each tree on a secondary lateral branch on the fourth whorl from the top of the tree. Ratings ranged from "0" corresponding to no pseudothecia present to "3" corresponding to greater that 50% of stomata occluded by pseudothecia. *Rhabdocline spp.* infection was rated using the same scale as *P.gaeumannii* and was also assessed on the north and south sides of the tree. Fruiting body presence was estimated over the entire crown on each respective side for *Rhabdocline spp.*

Preliminary results indicate that seed sources from southern Oregon and northern California are, on average, most susceptible to Rhabdocline needle cast (Figure 2a) and consistently exhibit low crown density, low needle retention and chlorotic crown color. These seed sources are from sites with low precipitation levels from May through September and high continentality index. Coastal and low elevation seed sources from northern Oregon and southern Washington had low to no Rhabdocline infection indicating a high level of resistance. Seed sources from these locations also exhibited higher crown density, higher needle retention and healthy green crown color. Climates of these seed sources are characterized by higher precipitation levels from May through September and low continentality index. High elevation seed sources were more susceptible to Rhabdocline needle cast than coastal or low elevation seed sources throughout the represented range. Minimal variation was observed in *P.gaeumannii* infection levels among the regions (Figure 2b).

a)

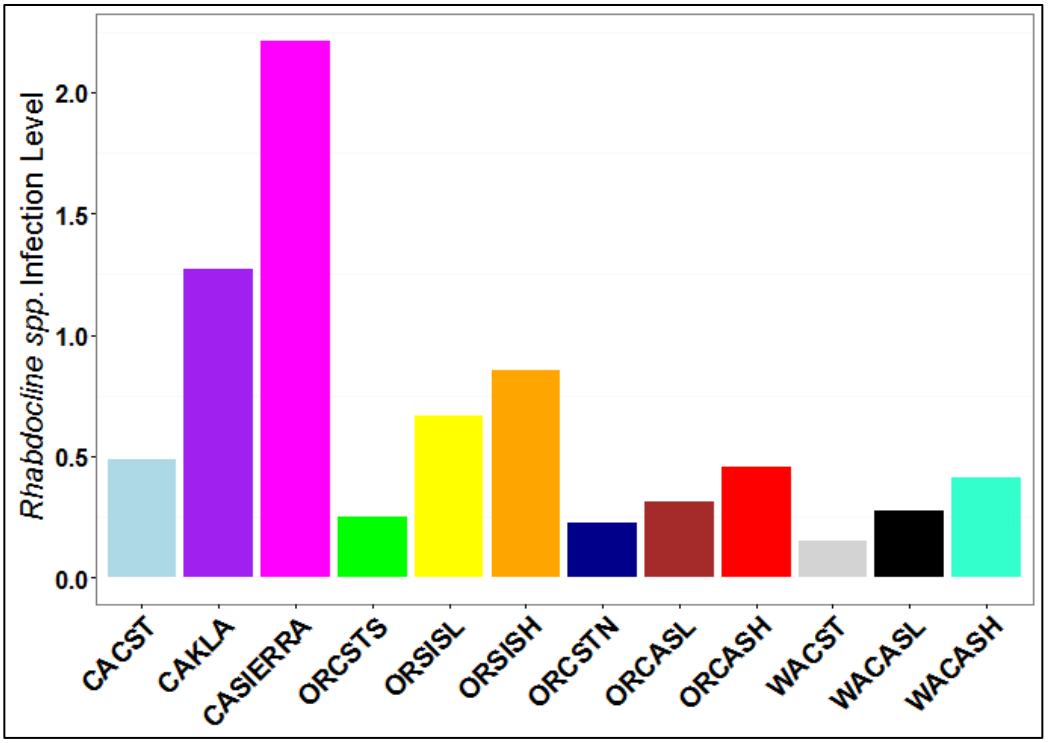

Figure 2. Levels of infection by **a)** Rhabdocline spp. and **b)** *P.gaeumannii.* California Sierra seed source was removed from *P.gaeumannii* evaluation due to high levels of Rhabdocline.

b)

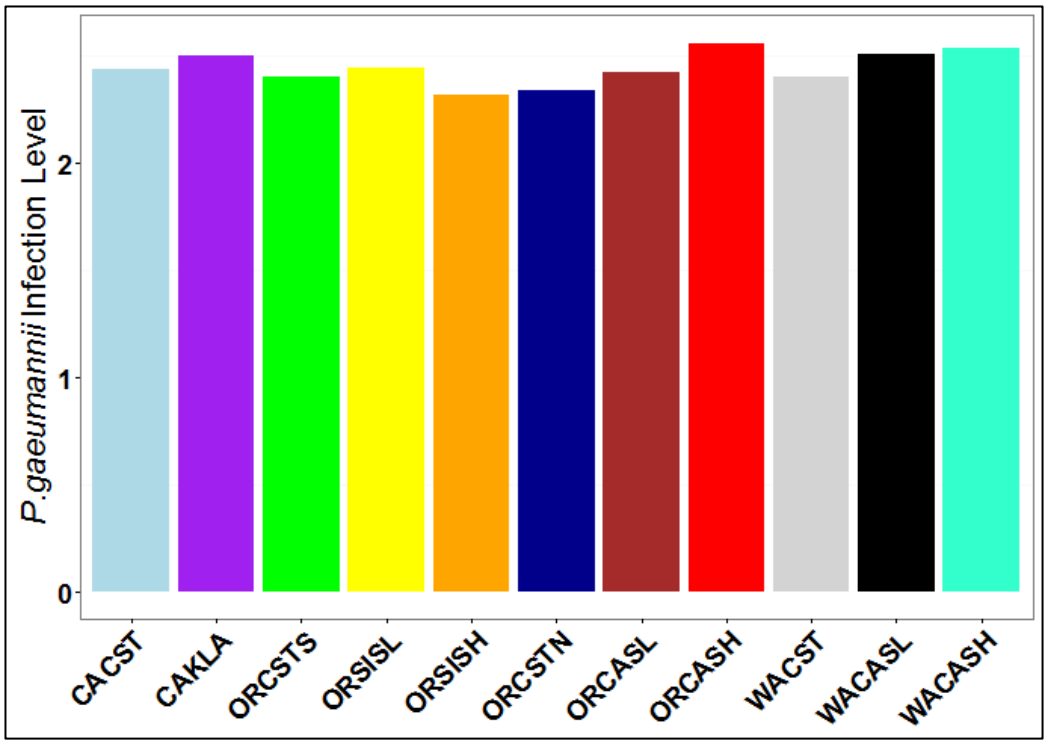

This project will provide a better understanding of the impact *P.gaeumannii,* and *Rhabdocline spp.* will have on different west side Douglas-fir seed sources under diverse climatic conditions. Understanding the levels of susceptibility/tolerance to these foliar pathogens will provide current land managers valuable information to assist in the identification of proper seed sources.

References

Boyce, J. S. 1940. A needle - cast of Douglas-fir associated with *Adelopus gaeumannii*. *Phytopathology*, 30(8), 649–655 pp.

Brandt, R. W. 1960. The Rhabdocline needle cast of Douglas fir. Syracuse: State University College of Forestry.

Hansen, E. M., Lewis, K. J. 1997. Compendium of conifer diseases. APS Press, the American Phytopathological Society.

Hansen, E. M., Stone, J. K., Capitano, B. R., Rosso, P., Sutton, W., Winton, L., McWilliams, M. G. 2000. Incidence and Impact of Swiss Needle Cast in Forest Plantations of Douglas-fir in Coastal Oregon. *Plant Disease*, 84(7), 773–778. doi:10.1094/PDIS.2000.84.7.773

Shaw, D. C., Filip, G. M., Kanaskie, A., Maguire, D. A., & Littke, W. A. 2011. Managing an Epidemic of Swiss Needle Cast in the Douglas-Fir Region of Oregon: The Role of the Swiss Needle Cast. *Journal of Forestry*, 109 (2), 109-119.

St Clair, Bradley, J., Howe, G. T. 2007. Genetic maladaptation of coastal Douglas-fir seedlings to future climates. Global Change Biology, 13(7), 1441–1454.

Can a fake fir tell the truth about Swiss needle cast?

E. Henry Lee[1], Peter A. Beedlow[1], Ronald S. Waschmann[1], Steve Cline[1], Michael Bollman[1], Charlotte Wickham[2], Nicholas Testa[3]

[1] US Environmental Protection Agency, 200 SW 35th Street, Corvallis, OR 97330, [2] Oregon State University, Department of Statistics, Corvallis, OR 97331, [3] Oregon Department of Transportation, Corvallis, OR 97330

Abstract

A key question in dendrochronology to reconstruct forest disturbance history is how to distinguish between the effects of Swiss needle cast (SNC) and other forest disturbance agents (e.g., *Arceuthobium* spp., *Armillaria*, *Phaseolus schweinitzii*, *Dendroctonus ponderosae*, *Dendroctonus pseudotsugae*, *Choristoneura occidentalis* Freeman, *Orgyia pseudotsugata* McDunnough) on radial stem growth of Douglas-fir (*Pseudotsuga menziesii* (Mirb.) Franco). SNC impacts physiological processes of carbon and water relations by stomatal occlusion and early needle abscission resulting in a reduction of tree growth with a distinct periodicity, whereas phytophagous pests reduce tree growth by defoliation with epidemics following less regular pseudo-periodicities. Outbreaks of the various forest disturbance agents differ in their magnitude, frequency, and duration. In particular, SNC impacts on Douglas-fir growth display a primary periodicity of 6-30 years and a secondary periodicity of 3-5 years which is unique to the causal fungus *Phaeocryptopus gaeumannii* (Rhode) Petrak. We use frequency domain analysis of tree-ring chronologies of Douglas-fir to identify the SNC disease cycle and separate the confounding effects of climate and SNC. We demonstrate the dendroecological reconstruction of SNC impacts on ancient Douglas-fir trees dated ~65K radioactive years B.P. from Eddyville, OR that were unearthed by the Oregon Department of Transportation.

Introduction

The ascomycete fungus *Phaeocryptopus gaeumannii* (Rhode) Petrak is ubiquitous in native Douglas-fir (*Pseudotsuga menziesii* (Mirb.) Franco, *P. menziesii* var. *glauca* [Beissn.] Franco) forests and is the cause of Swiss needle cast (SNC) (Hansen et al., 2000). SNC is most severe in forests and plantations on the western slopes of the Oregon Coast range within the coastal fog zone and is widely believed to be present but innocuous across much of the natural range of Douglas-fir (Hansen et al., 2000). Because of its generally inconspicuous and innocuous behavior, the history and spatial extent of SNC impacts on Douglas-fir growth are largely unknown. Evidence from dendrochronological studies indicates that SNC impacts on growth of Douglas-fir have occurred periodically as far back as 1592, which was the earliest of the available tree-ring records (Lee et al., 2013), and everywhere that its host is found in western Oregon (Lee et al., 2016a, 2016b). However, attribution of SNC as the cause of the anomalously low growth patterns in tree-ring chronologies is open to debate because the forested ecosystems in the Pacific Northwest (PNW) are host to many other forest pathogens (e.g., *Arceuthobium* spp., *Armillaria*, *Phaseolus schweinitzii*) and pests (e.g., *Dendroctonus ponderosae*,

Dendroctonus pseudotsugae, *Choristoneura occidentalis* Freeman, *Orgyia pseudotsugata* McDunnough). Differences in the magnitude, duration, and periodicity between forest disturbance agents allow one to separate the confounding effects of climate and multiple forest disturbances on Douglas-fir growth. We developed a conceptual model of the SNC disease cycle that quantifies the magnitude, duration, and periodicity of SNC impacts on annual radial stem growth based on empirical and epidemiological findings. Identification of the SNC disease cycle is illustrated with a dendrochronological example.

The Disease Cycle

The key growth pattern in master chronologies of coastal Douglas-fir is a sinusoidal cycle of anomalously low growth having a primary periodicity of ~6-30 years and a secondary periodicity of ~ 4 years associated with SNC (Lee et al., 2013). The periodic patterns of SNC impact on Douglas-fir radial growth increment occur throughout the life of the tree and because of the effects of synoptic seasonal weather patterns on fungal growth, are coherent across coastal Oregon. We synthesized our dendrochronological findings with the epidemiology of SNC to develop a conceptual model of the disease cycle driven by needle retention and fungal fruiting body abundance which have commonly been used as indices of disease severity (Hood 1982; Michaels and Chastagner 1984; Hansen et al. 2000; Manter et al. 2005). SNC reduces assimilation of carbon and tree growth by stomatal occlusion and early needle abscission (Manter et al. 2000; Hansen et al. 2000). Consequently, annual changes in SNC impacts depend upon inoculum abundance, ascospore germination, and pathogen colonization in association with climatic conditions which affect the proportion of stomata occluded and needle retention. Coastal Douglas-fir trees generally retain up to four years of needles but may only have current and 1-year-old foliage due to early needle abscission in severely affected plantations (Hansen et al 2000; Maguire et al. 2002; Zhao et al. 2011). In our conceptual model, the disease cycle begins when pathogen abundance is at epidemic levels, resulting in loss of 2-year-old and older needles and a significant reduction in tree ringwidth (Figure 1) (Lee et al., 2016a). The pathogen population will be reduced due to premature needle abscission resulting in fewer infected needles and a reduction in inoculum. Peak SNC outbreaks reduce tree ringwidth increment for several consecutive years because photosynthetic capacity is restored to normal only after all needle classes have formed (Saffell et al., 2014). A delay of several years between inoculation and growth of the fungus and radial stem growth reduction is expected because *P. gaeumannii* infects only the newly emerged needles (Hood and Kershaw 1975; Stone et al. 2008). This lagged growth response to SNC is represented by a 4-year periodicity in disease impacts (Figure 1). The slow buildup of pathogen abundance from endemic to epidemic levels over several life cycles is represented by a 20-year periodicity. The primary periodicity of 20 years varies by site and is as low as 6 years at Tillamook where more favorable climatic conditions enhance fungal development (Stone et al. 2008; Lee et al., 2013). Pseudothecia are commonly found on 4 to7-year-old needles in the Cascade Range of Oregon and Washington, and on 1 to 2-year-old needles in some areas of the Coast Range where pathogen dynamics are enhanced by more favorable climatic conditions (Stone et al. 2008). Pathogen abundance is not reset to endemic

levels by abscission of 2-year-old and older needles in areas where disease is constantly severe as indicated by a <10-year disease cycle and the presence of pseudothecia on 1 to 2-year-old needles.

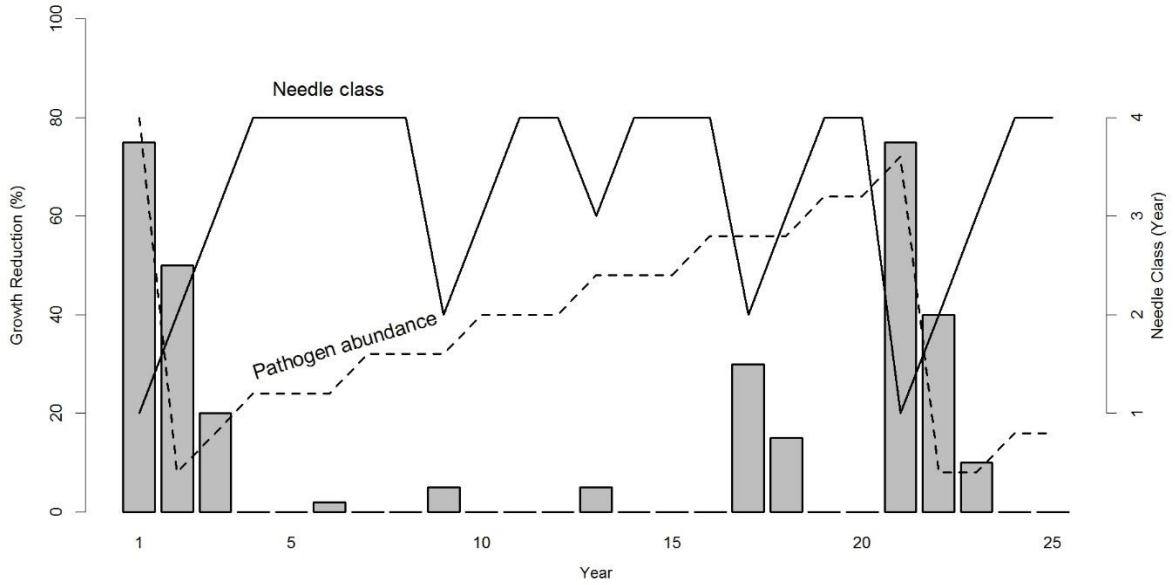

Figure 2. Conceptual model of Swiss needle cast (SNC) impact on radial growth increment in association with the abundance of Phaeocryptopus gaeumannii and number of needle classes retained (Lee et al., 2013). The number of needle classes retained varies from one (when the tree is heavily infected) to four (least infected). Pathogen abundance increases from endemic (when two-year-old and older needles are abscised) to epidemic levels (when tree is heavily infected) over several decades. The disease cycle begins anew with a peak reduction in growth when pathogen abundance reaches epidemic levels and is then reset to endemic levels following the early abscission of two-year-old and older needles. Growth reductions display 4- and ~20-year periodicities because P. gaeumannii infects only the newly emerged needles at time of sporulation and has a four-year life cycle.

Spectral Analysis of the SNC Disease Cycle

A time series displaying pseudo-periodic patterns is best examined using spectral or frequency domain analysis. We examine a Fourier transformation of five replications of the SNC disease cycle to illustrate the representation of the disease cycle in the frequency domain (Figure 2). The dominant pattern in the disease cycle is a peak impact occurring every 20 years (Figure 2A) which is represented in the frequency domain by a peak in its spectrum at a frequency of 0.05 cycles/year (i.e., periodicity of 20 years) (Figure 2B). The spectrum also has a secondary periodicity of 4 years (frequency = 0.25 cycles/year) which is seen in the time domain as a periodic impact on radial stem growth increment every four years. The other local peaks in the spectrum occur at the harmonic frequencies, e.g., twice and thrice the secondary frequency. The spectrum in Figure 2B is the signature of SNC impact that is unique and can be used to identify a SNC disease cycle and separate the confounding effects of climate, SNC, and other forest disturbances at a site.

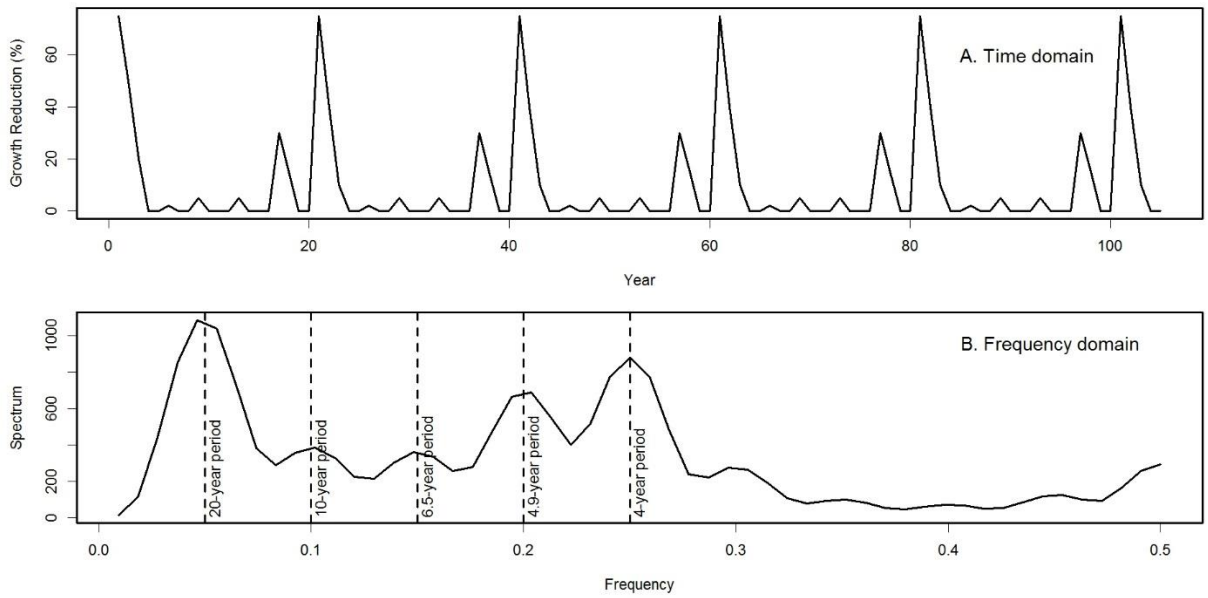

Figure 3. The sinusoidal pattern of Swiss needle cast (SNC) impact on radial growth increment of Douglas-fir is represented by five repetitions of the 20-year disease cycle. The SNC index has a primary periodicity of ~ 20 years and secondary periodicity of ~ 4 years as seen in the A) time and B) frequency domain. The total area under the spectrum is equal to the variance of the time series.

Example: Ancient Douglas-fir near Eddyville, Oregon

We developed tree-ring chronologies from eight of 11 Douglas-fir logs that were unearthed in 2008-2010 by the Oregon Department of Transportation along the U.S. Highway 20 reconstruction site due east of Eddyville, OR (N44º39´, W123º47´) (Figure 3). The logs, needles, and seed cones were encased in ancient landslide deposits at 7.6 to 24.4 m below the surface and were remarkably preserved (Figure 4). Radiocarbon dating estimates ages ~53K Before Present (BP) in the Marine Isotope Stage 3 (MIS3, ca. 60 to 27 K BP) period which was generally cold but with intermittent Dansgaard-Oeschger warm phases (Panyushkina et al., 2012). A more recent radiocarbon dating estimates the logs may be as old as ~65K BP (Nick Testa personal communication). Stem diameters range from 64 to 128 cm and are comparable in size to contemporary coastal Douglas-fir trees of the same age. The similar growth rates indicate that the ancient Douglas-fir come from a temperate rainforest environment comparable to present day. Needles of the ancient Douglas-fir appear to have significant stomatal occlusion by structures resembling pseudothecia of *P. gaeumannii*, as seen under a scanning electron microscope (Figure 5). The eight tree-ring series were successfully cross-dated and displayed different patterns of anomalously low growth, indicative of a non-climatic forest disturbance agent that affected some trees more than others rather than a climate stress that affected all trees uniformly (Figure 6). The divergence in tree ringwidth growth patterns was most evident for tree 351 that displayed several 3-year periods of growth reduction approximately every 7.5 years (Figure 6A).

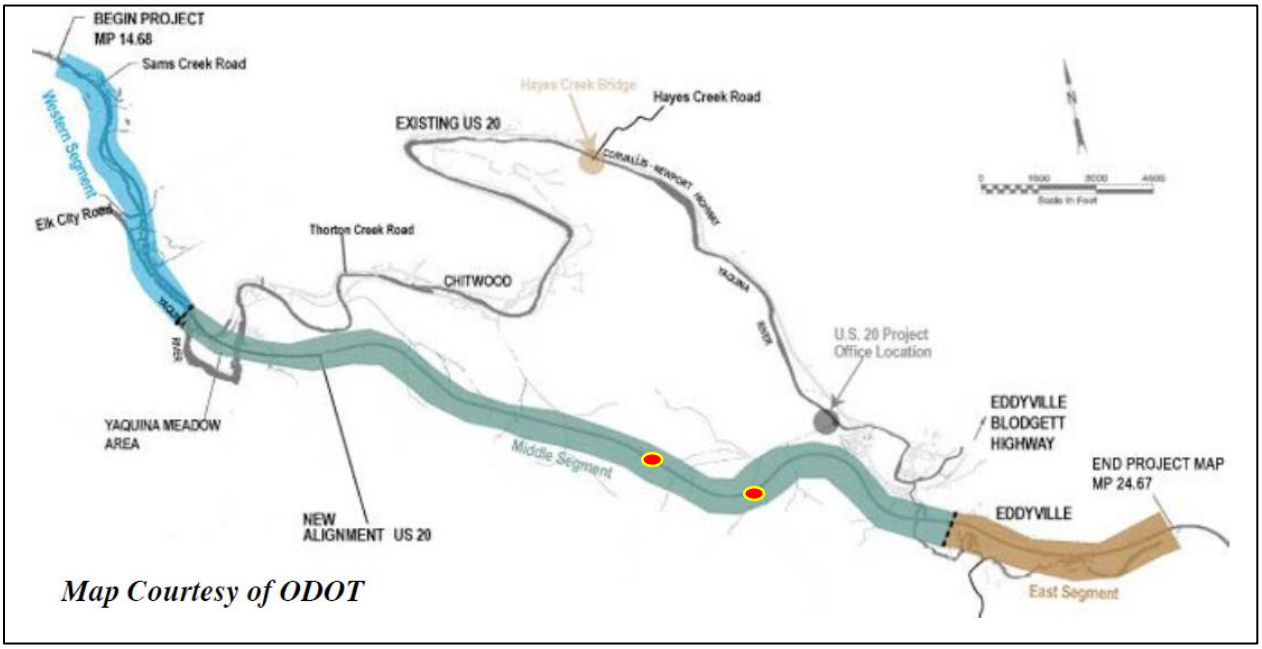

Figure 4. Logs, needles, and seed cones of ancient Douglas-fir were found down to 7.6 to 24.4 m below the surface by the Oregon Department of Transportation (ODOT) along the U.S. Highway 20 reconstruction site near Eddyville, Oregon. The two red dots represent where most of the ancient logs were found.

Figure 5. The 11 ancient Douglas-fir logs from Eddyville, Oregon were assigned unique identification numbers (351-361) and temporarily stored on the front lawn of the Oregon Department of Transportation offices in Corvallis, Oregon. This represents the 9th find of intact ancient logs in the world. Photograph was taken by Nicholas Testa, Oregon Department of Transportation.

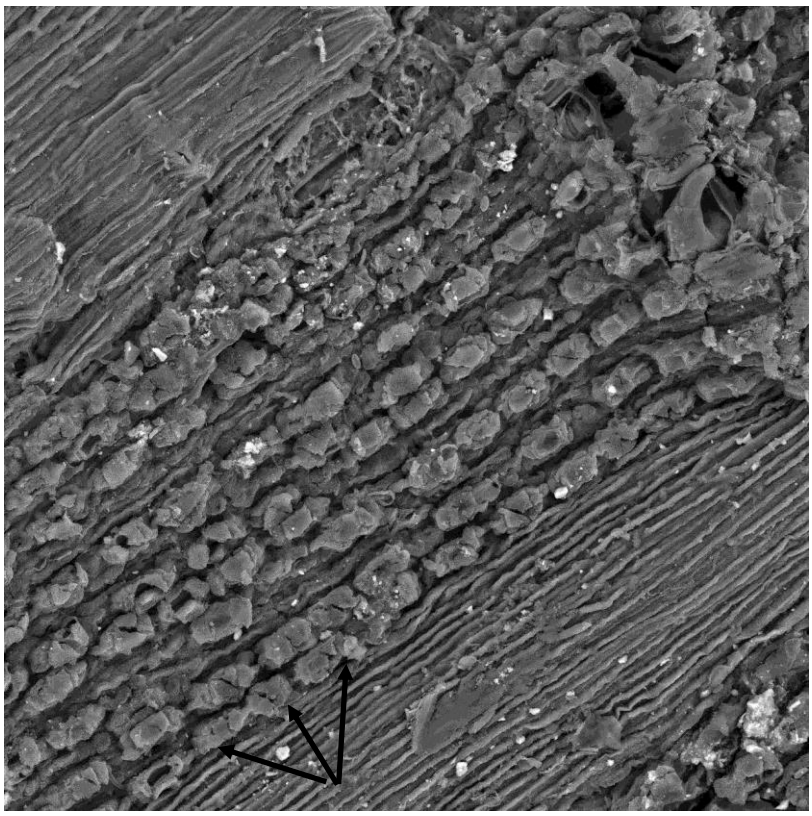

Figure 6. Scanning electron micrograph of pseudothecia primordia (see arrows) blocking the stomata of an ancient Douglas-fir needle found 29 m below the surface in landslide deposits near an Oregon Department of Transportation highway reconstruction project by Eddyville, Oregon. Image courtesy of William Rugh.

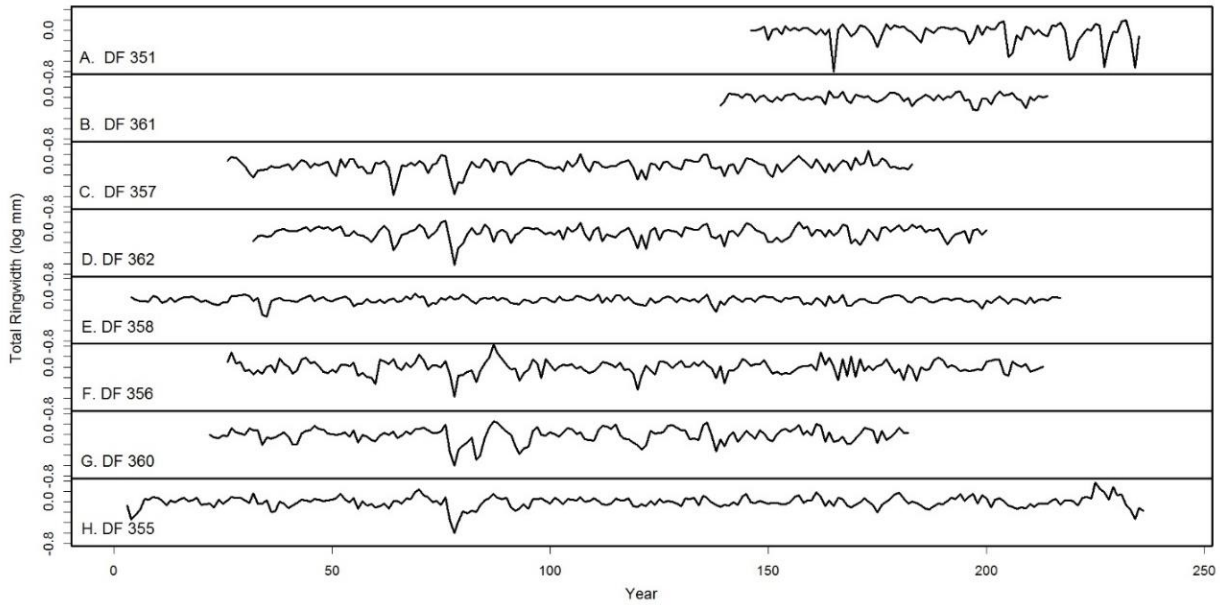

Figure 7. Chronologies of annual tree ringwidths for ancient Douglas-fir trees near Eddyville, Oregon were log transformed and detrended using a cubic spline smoother to remove the age-related growth trend. The length of the individual tree-ring time series ranged from 76 to 234 years.

Spectral analysis of the eight tree-ring chronologies of Douglas-fir indicated some displayed a significant SNC disease cycle signature (trees 351, 355, 356, 357, 360, 362) whereas others did not (trees 358, 361) (Figure 7). Tree 358 displayed the least variability and low pseudo-periodic patterns while tree 351 displayed the greatest variability and had a primary periodicity of 7.4 years and a secondary periodicity of 4.7 years (Figure 7). The chronology for tree 358 typically fluctuated by ±25% around 0, which is the typical range of climate effects on tree growth (Figure 8A). On the other hand, the chronology for tree 351 had sinusoidal patterns of anomalously low growth < -25% having periodicities of 7.4 years (Figure 8B). The 7.4-year disturbance cycle for tree 351 is similar to that of Tillamook Lower which has a periodicity of 6 years caused by SNC (Lee et al., 2016a). We reconstructed the history of SNC impact on Douglas-fir radial stem growth increment for each individual tree by taking the difference in the tree-ring chronologies between each tree and tree 358 (climate proxy) (Figure 9). The 20-year disturbance cycle of tree 355 is similar to the 25-year SNC cycle at Horse Creek Trail Lower in the Siuslaw National Forest (not shown). We attribute the 7.4-20 year disturbance cycles of the ancient Douglas-fir to SNC because the periodicities of low growth are similar to those of the SNC disease cycles of contemporary Douglas-fir and the stomata are possibly occluded. Drought stress is not a likely cause of the anomalously low growth patterns because soil moisture availability is not a primary limiting factor of growth of contemporary Douglas-fir in coastal Oregon (Lee et al., 2016b). Furthermore, the ground is unstable in this area and is prone to paleo-landslides due to erosional downcutting through stratigraphy caused by excessive precipitation, groundwater, and seismic activity (Hammond et al., 2009).

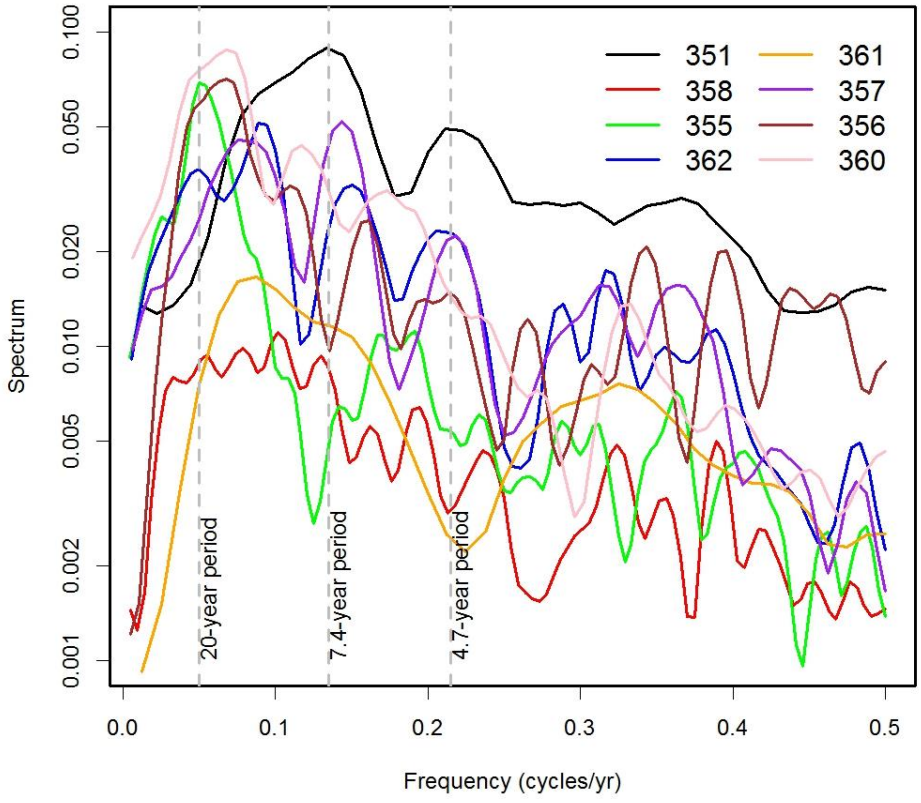

Figure 8. A comparison of the spectrum of the ancient Douglas-fir chronologies indicates a wide range of tree variability and pseudo-periodic tendencies. Tree 358 (in red) displays the least variability and has a broad primary periodicity ranging between 8 and 40 years. Tree 351 (in black) displays the greatest variability and has a primary periodicity of ~7.4 years and a secondary periodicity of ~4.7 years.

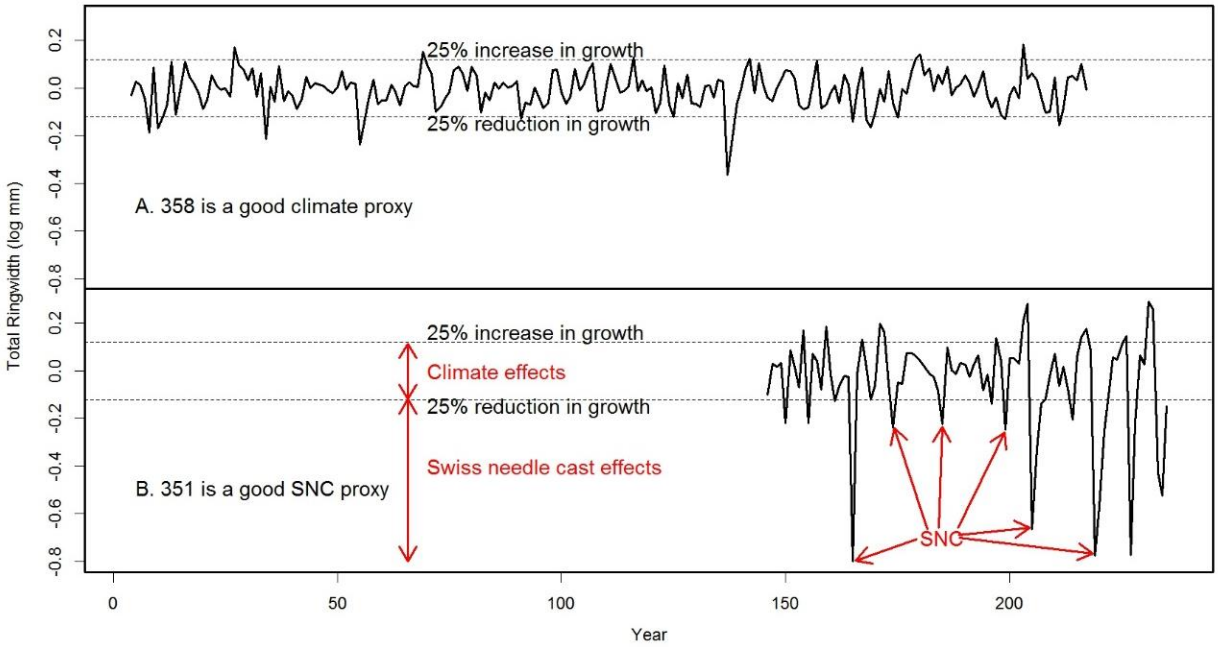

Figure 9. A) The chronology of tree 358 fluctuates between ±25% which is the range of growth response to climate. In comparison, B) the chronology of tree 351 represents a mixture of climate and Swiss needle cast (SNC) signals as indicated by the periodic patterns of anomalously low growth (red arrows). Drought stress was not a likely cause of the anomalously low growth patterns for tree 351 because growth reductions were not evident for tree 358 in these low growth years. These divergences in growth patterns are likely due to the inherent variability of SNC severity within a forest stand (Zhao et al., 2015).

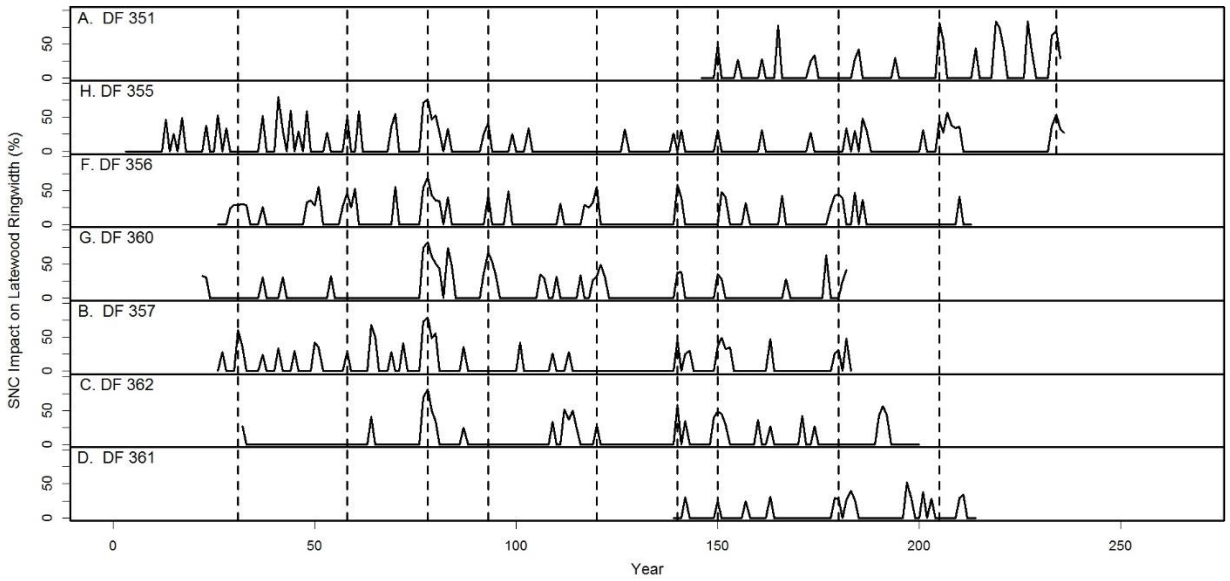

Figure 10. Tree-ring-based reconstruction of Swiss needle cast impacts on growth of ancient Douglas-fir trees near Eddyville, Oregon. Each host chronology was compared against the chronology for tree 358 (i.e., control) for purposes of reconstructing the forest disturbance history.

Conclusions

Differences in magnitude, duration, and periodicity between forest pests and diseases can be used as a means to reconstruct the disturbance history of each disturbance agent based on dendrochronological records. SNC impacts on Douglas-fir radial stem growth as seen in tree-rings display 6 to 30 year periodicities throughout the life of the tree. The higher frequencies in the disease cycle represent a lagged growth response to SNC caused by the infection of only the newly emerged needles at time of sporulation, followed by colonization of the needle over several years which is unique to *P. gaeumannii.* SNC impacts in the PNW date back to ~65K radioactive years BP as evidenced by the cyclical patterns of low growth in the master chronologies of ancient Douglas-fir that match the modern SNC disease cycles at coastal sites, and supported by the presence in the ancient needles of putative pseudothecia of *P. gaeumannii.* This long history of SNC predates forest management practices and improves our understanding of the climate factors affecting the causal fungus.

Acknowledgments

The authors thank William Rugh for his valuable assistance in scanning electron microscopy, Jay Simpkins, III for his valuable assistance with the transport of the ancient Douglas-fir logs to and from storage, and Caleb Naughton for his valuable assistance with preparation of the ancient Douglas-fir cross-sections for dendrochronological analysis. The research described in this article has been funded wholly by the U.S. Environmental Protection Agency. It has been subjected to review by the National Health and Environmental Effects Research Laboratory's Western Ecology Division and approved for publication. Approval does not signify that the contents reflect the views of the Agency, nor does mention of trade names or commercial products constitute endorsement or recommendation for use.

References

Hammond, C.M., Meier, D., and Beckstrand, D. 2009. Paleo-landslides in the Tyee Formation and highway construction, central Oregon Coast Range. In Volcanoes to Vineyards: Geological Field Trips through the Dynamic Landscape of the Pacific Northwest, O'Connor, J.E., Dorsey, R.J., and Madin, I.P. (eds.). Geological Society of America Field Guide 15, 481-494. doi: 10.1130/2009.fld015(23).

Hansen, E.M., Stone, J.K., Capitano, B.R., Rosso, P., Sutton, W., Winton, L., Kanaskie, A., and McWilliams, M.G. 2000. Incidence and impact of Swiss needle cast in forest plantations of Douglas-fir in coastal Oregon. Plant Disease **84**: 773-778.

Hood, I.A. 1982. *Phaeocryptopus gaeumannii* on Pseudotsuga menziesii in southern British Columbia. N. Z. J. For. Sci. **12**: 415-424.

Hood, I.A., and Kershaw, D.J. 1975. Distribution and infection period of *Phaeocryptopus gaeumannii* in New Zealand. N. Z. J. For. Sci. **5**: 201-208.

Lee, E. H., Beedlow, P. A., Waschmann, R. S., Burdick, C. A., Shaw, D. C. 2013. Tree-ring analysis of the fungal disease Swiss needle cast in Western Oregon coastal forests. Can. J. For. Res. 43, 677-690.

Lee, E. H., Beedlow, P. A., Waschmann, R. S., Cline, S., Bollman , M., Wickham, C., and Testa, N. 2016a. Tree-ring history of Swiss needle cast impact on Douglas-fir growth in western Oregon: Correlations with climatic variables. Proceedings of the 63rd Western International Forest Disease Work Conference, September 21-25, 2015, Newport, Oregon. (in press)

Lee, E. H., Beedlow, P. A., Waschmann, R. S., Tingey, D.T., Wickham, C., Cline, S., Bollman, M., and Carlile, C. 2016b. Douglas-fir displays a range of growth responses to temperature, water, and Swiss needle cast in western Oregon, USA. Agric. For. Meteor. (in press)

Maguire, D.A., Kanaskie, A., Voelker, W., Johnson, R., and Johnson, G. 2002. Growth of young Douglas-fir plantations across a gradient in Swiss needle cast severity. West. J. Appl. For. **17**: 86-95.

Manter, D.K., Bond, B. J., Kavanagh, K. L., Rosso, P. H., Filip, G. M. 2000. Pseudothecia of Swiss needle cast fungus, *Phaeocryptopus gaeumannii*, physically block stomata of Douglas fir, reducing CO2 assimilatio. New Phytologist 148, 481-491.

Manter, D.K., Reeser, P.W., and Stone, J.K. 2005. A climate-based model for predicting geographic variation in Swiss needle cast severity in the Oregon Coast Range. Phytopathol. **95**: 1256-1265.

Michaels, E., and Chastagner, G.A. 1984. Distribution, severity and impact of Swiss needle cast in Douglas-fir Christmas trees in western Washington and Oregon. Plant Disease **68**: 939-942.

Panyushkina, I., Van de Water P., Jull, A.T., Leavitt, S.W., Testa, N.R., Wiedenhoeft, A.J. 2012. High-resolution terrestrial MIS3 environment from trees encapsulated in landslide deposits of Oregon, USA. Abstract, Quaternary International 367-368.

Saffell, B.J., Meinzer, F.C., Voelker, S.L., Shaw, D.C., Brooks, R., Lachenbruch, B., McKay, J. 2014. Tree-ring stable isotopes record the impact of a foliar fungal pathogen on CO_2 assimilation and growth in Douglas-fir. Plant, Cell & Environment 37:1536-1547.

Stone, J.K., Capitano, B.R., and Kerrigan, J.L. 2008. The histopathology of *Phaeocryptopus gaeumannii* on Douglas-fir needles. Mycologia **100**: 431-444.

Zhao, J., Mainwaring, D.B., Maguire, D.A., and Kanaskie, A. 2011. Regional and annual trends in Douglas-fir foliage retention: correlations with climatic variables. For. Ecol. Manag. **262**: 1872-1886.

Zhao, J., Maguire, D.A., Mainwaring, D.B., and Kanaskie, A. 2015. The effect of within-stand variation in Swiss needle cast intensity on Douglas-fir stand dynamics. For. Ecol. Manag. **347**: 75-82.

Phylogeography and Hierarchical Population Structure of Two Lineages of *Phaeocryptopus gaeumannii* in the Pacific Northwest

Patrick Bennett and Jeffrey Stone
Department of Botany and Plant Pathology, Oregon State University

Introduction

The fungus *Phaeocryptopus gaeumannii*, the causal organism of Swiss Needle Cast (SNC) disease, exists as two distinct reproductively isolated subpopulations in the Pacific Northwest. These subpopulations, or lineages, differ in their geographic distributions in this region and their distributions may be correlated with disease severity in the Coast Ranges of Oregon and Washington. There is some evidence to suggest that these populations may also differ in virulence (Winton 2001). Studies of genetic diversity, population structure, and reproductive mode(s) may provide insights into the factors influencing disease severity, and the potential for evolutionary adaptation in this organism. The findings of these studies may be useful in developing management strategies to mitigate the impacts of this disease in Douglas-fir forests in western Oregon and Washington. The methods described below, as well as some preliminary analyses of genotype data from the isolates collected in 2014 were reported in the 2014 SNCC annual report, and are fully described in Bennett and Stone (2016).

Methods

Sample Collection

The genotypes included in the analyses presented here represent 482 isolates from 12 sites in the SNCC plot network in western Oregon Coast Range and two sites in the eastern Coast Range in southern Washington (Figure 1). Sites were sampled in a hierarchical fashion such that diversity and population structure could be described at various scales ranging from single needles to canopy sections within trees, to trees within sites, and also to sites within the larger geographic region. For a full description of the sampling strategies see Bennett and Stone (2016).

Isolations and Culturing

Foliage bearing pseudothecia of *P. gaeumannii* were attached to the lids of Petri dishes and incubated to allow spores to disperse onto the agar surface below. Single spores were isolated onto 2% malt agar plates and incubated for 2-6 months prior to DNA extraction.

DNA Extractions

Total genomic DNA was extracted from agar plugs containing mycelium of *P. gaeumannii*. The agar plugs were added to cryogenic vials containing glass beads, frozen in liquid nitrogen, and macerated using a mini beadbeater. The Qiagen DNeasy Plant Mini Kit (Qiagen, Hilden, Germany) was used to purify the DNA prior to microsatellite amplification.

Microsatellite PCR, Genotyping

The 10 microsatellite loci identified by Winton (2007) were amplified in three multiplex PCR reactions for each isolate. The primers were designed to target the conserved sequences flanking the microsatellite repeats, and a fluorescent dye label was added to the reverse primer such that each amplified product could be distinguished from other amplicons in the multiplex. The amplified microsatellite regions were then submitted to the OSU Center for Genome Research and Biocomputing (CGRB) for analysis. The sizes of the microsatellite amplicons were assessed using capillary electrophoresis on the ABI 3730 BioAnalyzer (Applied Biosystems). Allele sizes were determined using Applied Biosystems software GeneMapper 4.0 using the standard microsatellite method. The bins and panels were set to recognize allele size ranges described by Winton (2007). Allele sizes were confirmed visually for each locus for each isolate before exporting for analysis.

Data Analysis

The allele size data were assembled into multilocus genotypes and formatted with the aid of GenAlEx (Peakall and Smouse 2006, 2012) before importing to the statistical computing software *R* (R Core Team 2013) for use with *Poppr* 2.0 (Kamvar et al. 2014). Indices of genotypic diversity, as well as the unweighted pair-group-method using arithmetic means (UPGMA) were calculated with the *Poppr 2.0* package. Estimates of population structure such as K-means hierarchical clustering and discriminant analysis of principal components (DAPC) utilized Adegenet 2.0.0 (Jombart 2008). For a full description of the parameters used for the analyses of diversity, hierarchical AMOVA, UPGMA, and Mantel's test, see Bennett and Stone (2016). The number of genetic clusters selected for K-means clustering was determined by identifying the number of clusters that yielded the lowest value of the Bayesian Information Criterion (BIC). The clusters were then displayed on UPGMA dendrograms depicting genotypic similarities among 100 randomly selected isolates (Figure 4). For the discriminant analysis of principal components (DAPC), the maximum number of discriminant functions and principal components were retained given the sample size and displayed in scatter plot or density plot formats (Figure 3).

Results

The 2014 sampling yielded a total of 482 complete multilocus genotypes (MLGs) from 14 sites in the Coast Range in Oregon and Washington (Table 1). A total of 454 unique MLGs were identified, of which 358 isolates corresponded with previous identified allele profiles of Lineage 1, and 124 corresponded with profiles of Lineage 2 (Winton 2007).

Phylogeography

Our assessments of the distributions of the two lineages across the sites sampled in 2014 suggest that sites along the northern Oregon coast possess roughly equal proportions of Lineages 1 and 2 in sympatric populations (Figure 1, Table 1). These sites near Tillamook also exhibit the most severe symptoms of Swiss Needle Cast. Lineage 2 appears to be restricted to the

westernmost Coast Range in the northern parts of the state, as only a single isolate of Lineage 2 was recovered from sites greater than 25 miles east of Tillamook (N= 159, Figure 1, Table 1).

Table 1. Sample sizes, genotypic richness, and lineage distributions determined for 482 *P. gaeumannii* isolates from the 14 sites sampled for this study.

Site	N[a]	MLG[b]	eMLG[c]	L1[d]	L2[e]
T-01	49	48	9.96	23	26
T-02	10	9	9	4	6
T-03	17	17	10	9	8
T5-3	29	29	10	22	7
T5-5	21	20	9.79	17	4
T15-1	46	45	9.96	23	23
T15-2	24	23	9.84	10	14
T25-2	99	90	9.85	99	0
T25-3	60	59	9.97	59	1
F15-1	29	27	9.78	27	2
F15-3	15	15	10	4	11
F25-2	37	32	9.61	25	12
DNRL25-2	25	25	10	19	6
DNRS25-2	21	16	8.93	13	8
Total	**482**	**454**	**9.99**	**358**	**124**

[a]N= number of isolates; [b]MLG= number of multilocus genotypes; [c]eMLG= genotypic richness (expected number of multilocus genotypes in a rarefied sample of 10 isolates); [d]L1= abundance of Lineage 1; [e]L2= abundance of Lineage 2.

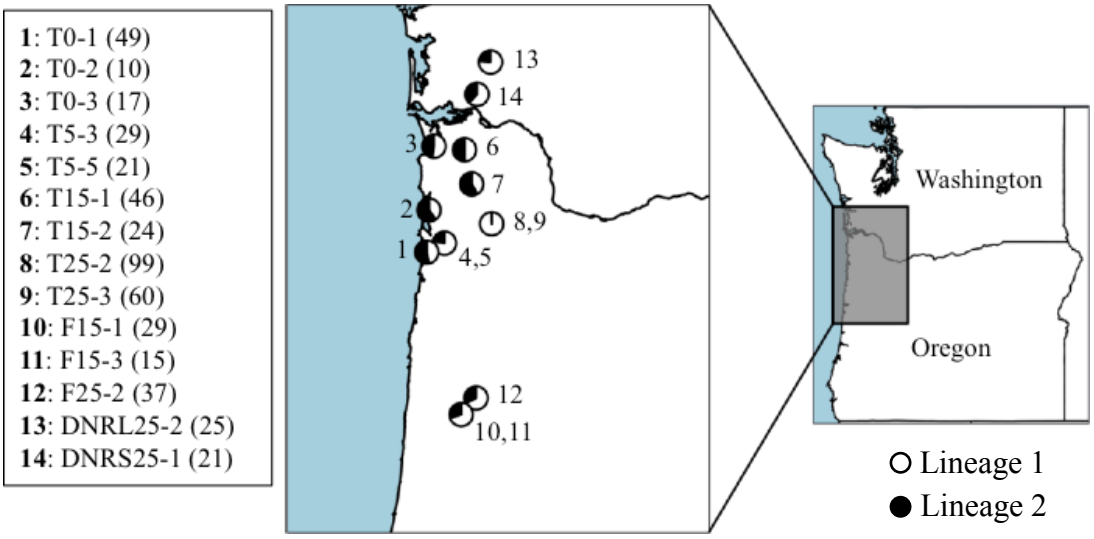

Figure 1. Map showing the relative distributions of two lineages of *P. gaeumannii* across the 14 sites sampled for this study. The numbers next to each pie chart correspond to the site names in the legend at left, and the numbers in parentheses indicate sample sizes. Lineage proportions from sites 4 and 5, 8 and 9, 10 and 11, respectively, were pooled and displayed as single pie charts to avoid overlap.

Genotypic Diversity

A comparison of genetic diversity among *P. gaeumannii* isolates from sites sampled in 2014 revealed that T-02 (Rockaway) had the least diversity of all sites based on a rarefied sample of 10 isolates (*H*= 2.16, Table 2, Figure 2). Sites T25-2 and T25-3 had the greatest diversity (*H*= 4.43, 4.07, respectively) of all sites sampled in 2014. Genotypic diversity was also compared between rarefied samples of isolates from the two reproductively isolated lineages. Isolates belonging to Lineage 1 had significantly higher diversity (*H=5.78)* than those of Lineage 2 (*H=4.76)* (Table 2) (Bennett and Stone 2016).

Table 2. Diversity and heterozygosity measured for *P. gaeumannii* isolates from each sampling site (*N* = 10) and each lineage (*N* = 128).

Site	**H** [a]	**G** [b]	**λ** [c]	**H_e** [d]
T-01	3.864 (3.69, 4.04)	47.08 (42.0, 52.1)	0.979 (0.97, 0.99)	0.821
T-02	2.164 (1.79, 2.54)	8.333 (6.30, 10.37)	0.880 (0.79, 0.97)	0.749
T-03	2.833 (2.56, 3.11)	17.00 (14.3, 19.8)	0.941 (0.90, 0.98)	0.806
T5-3	3.367 (3.16, 3.57)	29.00 (25.5, 32.5)	0.966 (0.95, 0.98)	0.781
T5-5	2.979 (2.72, 3.23)	19.17 (16.0, 22.3)	0.948 (0.92, 0.98)	0.726
T15-1	3.799 (3.62, 3.97)	44.08 (39.3, 48.9)	0.977 (0.97, 0.99)	0.778
T15-2	3.120 (2.88, 3.36)	22.15 (18.8, 25.6)	0.955 (0.93, 0.98)	0.804
T25-2	4.433 (4.30, 4.57)	73.69 (65.1, 82.3)	0.986 (0.98, 0.99)	0.630
T25-3	4.071 (3.92, 4.22)	58.07 (52.8, 63.3)	0.983 (0.98, 0.99)	0.717
F15-1	3.272 (3.05, 3.50)	25.49 (21.8, 29.2)	0.961 (0.94, 0.98)	0.751
F15-3	2.708 (2.43, 2.99)	15.00 (12.5, 17.5)	0.933 (0.89, 0.98)	0.810
F25-2	3.409 (3.20, 3.62)	27.94 (23.6, 32.3)	0.964 (0.95, 0.98)	0.815
DNRL25-2	3.219 (2.99, 3.45)	25.00 (21.7, 28.3)	0.960 (0.94, 0.98)	0.787
DNRS25-1	2.714 (2.45, 2.98)	14.23 (11.5, 17.0)	0.930 (0.89, 0.97)	0.759
Total	6.089 (6.03, 6.14)	417.8 (401, 435)	0.998 (0.997, 0.998)	0.820
Lineage	**H**	**G**	**λ**	**H_e**
1	5.780 (5.71, 5.85)	303.7 (289, 318)	0.997 (0.996, 0.997)	0.728
2	4.764 (4.66, 4.87)	114.7 (107, 122)	0.991 (0.989, 0.993)	0.745
Total	6.089 (6.03, 6.15)	417.8 (400, 435)	0.998 (0.997, 0.998)	0.820

[a] H = Shannon-Weiner diversity index; [b] G = Stoddart and Taylor's index; [c] λ = Simpson's index;
[d] H_e = Nei's expected heterozygosity. Numbers in parentheses are 95% confidence intervals calculated by bootstrapping.

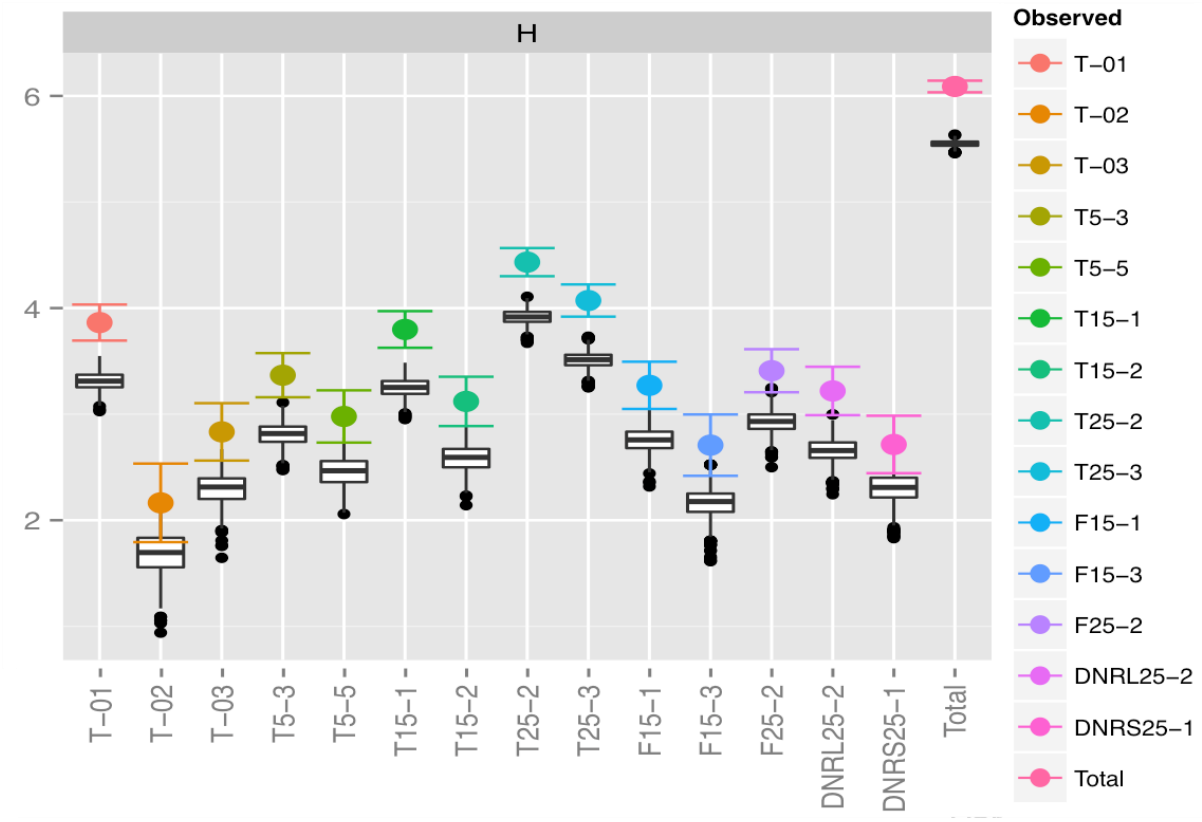

Figure 2. Comparison of *P. gaeumannii* genotypic diversity among sampling sites. *N* = 10. H= Shannon-Weiner diversity. The colored dots with error bars represent the observed statistics and their associated 95% confidence intervals. The black and white box and whisker plots represent the values estimated via bootstrapping with 1000 replicates.

Population Structure

AMOVA The results of our hierarchical AMOVA analysis revealed that most of the genetic variation occurred within individual trees (61.8%, Table 3). Approximately 22.7% of the variation could be explained by differences between the lineages, and the lineages were strongly and significantly differentiated genetically (Φ = 0.227, p = 0.001). While genetic variation among sampling sites accounted for only a small proportion of the total variance (4.719%), sites were weakly, but significantly, differentiated from one another (Φ = 0.061, p = 0.001). The genetic variation among isolates obtained from individual trees within each sampling site accounted for approximately 10.8% of the total variance, and isolates were moderately differentiated from one another (Φ= 0.148, p = 0.001).

Table 3. Table summarizing the results of the analysis of molecular variance (AMOVA) performed with the 454 *P. gaeumannii* isolates possessing unique MLGs.

Hierarchical Level	Variance (%)	Φ	p *
Φ_{LT} (between lineages)	22.671	0.227	0.001
Φ_{SL} (among sites within lineages)	4.719	0.061	0.001
Φ_{TS} (among trees within sites)	10.772	0.148	0.001
Φ_{TT} (within trees)	61.838	0.382	0.001

* p-Value was obtained for the Φ statistic using a randomization test with 999 permutations.

Discriminant Analysis of Principal Components

When sites were analyzed as populations in the Discriminant Analysis of Principal Components (DAPC), a data transformation that maximizes between-population variance to highlight genetic differentiation, sites T-02 and DNRS25-1 were the only sites differentiated from all other sites sampled (Figure 3b). Coastal Tillamook sites such as T-01, T5-3, and T5-5 appeared to be differentiated from those further inland (T25-2, T25-3) (Figure 3b). The two lineages were also strongly differentiated from one another in a DAPC analysis (Figure 3a).

a)

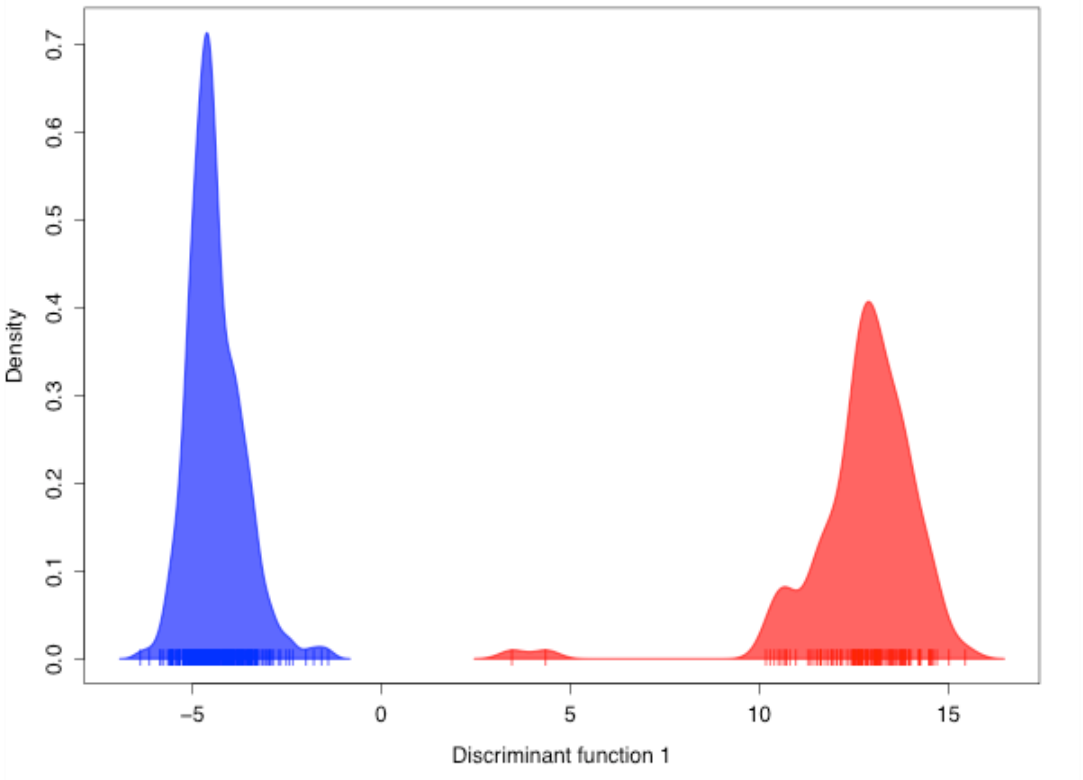

b)

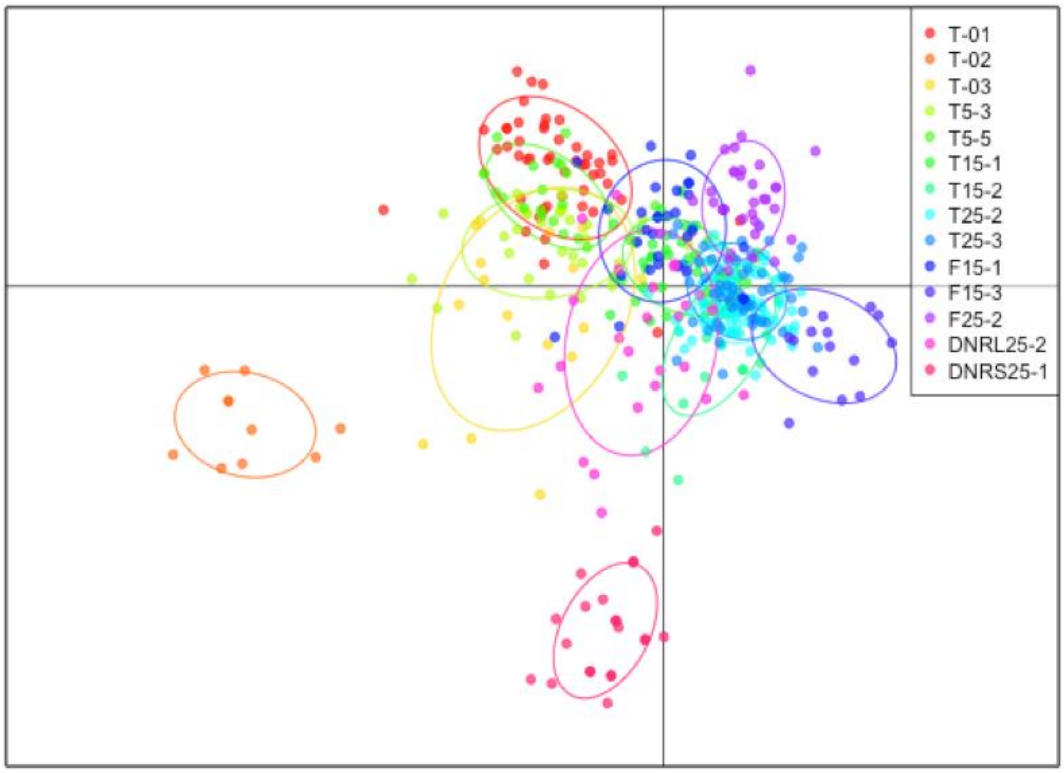

Figure 3. DAPC plots showing relationships among subpopulations. **a)** Colors correspond with lineages. Blue = Lineage 1, Red = Lineage 2. **b)** Colors correspond to sampling sites, and points correspond to individuals.

K-means Hierarchical Clustering

K-means clustering identified multiple genetic clusters within the 2014 sample population, however these groupings did not correspond to geographic sources or lineage designations. The optimal K-means model for this data set included 12 distinct genetic clusters (K=12). When these clusters were superimposed on a UPGMA dendrogram, individuals from different K-means genetic clusters grouped together on the same branches, suggesting a panmictic population structure with random mating (Figure 4a). If divergence between lineages were the only factor driving the population differentiation, one might expect K=2, or the existence of only two distinct genetic clusters corresponding to the reproductively isolated lineages, to be the optimal model. This was not the case, as there seems to be significant differentiation within both lineages. However, when the K-means clustering analysis was restricted to K=2 and again combined with UPGMA, the two K-means genetic clusters corresponded with the two lineages (Fig. 4b).

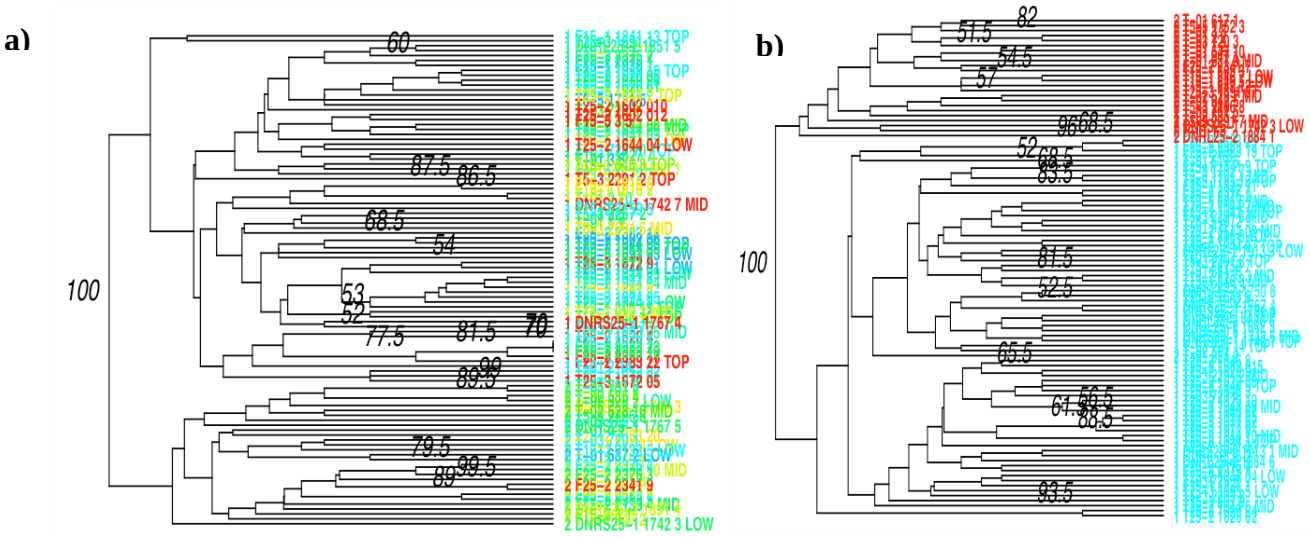

Figure 4. UPGMA dendrograms constructed with 100 randomly selected isolates. Colors represent genetic clusters identified using a K-means approach. Node labels represent bootstrap statistics for 1000 replicate trees. a) The optimum number of clusters (K=12) was chosen based on Bayesian information criterion (BIC). b) K=2 was chosen, and the two clusters correspond to the two lineages. Here, blue = Lineage 1, red = Lineage 2.

Linkage Disequilibrium

Estimates of the multi-locus Index of Association (I_A), such as $\bar{r}_d$, serve as a measure of linkage disequilibrium (LD) among loci (Agapow and Burt 2001). We used estimates of $\bar{r}_d$ to determine whether linkage exists between our microsatellite loci, and infer the mode(s) of reproduction occurring in *P. gaeumannii* populations. The null hypothesis is that no linkage exists among loci, or $\bar{r}_d$ is not significantly different from 0. An $\bar{r}_d$ value of 0 indicates that alleles assort randomly during sexual reproduction. Comparisons of $\bar{r}_d$ between a simulated null distribution and *P. gaeumannii* microsatellite genotypes indicate that the *P. gaeumannii* population structure is consistent with that of a clonal population or a population in which reproductively isolated subpopulations exist ($\bar{r}_d$ = 0.141, p = 0.001, Figure 5).

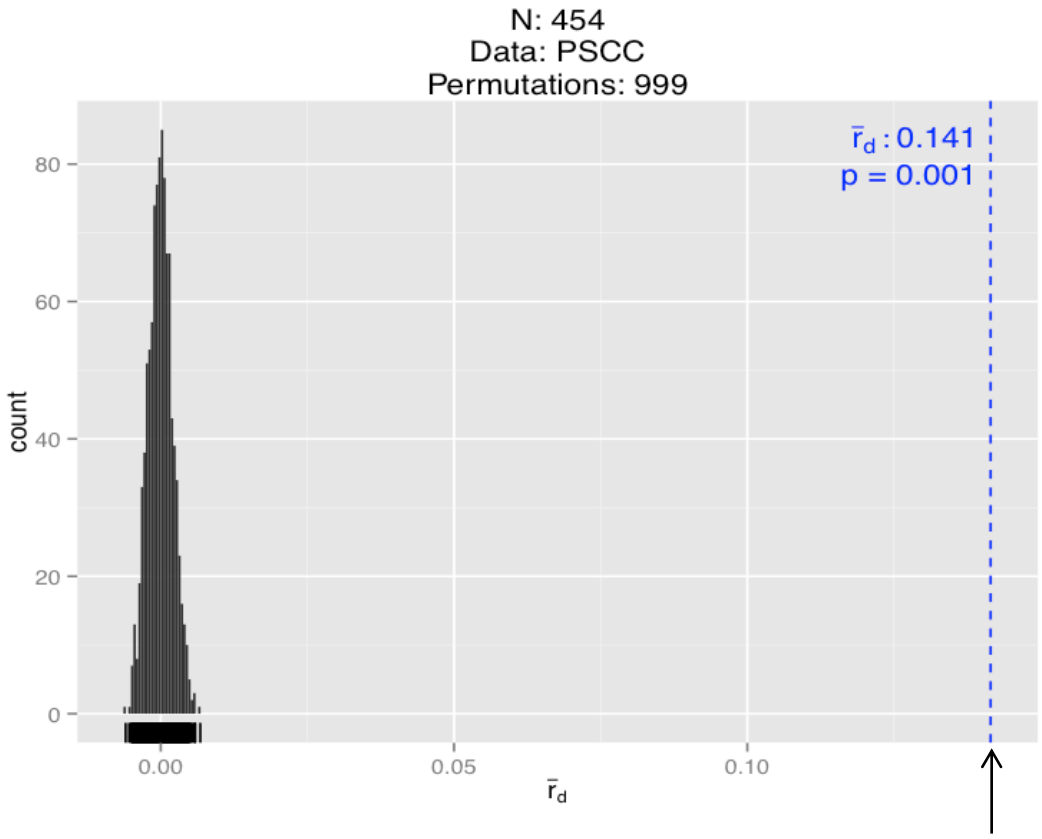

Figure 5. Plot showing observed estimates of linkage disequilibrium $\bar{r}_d$ (arrow and dotted line at right) compared with a simulated null distribution centered around 0 (histogram at left). The P-value was obtained by permuting the data 999 iterations. The data were clone censored such that only the 454 distinct genotypes are represented here.

Discussion

Phylogeography

The distributions of the two *P. gaeumannii* lineages appear to vary geographically, and genetic diversity within the two lineages also seems to have a geographic pattern. The occurrence of the two lineages in sympatric populations is intriguing, as the factors driving this divergence are not well understood. It could be that the two lineages have diverged within these sympatric populations and northwestern Oregon represents a region where the two lineages overlap, or alternatively there may have been a recent migration and mixing of two previously separate populations in northwestern Oregon.

Diversity

Measures of genetic diversity and variability based on molecular markers such as microsatellites can provide valuable insights into the life history and epidemiological dynamics of pathogenic fungi. Genetic diversity, along with population size and gene flow, are major factors used to assess the potential of phytopathogens to adapt to their hosts and develop mechanisms for increased virulence (McDonald and Linde 2002). In this sample population, genetic diversity varied as a function of geography, although this relationship was confounded by

the geographic distributions of the two lineages, which also differed along a latitudinal gradient from west to east in the northwestern part of the state. Sites with the lowest genotypic diversity were located on the western slopes of the Oregon Coast Range near Tillamook and Astoria and comprised roughly equal proportions of the two subpopulations. Sites with the greatest diversity, consisting almost exclusively of Lineage 1 isolates, occurred on the eastern side of the Coast Range approximately 25 – 35 miles east of Tillamook. This pattern, along with the observation that Lineage 1 is more diverse than Lineage 2, could indicate that the more eastern populations consist of native or endemic isolates of *P. gaeumannii*, while those found further west near the epidemic area consist of isolates that have recently migrated to, or emerged in, the area and thus are relatively uniform in their genetic composition. There are two possible explanations for these trends in diversity. A recent "founder" population of Lineage 2 isolates may have migrated to the northern coast of Oregon from endemic populations further south, or individuals with favorable characteristics that provided some evolutionary advantage may have been favored by natural selection and were thus driven to occupy a larger portion of the populations in the coastal epidemic area. Each of these scenarios, or a combination of the two, could result in drastically decreased genotypic diversity of isolates from sites in the SNC epidemic zone compared to endemic populations outside of this area.

Population Structure

Due to the hierarchical sampling methods with which the foliage samples were collected, the population genetic structure of our sample isolates could be described in a similar hierarchical fashion. The analysis of molecular variance (AMOVA) aimed to describe the variation in microsatellite genotypes within and among various levels of population hierarchy such that gene flow and genetic differentiation could be inferred. The results of the AMOVA suggest that site-level populations are genetically differentiated to some extent, indicating that local adaptation has occurred. However, across all sites there is a general panmictic population structure due to dispersal and gene flow within the region.

Much of the genetic variance in the microsatellite genotypes could be explained by the existence of the two lineages, or subpopulations. This resulted in a large Φ_{LT} value in the AMOVA analysis, indicating strong differentiation and a lack of gene flow. Similarly, the clear separation between the two lineages in the DAPC plot (Figure 3b) is likely due to divergence in the microsatellite genotypes due to reproductive isolation. This result supports the findings of the hierarchical AMOVA. These factors support the assertion that the two lineages are reproductively isolated and may be undergoing speciation.

The differentiation of sites T-02 and DNRS25-1 in the DAPC ordination is likely due to the presence of a rare allele(s) that occur in few other populations. While this may be the result of random variation, it could also indicate that these populations consist of a high proportion of some well-adapted individuals that possess similar genotypes. Because T-02 is in an area that has particularly severe disease, the latter possibility is intriguing. Site T-02 also had the lowest index

of diversity for all sites. This observation is consistent with descriptions of "epidemic" population structure, and previous observations by Winton et al. (2006), in which sites of disease outbreak are dominated by one or a few genotypes that are unique to the isolates responsible for the outbreak (Maynard Smith et al. 1993).

A K-means clustering algorithm was used to assign each isolate to a genetic cluster based on allelic similarities without any *a priori* knowledge of lineage designation, geography, or genetic differentiation. When K-means clustering is combined with the UPGMA analyses, factors influencing population structure such as reproductive mode(s) and gene flow can be inferred. The arrangement of isolates from K-means clusters on the branches of a UPGMA dendrogram allowed for the inference of gene flow as well as reproductive mode. If the sample isolates were mating only within sites, with no transfer of genetic material (spores) between sites, the K-means clusters would correspond perfectly with sampling sites. The results of our analyses suggest panmixia, a condition in which there is a lack of barriers to gene flow between sites resulting in a relatively homogeneous distribution of genetic variation across the sample sites. When this analysis was restricted such that K=2, the arrangements of clusters on the branches of the UPGMA dendrogram were consistent with assortative mating and reproductive isolation between the lineages (Figure 4b).

Analyses of genotypic diversity and population structure indicate that populations of *P. gaeumannii* are capable of reproduction through homothallism, a form of self-fertilization where sexual reproduction occurs in a single individual. Although uncommon, there were several occurrences of isolates sharing identical multilocus genotypes within the same site that were likely the result of homothallic reproduction. Of 482 total isolates there were 454 distinct genotypes (Table 2), i.e. 94.2% of isolates had unique MLGs resulting from heterothallic reproduction. In heterothallic populations where recombination occurs exclusively between individuals with dissimilar genotypes via random mating, alleles are inherited independently at each locus. In populations where homothallism or asexual reproduction predominates, or where reproductively isolated subpopulations exist, there may be a non-random association of alleles in multilocus genotypes.

There is no evidence to suggest that *P. gaeumannii* reproduces asexually, and thus its populations do not consist of clones, though they exhibit a population substructure in which alleles do not pair randomly. The high value of $\bar{r}_d$ likely reflects high linkage disequilibrium resulting from the presence of reproductively isolated subpopulations (ie: "lineages") within the larger *P. gaeumannii* population. This organism reproduces only via sexual reproduction (asci/ascospores), though the effects of population subdivision as well as the ability to reproduce through homothalism influence the genetic structure of its populations. Information about reproductive modes and reproductive isolation are useful in determining the potential for local adaptation and evolutionary capacity, and are essential for a thorough understanding of the *P. gaeumannii* disease cycle.

References

Agapow P-M., Burt A. Indices of multilocus linkage disequilibrium. *Molecular Ecology Notes 2001*, 1, 101–102.

Balloux, F., Lugon Moulin, N. The estimation of population differentiation with microsatellite markers. *Mol. Ecol.* 2002, *11*, 155–165.

Bennett, P., Stone, J. Assessments of Population Structure, Diversity, and Phylogeography of the Swiss Needle Cast Fungus (*Phaeocryptopus gaeumannii*) in the U.S. Pacific Northwest. *Forests* 2016, 7, 14.

Jombart, T. Adegenet: an R package for the multivariate analysis of genetic markers. *Bioinformatics* 2008, *24*, 1403-1405.

Kamvar Z.N., Tabima J.F., Grünwald N.J. Poppr: an R package for genetic analysis of populations with clonal, partially clonal, and/or sexual reproduction. *PeerJ* 2014, 2:e281.

Maynard Smith J, Smith NH, O'Rourke M, Spratt BG. How clonal are bacteria? *PNAS* 1993, *90*, 4384–4388.

McDonald, B.A., Linde, C. Pathogen Population Genetics, Evolutionary Potential, and Durable Resistance. *Annu. Rev. Phytopathol.* 2002, 40, 349–79.

Oregon Department of Forestry. Swiss Needle Cast (SNC) Aerial Survey, 1996–2015. Avaliable online: http://www.oregon.gov/odf.

Peakall, R., Smouse P.E. Genalex 6: Genetic analysis in Excel. Population genetic software for teaching and research. *Mol. Ecol. Notes* 2006, *6*, 288–295.

Peakall, R., Smouse, P.E. Genalex 6.5: Genetic analysis in Excel. Population genetic software for teaching and research - An update. *Bioinformatics* 2012, *28*, 2537–2539.

R Core Team. R: A Language and Environment for Statistical Computing. R Foundation for Statistical Computing, Vienna, Austria. Avaliable online: http://www.R-project.org.

Stone, J.K., Capitano, B.R., Kerrigan, J.L. The histopathology of *Phaeocryptopus gaeumannii* on Douglas-fir needles. *Mycologia* 2008, *100*, 431–444.

Winton, L.M., E.M. Hansen, and J.K. Stone. Population structure suggests reproductively isolated lineages of *Phaeocryptopus gaeumannii*. *Mycologia* 2006, *98*, 781-791.

Winton, L.M.; Stone, J.K.; Hansen, E.M. Polymorphic microsatellite markers for the Douglas-fir pathogen *Phaeocryptopus gaeumannii*, causal agent of Swiss Needle Cast disease. *Mol. Ecol. Notes* 2007, *7*, 1125–1128.

Phytophthora in Western Conifers

Everett Hansen, Professor Emeritus
Department of Botany and Plant Pathology, Oregon State University

2015 brought an early spring after a mild winter and in the central Oregon Coast Ranges it also brought alarming foliage symptoms on Douglas-fir (Figure 1). It took several guesses, and a lot of surprise to come up with the causal agent(s): a new *Phytophthora*, and a *Rhizoctonia*! The *Rhizoctonia* webblight was first described in 1996 on Christmas trees (Reeser et al. 1996), then largely disappeared (Reeser et al. 2001). We hadn't suspected it capable of forest defoliation. But that is another, still unfolding, story. This is about *Phytophthora*. These water molds shouldn't have been a surprise either—there are 32 or more species described from Oregon forests (Hansen et al. 2012), and our mantra since the advent of Sudden Oak Death has been "Look up for *Phytophthora*!" But surely not in Douglas-fir!

Actually, the northwestern conifer *Phytophthora* story started with Douglas-fir, and *P. cinnamomi* (Roth and Kuhlman 1966). Lew Roth concluded that exciting episode with the statement "It is too cold in the winter when it is wet enough, and too dry in the summer when it is warm enough." *P. cinnamomi* remains a problem in landscapes that receive summer irrigation. But the climate is changing…….

Phytophthora lateralis on Port Orford cedar started in horticultural nurseries in the 1920s, and was carried to the forest near Coos Bay in about 1950. It is at once a too common story of the relentless invasion of an exotic pathogen facilitated by human activities, and the best example of integrated management of a destructive forest disease. The lateralis story continues to unfold in Taiwan, now thought to be the pathogen's ancestral home, and in Europe where it exhibits frightening aerial behavior (Figure 2).

Phytophthora became a major factor limiting nursery production of forest planting stock and the survival of outplanted trees in the 1970s (Figure3). As the harvest of western forests intensified, demand for planting stock for regeneration increased dramatically. Forest tree nurseries became large agricultural operations, with all of the pathogen problems associated with intensive agriculture, including *Phytophthora*. We were lucky, though- the *Phytophthora* species that plagued the irrigated nurseries were poorly adapted for forest survival (Hansen et al. 1980). Infected seedlings died when outplanted, but the pathogen didn't spread or even survive on the outplanting sites. The nursery story was repeated in Christmas tree plantations, with infested stock dying in the plantations. In these foothill sites, however, the *Phytophthora* species have persisted and continue to plague susceptible trees, especially *Abies* species.

The story is still more dramatic in other forest ecosystems. Several *Phytophthora* species are invasive and destructive on conifers around the world. *Phytophthora austrocedri* kills the indigenous *Austrocedrus chilensis* in Patagonia (Greslebin et al. 2007). Its epidemiology is very

reminiscent of *P. cinnamomi* in Australia and *P. lateralis* in SW Oregon. It is spread on equipment in the forest, and by free ranging cattle. The same pathogen showed up on the opposite side of the world, killing junipers in Britain, and threatening heritage stands of this endemic conifer. The iconic New Zealand kauri, *Agathis* in the Aracareaceae (Figure 4), is threatened by *P. agathidicida* (Weir et al. 2015). In 2005 *P. pinifolia* seemingly came from nowhere and erupted into a spectacular epidemic of foliage disease on radiata pine in Chile (Duran et al. 2008). As quickly as it appeared the disease subsided, leaving many unanswered questions. *P. ramorum* is familiar to us, on tanoak and other hardwood trees and shrubs. We know that Douglas-fir and some other western conifers are susceptible in favorable environments and with high inoculum, but disease is limited to a twig blight in our forests (Figure 5). In Great Britain, however, again for reasons unclear, it exploded into a devastating epidemic in mature larch plantations. As these examples show, we should not be complacent about *Phytophthora* and our ecologically and economically irreplaceable conifers. The unfolding story of *P. pluvialis* in Douglas-fir is case in point.

Phytophthora pluvialis was first reported as a distinct species in 2011, isolated occasionally from tanoak and from raintraps in mixed forests in SW Oregon. Shortly on the heels of its formal description, and posting of its partial DNA sequence on GenBank (Reeser et al. 2013) pathologists in New Zealand recognized it as cause of the disease they were calling red needle cast in radiata pine, and in Douglas-fir plantations growing adjacent to the pine (Dick et al. 2014). This report in turn triggered us to look for *P. pluvialis* in our own Douglas-fir plantations, and we found it (Hansen et al. 2015)! At first there was no association with obvious disease symptoms, but that changed in the early spring of 2015.

In our one year's experience, symptoms of red needle cast of Douglas-fir in Oregon appeared in February. The disease was marked by dramatic foliage reddening and unseasonal needle fall, with many needles dropping while still green. Individual needles were often mottled chlorotic (Figure 6). Sporangia were observed emerging from a symptomatic needle. *P. pluvialis* was isolated on selective medium from 10-80% of fallen needles in many cases, although the situation was complicated by a simultaneous epidemic of foliar web blight, caused by a *Rhizoctonia* species (Figure 7). Disease symptoms were observed and *P. pluvialis* was isolated broadly in the central Oregon Coast Range and occasionally in the Cascade foothills.

Defoliation symptoms were most frequently noted on stand edges, often south-facing. Defoliation often extended in an inverted "V" from near the ground into the upper crown of the tree. By April and May affected branches on many trees were bare of needles, although at least many buds were unaffected and produced new growth in May. The resulting "tufted" appearance of severely defoliated trees became the lasting symptom visible through the year. We await 2016 with bated breath. Will red needle cast pick up where it left off in 2015, or is the disease going to be sporadic, dependent on particular microsites and weather patterns?

References

Dick M.A., N.M. Williams, M. Bader, J. Gardner, L.S. Bulman. 2014. Pathogenicity of *Phytophthora pluvialis* to *Pinus radiata* and its relation with red needle cast disease in New Zealand. New Zealand Journal of Forestry Science 44:1-12.

Duran A, Gryzenhout M, Slippers B, Ahumada R, Rotella A, Flores F, Wingfield, B.D, Wingfield, M.J.. 2008. *Phytophthora pinifolia* sp. nov. associated with a serious needle disease of *Pinus radiata* in Chile. *Plant Pathol.* 57:715–27

Greslebin, A., E.M. Hansen and W. Sutton. 2007. *Phytophthora austrocedrae* sp. nov., a new species associated with *Austrocedrus chilensis* mortality in Patagonia (Argentina). Mycol. Res. 111:308-316.

Hansen, E.M., L.F. Roth, P.B. Hamm, and A.J. Julis. 1980. Survival, spread, and pathogenicity of *Phytophthora* spp. on Douglas-fir seedlings planted on forest sites. Phytopathology 70:422-425.

Hansen, E.M., P. Reeser, W. Sutton, L. Sims. 2012. Host and Habitat Index for *Phytophthora* Species in Oregon. 2: http://journals.oregondigital.org/ForestPhytophthora/article/view/3026

Hansen, E.M., P. Reeser, W. Sutton, J. Gardner and N. Williams. 2015. First report of *Phytophthora pluvialis* causing needle loss and shoot dieback on Douglas-fir in Oregon USA and New Zealand. Plant Disease 99:727.

Pratt, R.G., L.F. Roth, E.M. Hansen, and W.D. Ostrofsky. 1976. Identity and pathogenicity of species of *Phytophthora* causing root rot of Douglas-fir in the Pacific Northwest. Phytopathology 66:710-714.

Reeser, P., W. Sutton, and E. Hansen. 2013. *Phytophthora pluvialis*, a new species from mixed tanoak-Douglas-fir forests of western Oregon U.S.A. *North American Fungi* 8(7): 1-8. http://dx.doi: 10.2509/naf2013.008.007

Reeser, P.W., Putnam, M.L., Winton, L. M., Nesson, M. 2001. Characterization of a *Rhizoctonia*-like fungus causing web-blight of Douglas-fir and true fir Christmas trees. Phytopathology 91:S189.

Roth L.F. & Kuhlman E.G. 1966. *Phytophthora cinnamomi*, an unlikely threat to Douglas-fir forestry. *For. Sci.* 12:147-159.

Weir B.S., Paderes E.P., Anand N., Uchida J.Y., Pennycook S.R., Bellgard S.E., Beever R.E. 2015. A taxonomic revision of *Phytophthora* Clade 5, including two new species, *Phytophthora agathidicida* and *P. cocois*. Phytotaxa 205: 21–38. http://dx.doi.org/10.11646/phytotaxa.205.1.2

Figure 1. Symptoms of red needle cast and webblight on Douglas-fir in the Oregon Coast Range, early spring 2015.

Photo credit: E. Hansen

Figure 2. Symptoms of aerial infection by *Phytophthora lateralis* on *Chamaecyparis lawsoniana* in Scotland.

Photo credit: E. Hansen

Figure 3. Phytophthora root rot in Douglas-fir nursery established on poorly drained agricultural land.

Photo credit: E. Hansen

Figure 4. Kauri dieback caused by *Phytophthora agathadicida*.

Photo credit: E. Hansen

Figure 5. Twig dieback of Douglas-fir caused by *Phytophthora ramorum*.

Photo credit: E. Hansen

Figure 6. Symptoms of red needle cast on Douglas-fir needles.

Photo credit: E. Hansen

Figure 7. Webblight on Douglas-fir, caused by *Rhizoctonia*.

Canopy Ecology of Swiss Needle Cast in Young, Mature, and Old-growth Douglas-fir Forests in Western Oregon

Yung-Hsiang Lan[1] and Dave Shaw[2]
[1] Forest Ecosystems and Society, Oregon State University, [2] Forest Engineering, Resources, and Management, Oregon State University

Swiss Needle Cast (SNC) is a foliar disease afflicting Douglas-fir (*Pseudotsuga menziesii* (Mirb.) Franco) trees caused by the fungus *Phaeocryptopus gaeumannii* (T.Rohde) Petrak. SNC is causing growth loss in forests across coastal Oregon and Washington, and is thought to be one of the largest threats to Douglas-fir plantation management in these regions. The fungal reproductive structures, pseudothecia emerge from within the needle and subsequently grow into the stomata. This fungus blocks gas exchange, thereby reducing photosynthetic rates and productivity of Douglas-fir trees. Disease severity varies with canopy position in younger forests, with the greatest severity in the upper crown (Manter *et al.* 2003, Shaw *et al.* 2014). This is unusual for a foliar disease because disease severity is usually greatest in the most humid portion of the crown, which for conifers is typically the lower and inner portion of the crown.

The structural complexity of canopies is well known as having differences in microclimate and nutrient allocation depending upon position in the canopy (Schoettle & Smith 1998, Leal & Thomas 2003). As forests mature, vertical and structural complexity increase, and diversity of biota inhabiting canopies increases (Franklin *et al.* 1991). However, disease patterns in canopies are poorly understood. What does SNC look like on young and mature Douglas-fir trees? SNC has been well studied in young stands but there is still uncertainty regarding the influence of foliar nitrogen on disease severity. In addition, SNC data from mature and old-growth forests is rare, and therefore understanding of the disease ecology in older forests is not well known. We are involved in studies exploring the relationship between disease severity of SNC and canopy position, climate, and foliage nitrogen in young, mature and old-growth forests. These studies will provide a database for mature and old-growth trees serving as background information for future research, especially for those studies regarding climate change issues.

Some researchers have suggested that climate and environmental factors are related to SNC disease severity. Temperature and moisture are important requirements for fungus survival and reproduction. Capitano (1999) found that 18˚C was the most appropriate temperature for *Phaeocryptopus gaeumannii* to germinate (in lab treatments). In the field, spring and winter temperatures, as well as summer precipitation were important factors affecting disease severity. Although anecdotal observations suggest that SNC is more severe in young trees than in mature trees, this has not been measured quantitatively. In particular, the effects of leaf wetness, canopy structure, and canopy microclimate on the severity of SNC are poorly understood. We will study the relationships between canopy structure, microclimate, and SNC severity (percent of stomata occluded by pseudothecia) among different ages of Douglas-fir forests. We hypothesize that the

complexity of crown structure in mature forests may relate to microclimatic differences within canopy. We expect a greater diversity in branch structures and a greater variety of micro-environments within the canopy of mature forests as compared to young forests, which may be related to SNC disease severity. We also propose that the moisture on needle surfaces is positively related to infection susceptibility.

However, nitrogen may also be an important factor for SNC presence. Kavanagh *et al.* (2003) suggested that *Phaeocryptopus* may acquire nitrogen and carbon from apoplastic spaces within Douglas-fir needles. They found a positive association between the concentration of nitrogen in conifer needles and in the pseudothecia of the fungus, but there was only a weak relationship between carbon in pseudothecia and infected needles. Kavanagh *et al.* (2003) hypothesized that fertilization might be associated with increasing nitrogen availability in Douglas-fir forests and the interaction between fungus and host trees. However, Kavanagh *et al.* (2003) found no strong relationships between fertilization and levels of ^{13}C or ^{15}N in pseudothecia of *Phaeocryptopus gaeumannii*. So, is nitrogen concentration in foliage correlated with either the incidence (percent of needles infected by *Phaeocryptopus gaeumannii*) or severity of SNC in young-growth Douglas-fir stands? We hypothesize that foliage and soil nitrogen will be positively correlated with SNC severity. We will use the Swiss Needle Cast Cooperative Research and Monitoring plot network (http://sncc.forestry.oregonstate.edu/) to study young Douglas-fir plantations in western Oregon, from southern Washington to northern California, and from coast stands to inland stands within 56 kilometers of the coast (Ritokova *et al.* 2014), including SNC severity data and nitrogen concentration in foliage and in soil. The complex vertical gradients in mature and older trees should allow us to test ideas about foliage disease distribution in a way that young stands do not provide. Is foliage nitrogen related to SNC in mature and old-growth Douglas-fir stand? Studying older sites in the coast range and in the Cascades in Oregon, we hypothesize the foliage nitrogen would be related to SNC severity, and expect there is a significant relationship between disease and nitrogen concentration both in coastal and inland area.

We hope our studies will provide insight into the ecology of foliage disease in the coastal Pacific Northwest of North America. Also, we hope to increase knowledge about the structural architecture and environment of mature forest canopies (i.e. crown structure and microclimate). In addition, we hope to discover the relationship between disease and climate using canopy station data, and ultimately make inferences on climate change impacts for Douglas-fir communities.

References

Capitano, B. (1999) The infection and colonization of Douglas-fir by *Phaeocryptopus gaeumannii*. M.Sc. thesis. Department of Botany and Plant Pathology, Oregon State University, Corvallis, Oregon.

Kavanagh, K., El-Hajj, Z., and Rose, C.L. (2003) The effect of nutritional status of Douglas-fir on *Phaeocryptopus gaeumannii*: evidence from foliar chemistry and stable isotopes. Swiss Needle Cast Cooperative Annual Report: p75-83.

Leal, D.B. and Thomas, S.C. (2003) Vertical gradients and tree-to-tree variation in shoot morphology and foliar nitrogen in an old-growth *Pinus strobus* stand. Canadian Journal of Forest Research, vol. 33(7), p1304-1314.

Manter, D.K., Winton, L.M., Filip, G.M., and Stone, J.K. (2003) Assessment of Swiss needle cast disease: temporal and spatial investigations of fungal colonization and symptom severity. Journal of Phytopathol, vol. 151: p344-351.

O'Neill, A.L., Kupiec, J.A. and Curran, P.J. (2002) Biochemical and reflectance variation throughout a Sitka spruce canopy. Remote Sensing of Environment 80: 134-142.

Richardson, A.D. (2004) Foliar chemistry of balsam fir and red spruce in relation to elevation and the canopy light gradient in the mountains of the northeastern United States. Plant and Soil 260: 291-299.

Ritokova, G., Shaw, D., Maguire, D., Mainwaring, D., Browning, J., Gourley, M., Filip, G., and Kanaskie, A. (2014) SNCC research and monitoring plot network. SNCC Annual Report: p.20-24.

Schoettle, A.W. and Smith, W.K. (1998) Interrelationships among light, photosynthesis and nitrogen in the crown of mature *Pinus contorta* ssp. *latifolia*. Tree Physiology 19: 13-22.

Shaw, D.C., Woolley, T., and Kanaskie, A. (2014) Vertical foliage retention in Douglas-fir across environmental gradients of the western Oregon coast range influenced by Swiss needle cast. Northwest Science, vol. 88: p23-32.

Forest Ecology and Management 347 (2015) 75–82

Contents lists available at ScienceDirect

Forest Ecology and Management

journal homepage: www.elsevier.com/locate/foreco

The effect of within-stand variation in Swiss needle cast intensity on Douglas-fir stand dynamics

Junhui Zhao [a], Douglas A. Maguire [b,*], Douglas B. Mainwaring [b], Alan Kanaskie [c]

[a] Arbor Research Collaborative for Health, Ann Arbor, MI, USA
[b] Department of Forest Engineering, Resources and Management, College of Forestry, Oregon State University, USA
[c] Oregon Department of Forestry, Salem, OR, USA

ARTICLE INFO

Article history:
Received 12 December 2014
Received in revised form 3 March 2015
Accepted 5 March 2015
Available online 24 March 2015

Keywords:
Swiss needle cast
Foliage retention
Diameter increment
Growth differentiation
Thinning guidelines

ABSTRACT

Swiss needle cast (SNC) is a foliar disease of Douglas-fir (*Pseudotsuga menziesii* (Mirb.) Franco) caused by the ascomycete *Phaeocryptopus gaeumannii* (Rohde) Petrak. The number of annual needle cohorts retained by a tree indicates SNC severity and associated growth losses. In previous studies growth losses have been predicted on the basis of plot-level foliage retention, and plot-level growth multipliers have been uniformly applied to all trees within a stand to simulate tree growth. In this analysis, the effects of within-stand variation in foliage retention on individual-tree growth impact and implied stand dynamics were analyzed. Models describing diameter increment of Douglas-fir were developed based on three different foliage retention ratings: (1) plot-level foliage retention; (2) tree-level foliage retention; and (3) a combination of plot-level foliage retention and the deviation of tree-level from plot-level foliage retention. Foliage retention at both the plot-level and tree-level was positively correlated with diameter increment, and a significant amount of additional variation in diameter growth was explained by the deviation of individual-tree foliage retention from the plot-level average. The SNC "effect" was assessed by comparing growth of trees with varying degrees of Swiss needle cast to growth of those that retained maximal amounts of foliage. Across all plots in the sampled population, the most severely affected dominant or co-dominant trees exhibited 30% diameter growth loss relative to trees of similar crown position with minimal SNC symptoms. Within a plot, diameter growth averaged about 12% higher on trees with the highest foliage retention relative to trees with the lowest foliage retention, implying that SNC intensifies stand differentiation. Rather than responding to SNC with proportionally uniform growth losses within a plot, these results suggest that individual trees tolerate or resist the disease differentially. Foliage retention should therefore be used as a criterion for selecting trees for removal during thinning operations in Douglas-fir stands with moderate to severe SNC.

1. Introduction

Swiss needle cast (SNC) is a foliar disease of Douglas-fir (*Pseudotsuga menziesii*) caused by the ascomycete *Phaeocryptopus gaeumannii* (Hansen et al., 2000). This pathogen causes premature loss of older foliage, resulting in needle longevity of only one year in the most severe cases, relative to a maximum of approximately four years in unaffected plantations of similar age and geographic location (Hansen et al., 2000; Maguire et al., 2002). Over the past 20 years, the Swiss needle cast epidemic in the Oregon Coast Range has significantly lowered productivity in affected Douglas-fir forests (Hansen et al., 2000; Maguire et al., 2002; Black et al., 2010). Aerial surveys conducted by the Oregon Department of Forestry annually since 1996 have detected fluctuating but gradually increasing areas in coastal Oregon with detectable SNC symptoms, amounting to 212,265 ha in 2013 (Kanaskie and McWilliams, 2013). Fruiting bodies of the fungal pathogen interfere with foliage gas exchange by physically blocking Douglas-fir stomata, thereby reducing or halting photosynthesis and leading to premature needle abscission (Manter et al., 2005). The mechanisms leading to growth decline of Douglas-fir include loss of photosynthetic surface area (Weiskittel et al., 2006) and physiological disruption of surviving foliage (Manter et al., 2005).

In plantations with severe symptoms of SNC, growth losses and reduced tree vigor have been evident (Maguire et al., 2002). Maguire et al. (2011) found that maximum periodic annual growth losses in cubic volume ranged between 36% and 59% in north coastal Oregon among four separate growth periods between

* Corresponding author at: FERM, College of Forestry, Oregon State University, Corvallis, OR 97331, USA. Tel.: +1 541 737 4215.
E-mail address: doug.maguire@oregonstate.edu (D.A. Maguire).

http://dx.doi.org/10.1016/j.foreco.2015.03.010
0378-1127/

1998 and 2008. In New Zealand, Douglas-fir enjoyed a disease-free period for a number of years after its introduction, providing a basis for estimating growth reductions after the appearance of SNC in 1959. Kimberley et al. (2011) estimated that average growth loss reached 25% for mean top height increment, 27% for basal area increment, and 32% for stem volume increment since 1959. Black et al. (2010) assessed the impacts of SNC by tree-ring analysis of mature Douglas-fir and western hemlock trees in the western Oregon Coast Ranges, concluding that radial growth was reduced by as much as 85% since 1984.

The negative effects of SNC-imposed reductions in foliage retention on Douglas-fir growth is well established, but most studies to date have quantified this relationship at the plot-level. To our knowledge the effects of tree-to-tree variation in foliage retention on stand dynamics and relative tree growth rates have not been quantified. Johnson (2002) observed variation in family tolerance to SNC in 11-year-old Douglas-fir progeny, but foliage retention was not a significant predictor of diameter or height growth. However, foliage retention was measured as the percentage of 2-yr-old or 3-yr-old needles rather than the number of retained annual needle cohorts (Johnson, 2002).

The question of whether within-stand variation in foliage retention induced by SNC has altered stand dynamics by differential effects on diameter increment has not been addressed directly. However, a tree-level analysis of diameter growth within commercially-thinned stands infected with SNC found marginally significant evidence of an interaction between foliage retention and tree diameter, suggesting that larger diameter trees maintain a higher percentage of their full growth potential than smaller trees as foliage retention decreased (Mainwaring et al., 2005). Whether smaller trees had lower levels of foliage retention than the larger trees in the same stand is unknown, leaving open the question of whether variation in foliage retention within a stand influences stand dynamics.

The goal of this study was to gain a better understanding of stand dynamics within SNC-infected stands, particularly by quantifying the effects of SNC on any departures from normal growth differentiation patterns among individual trees. The rate and intensity of these departures would have implications for the timing of thinnings and the selection of trees for removal. Similarly, shifts in the intensity of differentiation would have implications for growth and yield projections, harvest schedules, and harvested tree and log dimensions. The specific objective of this study therefore was to test the hypothesis that tree-to-tree variation in foliage retention (SNC severity) has intensified differentiation of Douglas-fir growth rates. If this hypothesis proves correct, then tree-level foliage retention should account for significantly more of the variation in tree growth than plot-average foliage retention, and the dynamics of SNC-impacted stands are characterized by more extreme differentiation in growth rate and size distribution than unimpacted stands. Three steps were followed in pursuit of this objective: (1) separate diameter increment models were developed for Douglas-fir based on plot-level versus individual tree-level foliage retention; (2) diameter increment models were developed for Douglas-fir that included both plot-level foliage retention and the deviation of individual-tree retention from this plot-level retention; and (3) the relative proportion of variation in Douglas-fir diameter increment explained by plot-level foliage retention, tree-level foliage retention, and the combination of plot-level foliage retention and tree-level deviations from the plot average were quantified and assessed graphically.

2. Methods

The target population for the Swiss Needle Cast Cooperative (SNCC) Growth Impact Study was 10- to 30-yr-old Douglas-fir plantations in north coastal Oregon (Maguire et al., 2002, 2011). A list of all 10- to 30-yr-old Douglas-fir stands was first compiled in 1996, with geographic bounds defined by Astoria to the north (N46°11′, W123°50′), Newport to the south (N44°38′, W124°04′), the Pacific Ocean to the west (W124°05′), and the crest of the Oregon Coast Ranges to the east (W123°30′). Over the last 40 years in this region, the mean January minimum temperature was 0 °C and the mean July maximum temperature was 25 °C. Total annual precipitation averaged 150–300 cm, with approximately 70% of the total falling between October and March.

A set of 76 stands was randomly selected from this list with probability proportional to area. The selected sample stands represented a range of SNC severity indicated by a minimum plot-level foliage retention of 1.01 years and a maximum of 3.85 years. The assumption made in this analysis was that SNC was the primary influence on foliage retention. Other factors known to influence foliage retention (Maguire et al., 2011) were controlled to some degree by specifying the target population, as well as by including the covariates described below.

A single, permanent plot was established in each sampled stand in the late winter/early spring of 1998. Plots were square, 0.08 ha in area (31.7 × 31.7 m), and centered on the fifth point of an ODF (Oregon Department of Forestry) transect established in spring 1997 (retrospective plots reported by Maguire et al. (2002) were centered on the third point). On each measurement plot, all trees with diameter at breast height (dbh) greater than 4 cm were tagged and measured (nearest 0.1 cm) at a height of 1.37 m. In addition, at least 40 Douglas-fir (largest 10 and smallest 4 by dbh, and the remaining 26 evenly distributed across the dbh distribution) were measured for total height (nearest 0.01 m) and height to crown base (nearest 0.01 m) at time of plot establishment. After two, four, and six growing seasons, all trees were remeasured for dbh, and all undamaged trees from the original height subsample were remeasured for total height and height to crown base. Some plots contained a significant amount of western hemlock (*Tsuga heterophylla* (Raf.) Sarg.), as well as various broadleaved species, most commonly cascara (*Rhamnus purshiana* D.C.), red alder (*Alnus rubra* Bong.), and red elderberry (*Sambucus racemosa* L.). Other conifers that occurred less frequently included Sitka spruce (*Picea sitchensis* (Bong.) Carr.), western redcedar (*Thuja plicata* Donn.), noble fir (*Abies procera* Rehder), and grand fir (*Abies grandis* (Dougl.) Forbes). Other hardwood species included bitter cherry (*Prunus emarginata* (Dougl.) Walp.) and bigleaf maple (*Acer macrophyllum* Pursh).

Ten dominant or codominant trees on each plot were also scored for SNC at time of plot establishment in 1998, and just prior to bud break in years 1999–2004. Needle retention of individual trees was visually estimated by first dividing the live crown into thirds, with the base of the live crown defined as the lowest live branch. Secondary or lateral branches on a primary or main branch were then examined in the center of each third, and the average number of needle age classes present at time of sampling was estimated to the nearest 0.5 yr (Maguire et al., 2002). The needle retention of the tree was then estimated by averaging these values across crown thirds. Plot-level foliage retention was the average of the ten SNC-scored trees.

2.1. Variables in the model

Diameter increment models were developed from the ten individual Douglas-fir trees that had been scored for foliage retention within each plot and for each growth period that the tree survived without any top damage, resulting in 2469 separate measurements (Tables 1 and 2).

Separate diameter increment models for Douglas-fir were developed using each of three different estimates of foliage

retention: (1) Model 1: plot-level foliage retention (PlotFR); (2) Model 2: tree-level foliage retention (TreeFR); and (3) Model 3: combination of plot-level foliage retention and the difference between tree-level and plot-level foliage retention (DiffFR = TreeFR–PlotFR, Fig. 1). Variables from the following four classes of additional explanatory variables were also tested:

1. *Tree size*: diameter at breast height, DBH (cm); total height, HT (m); height to crown base defined as the lowest live branch, HCB (m); crown ratio, CR.
2. *Stand density*: trees per ha, TPH (trees/ha); average diameter and average height of the 100 largest (by diameter) trees per ha, D100 (cm) and H100 (m), respectively; stand density index, SDI; quadratic mean diameter, QMD (cm); basal area, BA (m^2/ha); crown competition factor (Krajicek et al., 1961) using the maximum crown width equations described by Paine and Hann (1982), CCF (%).
3. *Tree social position*: basal area in trees with DBH greater than the subject tree, BAL (m^2/ha); crown competition factor in trees with DBH greater than the subject tree, CCFL (%).
4. *Site quality*: Bruce's (1981) site index, SI (m at 50 years).

In addition to the untransformed variables, the natural logarithm, square, and inverse of each were also tested.

2.2. Model development

The biological processes that influence tree growth are inherently non-linear. However, linear regression is a suitable tool for modeling growth curves if a linearizing relationship can be found between the key variables (Curtis, 1967) and biologically reasonable shapes are determined (Trasobares et al., 2004). Various linear and nonlinear regression models were fitted to the data to develop a series of equations describing diameter increment. Preliminary analysis revealed that nonlinear models tended to have more reasonable residual distribution as well as higher accuracy. Therefore, nonlinear regressions were adopted in this analysis.

Repeatedly measured growth and yield data are typically correlated, and they usually exhibit heteroskedasticity in model residuals as well (Gregoire, 1987). Preliminary analysis revealed that model residuals were not homogeneous and that the residual variance increased monotonically with increasing tree diameter. Although the logarithmic transformation was examined to correct for heteroskedasticity (Calama and Montero, 2005; Yang et al., 2009), the models continued to show a trend of increasing residual variance with tree diameter. Therefore, weighted nonlinear regression was used to homogenize the variance in residuals. A weight of DBH^{-m} was tested, with $m = 0, 1, 2, 3$, and 4.

To account for correlations among trees within a plot, a non-linear model with a random plot effect was estimated with PROC NLMIXED in SAS version 9.2 (SAS Institute 2008). A set of promising model forms was selected by a combination of all-subsets exploratory analyses on linearized models and numerous existing nonlinear diameter growth models. The final model for each of the three representations of foliage retention were nonlinear and chosen on the basis of residual analysis, minimization of AIC, and biological interpretability. Alternative variance–covariance matrices, including unstructured, compound symmetry, Toeplitz, and AR(1) structures, were tested on the linearized form of the final non-linear model. All parameter estimates were required to be significantly different from zero at $\alpha = 0.05$.

Table 1
Means and ranges of tree-level attributes from the Swiss needle cast growth impact study. See text in Section 2 for variable definitions.

Variable	Unit	*N*	Mean	Std Dev	Minimum	Maximum
dbh	cm	2469	26.77	8.23	3.90	57.30
ht	m	2469	16.78	4.88	3.32	35.40
hcb	m	2469	4.20	3.13	0.00	19.69
BAL	m^2/ha	2469	8.90	8.85	0.00	49.31
CCFL	%	2469	46.04	45.26	0.00	289.88
CR	–	2469	0.77	0.14	0.26	1.00
TreeFR	years	2469	2.39	0.58	0.67	4.77
DiffFR	years	2469	−0.01	0.40	−1.59	1.71

Table 2
Means and ranges of plot-level attributes from the Swiss needle cast growth impact study. See text in Section 2 for variable definitions.

Variable	Unit	*N*	Mean	Std Dev	Minimum	Maximum
SI	m	282	43.69	7.12	13.80	63.10
PlotFR	years	282	2.38	0.45	1.01	3.85
Age	years	282	22.67	5.93	11.00	38.00
D100	cm	282	29.44	8.08	5.58	49.00
H100	m/ha	282	17.25	4.76	4.01	34.14
BA	m^2	282	27.65	10.72	1.71	65.37
CCF	%	282	184.44	63.25	38.33	539.64
TPH	trees/ha	282	1121.57	548.90	345.80	4705.35
QMD	cm	282	18.71	5.76	4.12	35.76
SDI	25-cm trees/ha	282	611.98	213.07	69.20	1298.65
Douglas-fir BA	m^2/ha	282	21.77	9.50	0.62	48.35
Other conifer BA	m^2/ha	282	4.19	6.99	0.00	46.98
Hardwood BA	m^2/ha	282	1.70	2.66	0.00	17.29
% Douglas-fir BA	%	282	80	23	12	100
Douglas-fir TPH	trees/ha	282	118.59	14.33	37.05	135.85

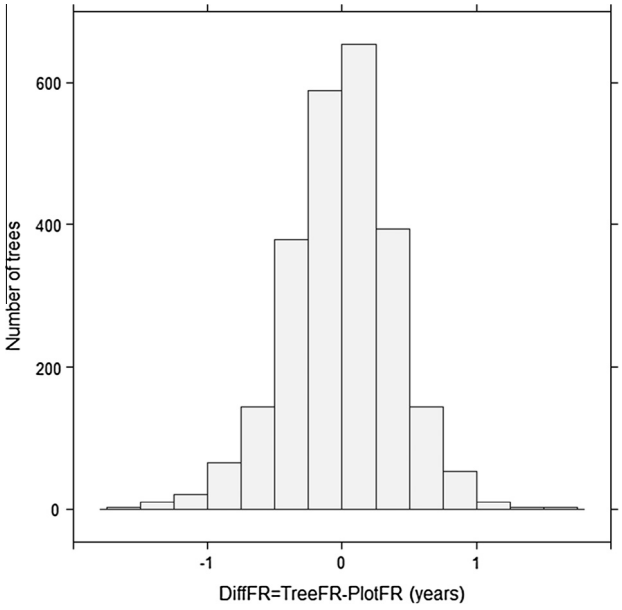

Fig. 1. Frequency of sample trees in each class of DiffFR, or deviation of tree-level foliage retention (TreeFR) from plot-average foliage retention (PlotFR) in the Swiss needle cast growth impact study.

2.3. Model evaluation

The models were evaluated by examining the magnitude and distribution of residuals plotted against the response variable and each of the separate predictor variables. The aim was to detect any obvious dependencies or patterns that indicated systematic biases. To determine the accuracy of model predictions, bias and precision of the models were computed directly. Mean difference (MD), mean squared difference (MSD), mean absolute difference (MAD), and R^2 were calculated on the original (unweighted) scale

(including any corrections for log bias from log-transformed models) as follows (Palahí et al., 2003):

$$\mathrm{MD} = \sum_{i=1}^{n}\left(\Delta\mathrm{dbh}_i - \widehat{\Delta\mathrm{dbh}}\right) \Big/ n$$

$$\mathrm{MSD} = \sum_{i=1}^{n}\left(\Delta\mathrm{dbh}_i - \widehat{\Delta\mathrm{dbh}}\right)^2 \Big/ n$$

$$\mathrm{MAD} = \sum_{i=1}^{n}\left|\Delta\mathrm{dbh}_i - \widehat{\Delta\mathrm{dbh}}\right| \Big/ n$$

$$R^2_{\mathrm{pseudo}} = 1 - \frac{\sum_{i=1}^{n}\left(\Delta\mathrm{dbh}_i - \widehat{\Delta\mathrm{dbh}}\right)^2}{\sum_{i=1}^{n}\left(\Delta\mathrm{dbh}_i - \overline{\Delta\mathrm{dbh}}\right)^2}$$

where Δdbh was the observed periodic annual diameter increment, $\widehat{\Delta\mathrm{dbh}}$ was the predicted periodic annual diameter increment, $\overline{\Delta\mathrm{dbh}}$ was the average value of observed periodic annual diameter increment, and i referred to the ith tree with $i = 1, 2, \ldots, n$.

2.4. Model application: growth multiplier

The greatest tree-level foliage retention (4.77 years) and plot-level foliage retention (3.85 years) were assumed to represent the most "healthy" condition of Douglas-fir trees and plots, respectively. The diameter growth impact and basal area growth impact for individual plots with foliage retention between 1.0 and 3.85 years, or for trees with average foliage retention between 1.0 and 4.77 years, were calculated using the model based on plot-level foliage retention (Model 1) or tree-level foliage retention (Model 2), respectively. Within a plot, the difference between TreeFR and PlotFR typically ranged between −0.75 and +0.75 years. Therefore, the SNC multiplier from the model based on both plot-level foliage retention and the deviation of tree-level from plot-level foliage retention (Model 3) was plotted across the range of PlotFR from 1 to 3.85 years under three different conditions of TreeFR: (1) TreeFR − PlotFR = −0.75 years; (2) TreeFR − PlotFR = 0 years; and (3) TreeFR − PlotFR = +0.75 years.

2.5. Within-stand variability in foliage retention

Little analysis has been done to date to test the hypothesis that foliage retention declines with lower or greater social status within a stand. Foliage retention values on more than 700 trees from more than 70 plots and four different measurement periods were available to test this hypothesis. Individual-tree foliage retention was regressed on the ratio of individual-tree dbh (D) to plot-level quadratic mean diameter of the Douglas-fir component (Q), treating plot as a random effect. This analysis was intended to facilitate interpretation of the final growth models relative to initial tree size versus initial foliage retention. As a means of illustrating the within-plot variation of foliage retention, the standard deviation in estimated foliage retention for the ten trees within each plot was calculated for each year of SNC rating, and an average value for each plot was determined as the average of all years during which SNC severity was rated for that plot.

3. Results

3.1. The model

The diameter increment models based on plot-level and tree-level foliage retention were as follows:

$$\Delta\mathrm{dbh} = \exp\left(\beta_{10} + \beta_{11}\cdot\log(\mathrm{dbh}) + \beta_{12}\log\left(\frac{\mathrm{CR}+0.2}{1.2}\right) + \beta_{13}\cdot\mathrm{CCFL} + \beta_{14}\cdot\mathrm{age} + \beta_{15}\cdot\mathrm{SDI} + \frac{\beta_{16}}{\mathrm{PlotFR}}\right) + \delta_1 + \varepsilon_1 \quad (1)$$

$$\Delta\mathrm{dbh} = \exp\left(\beta_{20} + \beta_{21}\cdot\log(\mathrm{dbh}) + \beta_{22}\cdot\log\left(\frac{\mathrm{CR}+0.2}{1.2}\right) + \beta_{23}\cdot\mathrm{CCFL} + \beta_{24}\cdot\mathrm{age} + \beta_{25}\cdot\mathrm{SDI} + \frac{\beta_{26}}{\mathrm{TreeFR}}\right) + \delta_2 + \varepsilon_2 \quad (2)$$

$$\Delta\mathrm{dbh} = \exp\left(\beta_{30} + \beta_{31}\cdot\log(\mathrm{dbh}) + \beta_{32}\cdot\log\left(\frac{\mathrm{CR}+0.2}{1.2}\right) + \beta_{33}\cdot\mathrm{CCFL} + \beta_{34}\cdot\mathrm{age} + \beta_{35}\cdot\mathrm{SDI} + \frac{\beta_{36}}{\mathrm{PlotFR}} + \beta_{37}\cdot\log(\mathrm{DiffFR}+2)\right) + \delta_3 + \varepsilon_3 \quad (3)$$

where dbh was diameter at breast height (cm); CR was crown ratio (live crown length/total tree height); CCFL was crown competition factor in larger trees (%); age was total stand age (years); SDI was stand density index (Reineke, 1933); PlotFR was plot-level foliage retention (years); TreeFR was tree-level foliage retention (years); DiffFR was the difference between tree-level foliage retention and average plot-level foliage retention (TreeFR − PlotFR); β_{10}–β_{16}, β_{20}–β_{26}, and β_{30}–β_{37} were parameters to be estimated from the data; δ_1, δ_2, and δ_3 were random plot effects assuming $\delta_i \sim N(0, {\sigma_{\delta i}}^2)$, with $i = 1$, 2, or 3; and ε_i are random errors assuming $\varepsilon_i \sim N(0, {\sigma_{\varepsilon i}}^2)$ with $i = 1$, 2, or 3. A weight of DBH^{-2} was used in all three of the above models. Variance covariance structures AR(1) and compound symmetry were significant in the linear form of these models, however, they had a slightly higher AIC. Therefore, the final model did not specify a variance covariance structure.

The above three models were evaluated with R^2_{pseudo}, MD, MSD, and MAD (Table 3). The model using tree-level foliage retention [2] had a greater R^2_{pseudo} than the model with plot-level foliage retention [1], as well as a lower MD, MSD, and MAD, indicating that tree-level foliage retention predicted Douglas-fir diameter increment more accurately. Model [3], incorporating both plot-level foliage retention and the deviation of tree-level retention from plot-level retention, performed almost as well as model [2], but with slightly less precision. However, all three models had similar accuracy, e.g., R^2_{pseudo} of Model [2] was only 0.0049 higher than that of Model [1] and only 0.0011 higher than Model [3]. Similarly, MAD of Model [2] was only 0.00190 lower than that of Model [1] and only 0.00044 lower than that of Model [3].

Parameter estimates in the final models were all significantly different from zero at $\alpha = 0.05$ (Table 4). In all models, diameter growth was positively correlated with dbh and crown ratio, and negatively correlated with SDI, CCFL, age, and the reciprocal of foliage retention. In general, diameter growth increased with increasing tree size, crown size and foliage retention, and decreased with higher stand density, lower social position, and greater age. Weighted residuals showed no serious departures from constant variance or biases across predictor variables (not shown). The random plot effect and alternative variance–covariance structures in

Table 3
Statistics for evaluation of diameter growth models for Douglas-fir trees from the Swiss needle cast growth impact study. See equations in Section 2 for exact definition of statistics.

Variable	Definition	Model [1]	Model [2]	Model [3]
MD	Mean difference	−0.000007	−0.000115	−0.000143
MSD	Mean squared difference	0.073561	0.072404	0.072667
MAD	Mean absolute difference	0.208572	0.206675	0.207118
R^2_{pseudo}	Pseudo-R^2	0.687629	0.692551	0.691441

the linearized mixed-effects version of this model provided no significant improvement over the model without these potential refinements, and residuals indicated better conformity of the non-linear model to the assumptions of least squares estimation.

3.2. Growth multiplier

Given the model forms and parameter estimates, the trends in implied diameter growth multipliers (DMOD) over initial foliage retention were as follows:

$$\mathrm{DMOD}_{\mathrm{model1}} = \frac{\exp\left(\frac{-0.4772}{\mathrm{plotFR}}\right)}{\exp\left(\frac{-0.4772}{3.85}\right)} = \exp\left[-0.4772\left(\frac{1}{\mathrm{plotFR}} - \frac{1}{3.85}\right)\right] \quad (4)$$

$$\mathrm{DMOD}_{\mathrm{model2}} = \frac{\exp\left(\frac{-0.4529}{\mathrm{treeFR}}\right)}{\exp\left(\frac{-0.4529}{4.77}\right)} = \exp\left[-0.4529\left(\frac{1}{\mathrm{treeFR}} - \frac{1}{4.77}\right)\right] \quad (5)$$

$$\mathrm{DMOD}_{\mathrm{model3,0}} = \left(\frac{0+2}{2}\right)^{0.1597}\left[\frac{\exp\left(\frac{-0.5069}{\mathrm{plotFR}}\right)}{\exp\left(\frac{-0.5069}{3.85}\right)}\right] = \left(\frac{0+2}{2}\right)^{0.1597}\exp\left[-0.5069\left(\frac{1}{\mathrm{plotFR}} - \frac{1}{3.85}\right)\right] = \exp\left[-0.5069\left(\frac{1}{\mathrm{plotFR}} - \frac{1}{3.85}\right)\right] \quad (6)$$

$$\mathrm{DMOD}_{\mathrm{model3,-0.75}} = \left(\frac{-0.75+2}{2}\right)^{0.1597}\left[\frac{\exp\left(\frac{-0.5069}{\mathrm{plotFR}}\right)}{\exp\left(\frac{-0.5069}{3.85}\right)}\right] = \left(\frac{-0.75+2}{2}\right)^{0.1597}\exp\left[-0.5069\left(\frac{1}{\mathrm{plotFR}} - \frac{1}{3.85}\right)\right] \quad (7)$$

$$\mathrm{DMOD}_{\mathrm{model3,+0.75}} = \left(\frac{+0.75+2}{2}\right)^{0.1597}\left[\frac{\exp\left(\frac{-0.5069}{\mathrm{plotFR}}\right)}{\exp\left(\frac{-0.5069}{3.85}\right)}\right] = \left(\frac{+0.75+2}{2}\right)^{0.1597}\exp\left[-0.5069\left(\frac{1}{\mathrm{plotFR}} - \frac{1}{3.85}\right)\right] \quad (8)$$

where PlotFR ranged from 1 to 3.85 years, and TreeFR ranged from 1 to 4.77 years.

The tree-level foliage retention multiplier exhibited a greater range for a given initial foliage retention than did the plot-level multiplier (Fig. 2). Where SNC was most severe, (PlotFR = TreeFR = 1 year), the value of the diameter growth multiplier was 0.70 for both plot-averages and individual-trees. As SNC became less severe, the multipliers for models [1] and [2] approached a value of 1 at foliage retention levels indicative of little to no SNC impact. A tree with a foliage retention that was 0.75 years greater than the plot average foliage retention (model [3], TreeFR = PlotFR + 0.75) was implied to have a diameter increment 5% larger than a tree with the plot-average foliage retention. In contrast, a tree with a foliage retention that was 0.75 years less than that of the plot average foliage retention (model [3], TreeFR = PlotFR-0.75) was implied to have a diameter increment 7% less than a tree with the plot-average foliage retention.

Table 4
Parameter estimates from the model for predicting diameter increment from plot-average foliage retention (Model 1; PlotFR), individual-tree foliage retention (Model 2: TreeFR), and the combination of individual-tree and plot-average foliage retention (Model 3: TreeFR + PlotFR). All parameters are significantly different from zero at $\alpha = 0.05$.

	Model [1]		Model [2]		Model [3]	
	Estimate	S.E.	Estimate	S.E.	Estimate	S.E.
β_{i0}	0.6723	0.1227	0.6524	0.09537	0.5797	0.1243
β_{i1}	0.3301	0.03811	0.3306	0.03601	0.3233	0.03802
β_{i2}	1.4187	0.09225	1.3888	0.09103	1.3848	0.09154
β_{i3}	−0.00246	0.00028	−0.00228	0.000265	−0.00235	0.000277
β_{i4}	−0.0399	0.004106	−0.03989	0.004029	−0.03978	0.004041
β_{i5}	−0.00056	0.000087	−0.00055	0.000086	−0.00054	0.000086
β_{i6}	−0.4772	0.113	−0.4529	0.06101	−0.5069	0.1142
β_{i7}					0.1597	0.02624
μ_i	0.03336	0.0062	0.03326	0.00616	0.03338	0.0062

3.3. Within-stand variability in foliage retention

The trees selected for SNC severity rating within this dataset were limited to dominant and co-dominant trees, so the average D/Q was 1.4 with a standard deviation of 0.37. Regardless, the mixed-effects model indicated that foliage retention increased significantly with increasing D/Q even over this limited diameter range. On average, foliage retention would increase by 0.19 years per unit increase in D/Q (Fig 3).

In the 76 plots analyzed, the average standard deviation in tree-level foliage retention for a given year and a given plot of scoring varied from 0.04 to 0.90 years, with an average of 0.39 years. The standard deviation in tree level foliage retention for each plot and year increased with increasing average tree height (Fig 4), indicating that as the stands matured and differentiated, the variation in foliage retention was increasing

4. Discussion

The diameter growth models (Eqs. (1–3)) were consistent with previously constructed diameter and basal area increment models (Wykoff, 1990; Monserud and Sterba, 1996; Hann and Hanus, 2002; Uzoh and Oliver, 2008); i.e., dbh and crown ratio (CR) were positively correlated with diameter increment, but stand age, crown competition factor in larger trees (CCFL), and stand density index (SDI) were negatively correlated with diameter increment. As expected, foliage retention was positively correlated with diameter increment at both the plot-level and tree-level. To date, all SNC-related growth impacts have been assessed using plot-average foliage retention. Although there is significant variation in tree-level foliage retention within a stand, plot-level averages have nonetheless provided a useful means of determining regional

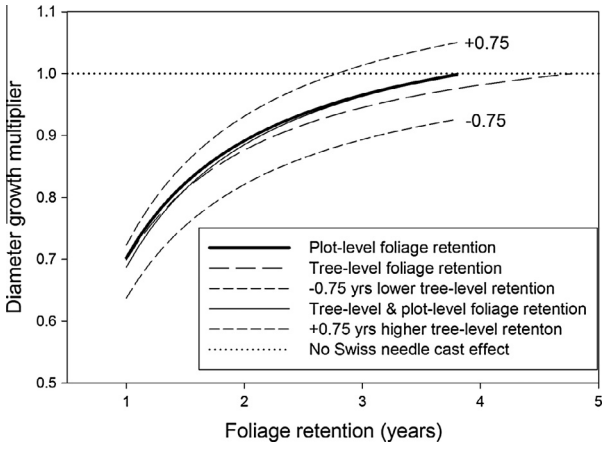

Fig. 2. Inferred diameter growth multipliers from the diameter increment model using plot-average foliage retention (Model 1; PlotFR), individual-tree foliage retention (Model 2: TreeFR), and the combination of individual-tree and plot-average foliage retention (Model 3: TreeFR + PlotFR).

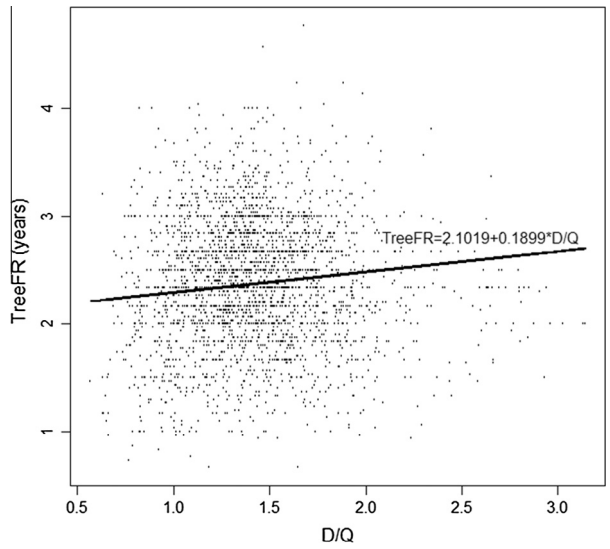

Fig. 3. Relationship between TreeFR and D/Q.

impacts of the disease and stand-level growth losses (Maguire et al., 2011). However, given the variation of foliage retention among trees within a plot and the correlation between tree-level foliage retention and individual-tree growth, plot-level averages mask the portion of within-stand variability in tree growth imposed by differences in SNC severity among individual trees. Accounting for this additional source of variation in individual tree growth increases the accuracy of simulated stand dynamics where significant tree-level differences in SNC severity persist, specifically by better representing the intensity of size differentiation. Likewise, this variation provides an opportunity to improve growth responses to thinning by considering foliage retention as a criterion for selecting retained trees.

In a previous analysis, Garber et al. (2007) applied plot-level foliage retention to the same growth data used in this analysis to calculate multiplicative adjustment factors. These SNC multipliers

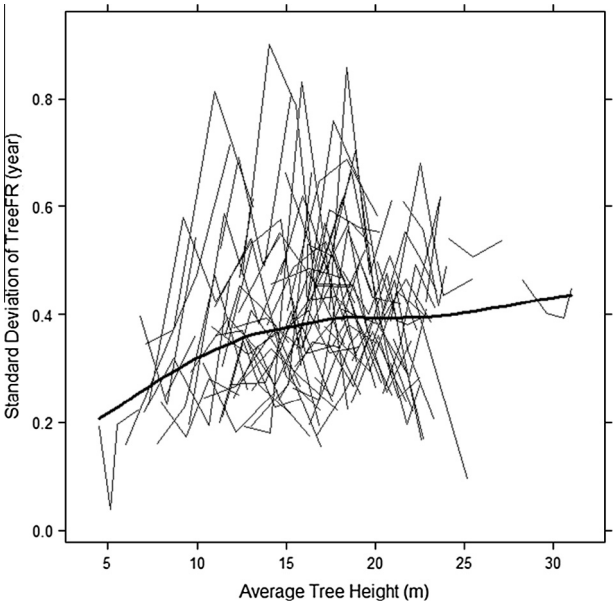

Fig. 4. Standard deviation and lowess trend line of tree-level foliage retention for all plot and measurement year combinations in the SNCC growth impact study. Lines connect time series for each individual plot.

were intended to enable users of the growth and yield model ORGANON to simulate growth dynamics of SNC-impacted stands. Garber et al. (2007) found that a foliage retention of one year at the plot level implied diameter and height growth averaging only 33% and 60%, respectively, of that expected in a healthy stand. Although these growth multipliers seemed to imply plot-level growth impacts that were consistent with volume growth losses estimated at the stand level (Maguire et al., 2011), the variability in multipliers observed in this analysis suggests that a constant multiplier across all trees within the stand will generate inaccuracies in simulated stand dynamics and resulting stand structure (e.g., diameter distributions). This inaccuracy will be compounded by corresponding effects on stand-structural covariates that are designed to represent relative social position in the stand (e.g., CCFL) and that therefore depend on the degree of size differentiation. In this case, a silvicultural regime selected to achieve a given stand management objective may not produce the expected stand structure if based on simulations that do not consider individual-tree variation in SNC effects.

In addition to these implications for stand dynamics and silvicultural manipulation of stand structure, the size distribution of trees and logs underlying a given stand volume has a strong influence on stand valuation. Product recovery and value will vary by log size, but further variation is introduced by the SNC effects on wood stiffness (Johnson et al., 2005). The effects of SNC on wood quality and stem form have not been fully quantified, but trees subjected to fungicidal exclusion of the fungus are known to grow significantly different wood than trees without fungicidal protection (Johnson et al., 2003). Likewise, SNC-impacted stems are generally more slender for a given dbh and height (Weiskittel and Maguire, 2004). Both these responses to SNC affect product recovery and value of Douglas-fir in regions where SNC is prevalent.

Plot-level average foliage retention is based on estimates from dominant and co-dominant trees only, so the full range of variability within the stand was probably not captured by this protocol. However, this stand component contributes the most to growth and value (O'Hara, 1988), so the practical implication of any bias introduced by extrapolating to lower crown classes may be minimal. Although foliage retention was generally estimated on dominant and codominant trees, foliage retention exhibited a significant increase with increasing relative diameter even over this limited diameter range. The degree to which this relationship is cause versus effect, and the degree to which it can be extrapolated to intermediate and suppressed trees, is unknown. Dendrochronological work attempting to identify historical fluctuations in SNC in the Oregon Coast Ranges included trees that make up part of the suppressed component of current stands (Black et al., 2010). Black et al.'s (2010) analysis showed that at the most severely impacted sites Douglas-fir radial growth was reduced by as much as 85%. In the current study, the largest diameter growth reduction was only 30% for the most severely impacted trees. Part of the difference may have resulted from comparing the effect of SNC between different stand components in the two studies, i.e., among dominants and co-dominants in the Swiss Needle Cast Cooperative growth impact study, but among all crown classes in Black et al.'s (2010) study. However, it is impossible to know retrospectively whether the greater growth impact of SNC in Black et al.'s (2010) dendrochronological study was largely or partly an effect of lower foliage retention by lower crown classes.

The link between foliage retention and crown position, and between foliage retention and growth is consistent with observations previously made within SNC-infected stands, i.e., that SNC is one of numerous drivers of differentiation within coastal Douglas-fir stands (Mainwaring et al., 2005). In severely impacted stands, it has been recommended that density be kept low to ensure long crowns, thereby sustaining sufficient foliar mass and

diameter growth. Arguments have also been made that a higher density of trees should be planted in these stands to ensure that enough crop trees produce sufficient volume to maintain net positive revenues from Douglas-fir stand management in SNC-impacted coastal regions. Meeting both of these objectives with a pre-commercial thinning will alter current management guidelines in coastal zones, affecting stand structure by providing more growing space and opportunity for recruitment and persistence of other under- and overstory species.

This growth analysis of plots from the Swiss Needle Cast Cooperative relied on our ability to accurately assess tree-level foliage retention. Measurement error in estimating foliage retention for a given crown third and the average for a given tree may reduce the appeal of accounting for within-stand variation in foliage retention. As the trees on these permanent plots become taller and foliage visibility declines, maintenance of estimation accuracy necessitated that the method for estimating tree-level foliage retention shift to estimating foliage retention on the southernmost branch pruned off the fifth whorl from the tip of the tree. Initial comparisons to the more conventional ground based visual estimates when needle cohorts were still visible from the ground indicated close agreement between the two approaches. Especially in older stands, visual estimates are easiest to get for dominant trees, because they tend to have some open space around them, and their branches can be more readily seen against the sky. However, intermediate and suppressed trees are more difficult to assess from the ground, due primarily to the low contrast in color between needles on a specific branch and those on neighboring branches. Incorporation of tree-level foliage retention values for predictive purposes on a large scale and on taller trees would probably necessitate further analysis of sampling strategies to ensure the required estimation accuracy.

Finally, it is widely recognized that other factors related to site quality, stand structure, and silvicultural history influence foliage retention, complicating efforts to quantify pure SNC impacts (Maguire et al., 2011). Both earlier and current work on *P. gaeumannii* indicate that this endemic fungus has been virtually ubiquitous on Douglas-fir foliage (Boyce, 1940; Hood, 1982; Stone et al., 2008). In fact, pseudothecia counts on foliage samples indicated the presence of the fungus at all the plots included in this study (unpublished data). Slower growth associated with lower fertility in unmanaged stands has been considered a cause of greater foliage retention rather than an effect (Reich et al., 1995; Shoettle, 1990), and foliage retention has been observed to decline as a result of positive growth responses to fertilization (Balster and Marshall, 2000). Because these trends are opposite to growth patterns observed over the range in SNC intensity characterizing the growth impact study, growth reductions quantified in this analysis are attributed predominantly to direct effects of *P. gaeumannii* on gas exchange and foliage retention (Manter et al., 2003).

5. Conclusion

Within-stand variation in individual-tree foliage retention has influenced individual-tree growth rates and stand dynamics. The most severely impacted plots exhibited 30% diameter growth loss for dominant and co-dominant trees. Within a plot, diameter growth averaged about 12% higher on dominant and co-dominant trees with the greatest foliage retention relative to trees with the least foliage retention. Results from this analysis indicated that use of a plot-average foliage retention will introduce bias into individual-tree growth predictions. Bias would result both from the projected growth of individual trees, and from the compounding effects over multiple growth periods on covariates that represent the relative size and social position of the tree in the stand. Furthermore, lack of knowledge about differential SNC growth effects on individual trees forfeits the opportunity to include foliage retention as a criterion for selecting trees for removal during thinnings.

Acknowledgements

This project was funded by the Swiss Needle Cast Cooperative (SNCC) hosted at Oregon State University. We gratefully acknowledge field work performed by many different field crews working for the SNCC and the Oregon Department of Forestry.

References

Balster, N.J., Marshall, J.D., 2000. Decreased needle longevity of fertilized Douglas-fir and grand fir in the northern Rockies. Tree Physiol. 20, 1191–1197.
Black, B.A., Shaw, D.C., Stone, J.K., 2010. Impacts of Swiss needle cast on overstory Douglas-fir forests of the western Oregon coast range. For. Ecol. Manage. 259, 1673–1680.
Boyce, J.S., 1940. A needle cast of Douglas-fir associated with *Adelopus gaeumannii*. Phytopathology 30, 649–659.
Bruce, D., 1981. Consistent height-growth and growth-rate estimates for remeasured plots. For. Sci. 27, 711–725.
Calama, R., Montero, G., 2005. Multilevel linear mixed model for tree diameter increment in stone pine (*Pinus pinea*): a calibration approach. Silva Fenn. 39, 37–54.
Curtis, R.O., 1967. Height diameter and height-diameter-age equations for second-growth Douglas-fir. For. Sci. 13, 356–375.
Garber, S., Maguire, D., Mainwaring, D., Hann, D., 2007. Swiss Needle Cast ORGANON module update. In: Shaw, D., (Ed.). 2007 Swiss Needle Cast Cooperative Annual Report. College of Forestry, Oregon State University, Corvallis, OR, pp. 63–66.
Gregoire, T.G., 1987. Generalized error structure for forestry yield models. For. Sci. 33, 423–444.
Hann, D.W., Hanus M.L., 2002. Enhanced diameter-growth-rate equations for undamaged and damaged trees in southwest Oregon. Forest Research Lab., Oregon State University, Corvallis, Oregon. Research Contribution 39, 54p.
Hansen, E.M., Stone, J.K., Capitano, B.R., Rosso, P., Sutton, W., Winton, L., Kanaskie, A., McWilliams, M., 2000. Incidence and impact of Swiss needle cast in forest plantations of Douglas-fir in coastal Oregon. Plant Dis. 84, 773–778.
Hood, I.A., 1982. *Phaeocryptopus gaeumannii* on *Pseudotsuga menziesii* in southern British Columbia. New Zealand J. For. Sci. 12, 415–424.
Johnson, G.R., 2002. Genetic variation of Douglas-fir to Swiss needle cast as assessed by symptom expression. Silvae Genetica 51, 80–86.
Johnson, G.R., Gartner, B.L., Maguire, D., Kanaskie, A., 2003. Influence of Bravo fungicide applications on wood density and moisture content of Swiss needle cast affected Douglas-fir trees. For. Ecol. Manage. 186, 339–348.
Johnson, G.R., Grotta, A.T., Gartner, B.L., Downes, G., 2005. Impact of the foliar pathogen Swiss needle cast on wood quality of Douglas-fir. Can. J. For. Res. 35, 331–339.
Kanaskie, A., McWilliams, M., 2013. Swiss Needle Cast aerial survey, 2013. In: Shaw, D., (Ed.). 2013 Swiss Needle Cast Cooperative Annual Report. College of Forestry, Oregon State University, Corvallis, OR, pp. 5–8.
Kimberley, M.O., Hood, I.A., Knowles, R.L., 2011. Impact of Swiss needle-cast on growth of Douglas-fir. Phytopathology 101, 583–593.
Krajicek, J.E., Brinkman, K.E., Gingrich, S.F., 1961. Crown competition: a measure of density. For. Sci. 7, 35–42.
Maguire, D.A., Kanaskie, A., Voelker, W., Johnson, R., Johnson, G., 2002. Growth of young Douglas-fir plantations across a gradient in Swiss needle cast severity. West. J. Appl. For. 17, 86–95.
Maguire, D.A., Mainwaring, D.B., Kanaskie, A., 2011. Ten-year growth and mortality in young Douglas-fir stands experiencing a range in Swiss needle cast severity. Can. J. For. Res. 41, 2064–2076.
Mainwaring, D.B., Maguire, D.A., Kanaskie, A., 2005. Interactive effects of Swiss needle cast and commercial thinning on Douglas-fir growth and development in north coastal Oregon: two year response from 30 permanent monitoring plots. In: Mainwaring, D., Shaw, D., (Eds.). Swiss Needle Cast Cooperative 2005 Annual Report. College of Forestry, Oregon State University, Corvallis, OR, pp. 23–33.
Manter, D.K., Bond, B.J., Kavanagh, K.L., Stone, J.K., Filip, G.M., 2003. Modelling the impacts of the foliar pathogen, *Phaeocryptopus gaeumannii*, on Douglas-fir physiology: net canopy carbon assimilation, needle abscission and growth. Ecol. Model. 164, 211–226.
Manter, D.K., Reeser, P.D., Stone, J.K., 2005. A climate-based model for predicting geographic variation in swiss needle cast severity in the oregon coast range. Phytopathology 95, 1256–1265.
Monserud, R.A., Sterba, H., 1996. A basal area increment model for individual trees growing in even- and uneven-aged forest stands in Austria. For. Ecol. Manage. 80, 57–80.
O'Hara, K.L., 1988. Stand structure and growing space efficiency following thinning in an even-aged Douglas-fir stand. Can. J. For. Res. 18, 859–866.

Paine, D.P., Hann, D.W., 1982. Maximum crown-width equations for southwestern Oregon tree species. Oregon State University, Forest Research Laboratory, Corvallis, OR, Research Pap. 46, 20p.
Palahí, M., Pukkala, T., Miina, J., Montero, G., 2003. Individual-tree growth and mortality models for Scots pine (*Pinus sylvestris* L.) in north-east Spain. Ann. For. Sci. 60, 1–10.
Reich, P.B., Koike, T., Gower, S.T., Schoettle, A.W., 1995. Causes and consequences of variation in conifer leaf life-span. In: Smith, W.K., Hinckley, T.M. (Eds.), Ecophysiology of Coniferous Forests. Academic Press, New York, USA, pp. 225–254.
Reineke, L.H., 1933. Perfecting a stand-density index for even-aged forests. J. Agric. Res. 46, 627–638.
SAS Institute Inc., 2008. SAS/STAT® 9.2 User's Guide. SAS Institute Inc., Cary, NC.
Schoettle, A.W., 1990. The interaction between leaf longevity and shoot growth and foliar biomass per shoot in *Pinus contorta* at two elevations. Tree Physiol. 7, 209–214.
Stone, J.K., Capitano, B.R., Kerrigan, J.L., 2008. The histopathology of *Phaeocryptopus gaeumannii* on Douglas-fir needles. Mycologia 100, 431–444.
Trasobares, A., Tomé, M., Miina, J., 2004. Growth and yield model for *Pinus halepensis* Mill. in Catalonia, north-east Spain. For. Ecol. Manage. 203, 49–62.
Uzoh, F.C.C., Oliver, W.W., 2008. Individual tree diameter increment model for managed even-aged stands of ponderosa pine throughout the western United States using multilevel linear mixed effects models. For. Ecol. Manage. 256, 438–445.
Weiskittel, A.R., Maguire, D.A. 2004. Influence of Swiss needle cast on Douglas-fir stem properties. In: Mainwaring, D., (Ed.). Swiss Needle Cast Cooperative 2004 Annual Report. College of Forestry, Oregon State University, Corvallis, OR, pp. 91–97.
Weiskittel, A.R., Maguire, D.A., Garber, S.M., Kanaskie, A., 2006. Influence of Swiss needle cast on foliage age class structure and vertical distribution in Douglas-fir plantations of north coastal Oregon. Can. J. For. Res. 36, 1497–1508.
Wykoff, R.W., 1990. A basal area increment model for individual conifers in the northern Rocky Mountains. For. Sci. 36, 1077–1104.
Yang, Y., Huang, S., Meng, S.X., Trincado, G., VanderSchaaf, C.L., 2009. A multilevel individual tree basal area increment model for aspen in boreal mixedwood stands. Can. J. For. Res. 39, 2203–2214.

forests

MDPI

Article

Assessments of Population Structure, Diversity, and Phylogeography of the Swiss Needle Cast Fungus (*Phaeocryptopus gaeumannii*) in the U.S. Pacific Northwest

Patrick Bennett * and Jeffrey Stone

Received: 2 October 2015; Accepted: 17 December 2015; Published: 6 January 2016
Academic Editors: Jan Stenlid, Jonas Oliva and Audrius Menkis

Department of Botany and Plant Pathology, Oregon State University, Corvallis, OR 97331, USA; stonej@science.oregonstate.edu
* Correspondence: bennetpa@science.oregonstate.edu; Tel.: +1-541-737-8380

Abstract: Swiss needle cast (SNC) is a foliar disease of Douglas-fir (*Pseudotsuga menziesii*) caused by *Phaeocryptopus gaeumannii* (Rohde) Petrak. This fungus is endemic to western North America, where it has historically had little impact in native forests. However, increasing disease severity in western Oregon since the 1990s has prompted renewed interest in *P. gaeumannii* and SNC. For this study, we analyze multilocus microsatellite genotypes from 482 single-spore isolates from 68 trees across 14 sites in the western Coast Range of Oregon and southwestern Washington. This study assesses genotypic variation and genetic structure at several levels of population hierarchy. Despite the observation that most of the genetic variation occurred within subpopulations, our analyses detected significant differentiation at all hierarchical levels. Clustering among the 482 isolates based on genetic distance clearly supports the existence of two previously described cryptic lineages of *P. gaeumannii* in the western United States. The two lineages occur in varying proportions along latitudinal and longitudinal gradients in western Oregon and Washington, suggesting a relationship between climate and phylogeography. Sites near Tillamook, Oregon, where SNC is most severe, consist of sympatric subpopulations in which the two lineages comprise roughly equal proportions.

Keywords: Douglas-fir; forest pathology; population genetics; microsatellites; mycology

1. Introduction

Defoliation caused by *Phaeocryptopus gaeumannii* (Rohde) Petrak was first observed in Douglas-fir plantations in Europe in the 1920s and was termed "Swiss needle cast" (hereafter SNC). It was later discovered that this fungus is abundant and widespread in western North America, with herbarium specimens bearing *P. gaeumannii* pseudothecia collected as early as 1916 [1]. It was widely accepted that this fungus is ubiquitous throughout Douglas-fir forests in the U.S. Pacific Northwest, although it had rarely been observed to cause noticeable impacts outside of the Christmas tree industry [2]. Beginning in the mid-1980s symptoms of the disease began to emerge in the western Oregon Coast Range near Tillamook. Foresters noted chlorotic foliage, thinning crowns, and reduced height and diameter growth of Douglas-fir in timber plantations. Subsequent research identified *P. gaeumannii* as the most likely cause [2]. Later studies of SNC disease physiology revealed that these symptoms are caused by reduced gas exchange in the needles due to the occlusion of the stomata by ascocarps (pseudothecia) produced by this fungus. This blockage of the stomata leads to a reduction in carbon assimilation proportional to the percentage of total stomates occupied by pseudothecia [3] Abscission occurs when a needle ceases to function as a carbon source [4]. Regional SNC aerial surveys conducted annually since 1996 have documented gradual expansions in the area affected by the disease and in

the magnitude of disease severity. By 2015, the total area in western Oregon displaying symptoms of SNC reached 237,250 ha, an increase of over 350% since the first survey in 1996 [5].

Although *P. gaeumannii* reproduces sexually through the formation of ascospores in the annual production of pseudothecia; no form of asexual sporulation has been observed [6]. Despite this absence of true clonal reproduction, previous population genetic studies that employed molecular techniques such as SSCP (single strand conformation polymorphisms) suggested that a clonal population structure predominates, although outcrossing likely occurs with low frequency [7]. Given that the vegetative thallus of this fungus contains haploid nuclei, these observations likely reflect the role of homothallism in *P. gaeumannii* populations. In addition to this population substructure due to reproductive mode, the presence of multiple lineages of *P. gaeumannii* in the United States was demonstrated through the use of multilocus gene-genealogies [7]. An analysis of the spatial distributions of these lineages suggested that they co-occur in sympatric populations in the western United States, particularly in the western Coast Range in Oregon. In a sampling of five plantations in the SNC epidemic area, an increasing proportion of one of these lineages, "Lineage 2", was negatively correlated with foliage retention, a common measure of disease severity [8]. This lineage was also twice as likely to be recovered from sites that were rated as having severe SNC infections than those with less severe disease [8]. This observation led these authors to suggest that Lineage 2 might be more aggressive than Lineage 1, and that its recent emergence may have been a significant factor in the intensification of SNC in northwestern Oregon. In a later analysis, 10 nuclear microsatellite loci were used to assess diversity and population structure in a sample of 60 isolates from western Oregon [9]. The authors noted that genotypic diversity was exceptionally high in their sample population. High diversity, combined with the apparent lack of linkage disequilibrium between many of the loci, led these authors to conclude that this particular set of microsatellite markers should serve as an appropriate tool for the estimation of population diversity and structure for *P. gaeumannii*. They also noted that sampling at finer spatial scales was needed to accurately assess these parameters and to determine the relationship between lineage phylogeography and the distribution of disease on the landscape [9].

The objectives of this study were to analyze the distributions of the two lineages of *P. gaeumannii* at multiple spatial scales across geographic and climatic gradients. Estimates of genotypic diversity and population differentiation were considered in an attempt to correlate population dynamics with possible factors influencing the observed distribution of disease severity in western Oregon. Our analyses aimed to assess the extent to which gene flow occurs between subpopulations at several levels of a population hierarchy. Lineages, sampling sites, and individual trees were considered as possible demes in which random mating may occur. This study also aims to assess the spatial scales at which populations of *P. gaeumannii* are structured in natural populations. To address this question, samples were collected and analyzed from several spatial scales ranging from trees to landscapes. Genetic clustering analyses were performed in which the similarity and relatedness between isolates from various spatial scales could be compared statistically as well as graphically.

2. Materials and Methods

2.1. Sample Collection

Included in these analyses are microsatellite genotypes from 482 isolates of *P. gaeumannii* collected from 68 trees in 14 Douglas-fir plantations in western Oregon and southwestern Washington. Nine sites were sampled in the Coast Range in northern Oregon near the town of Tillamook, with a central transect of five sites spanning 57 km west-to-east. Three sites were sampled in the central Oregon Coast Range spanning 24–57 km east of the town of Florence, and two sites were sampled approximately 40 km inland in southwestern Washington (Figure 1, Table 1). Foliage was collected from five randomly selected 10–30 year old Douglas-fir trees at each site. Second- and third-year internodes were sampled from secondary branches in the upper crown. From one tree at each site, branches were also collected from vertically stratified sections of the canopy including the lower, middle, and upper crown

(Figure 1B). The number of isolates obtained from each tree ranged from 10 to 30, and the number of isolates genotyped from each sampling site ranged from 10 to 99.

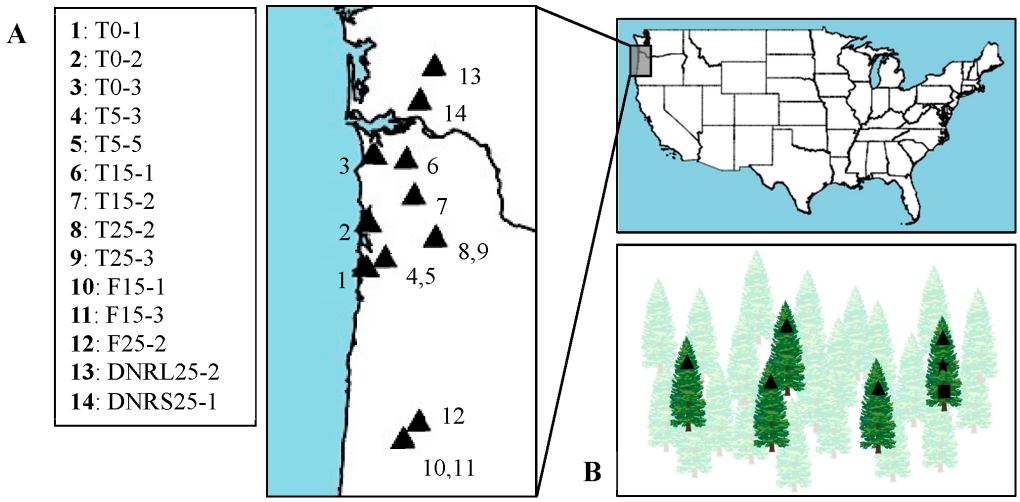

Figure 1. (**A**) Map of northwestern Oregon and southwestern Washington with markers indicating the locations of sites where *Pseudotsuga menziesii* foliage was collected for isolation of *Phaeocryptopus gaeumannii*. Legend at left shows the site names corresponding to marker numbers on map. T = Tillamook, F = Florence, DNR = Washington Department of Natural Resources. The number immediately following the letter corresponding to these locations represents the distance of the sampled stand from the coast. (ex: T25 = 25–35 miles (40–57 km) from coast at the latitude of Tillamook, Oregon); (**B**) Schematic diagram of foliage sampling at a given site. Triangles represent collections from the upper canopies of five randomly selected Douglas-fir trees at each site. The star and the square represent collections of foliage from the middle and lower canopy, respectively, of one of the five trees sampled at each site.

Table 1. Sample sizes, genotypic richness, and lineage distributions determined for 482 *P. gaeumannii* isolates from the 14 sites sampled for this study.

Site	N [a]	MLG [b]	eMLG [c]	L1 [d]	L2 [e]
T-01	49	48	9.96	23	26
T-02	10	9	9	4	6
T-03	17	17	10	9	8
T5-3	29	29	10	22	7
T5-5	21	20	9.79	17	4
T15-1	46	45	9.96	23	23
T15-2	24	23	9.84	10	14
T25-2	99	90	9.85	99	0
T25-3	60	59	9.97	59	1
F15-1	29	27	9.78	27	2
F15-3	15	15	10	4	11
F25-2	37	32	9.61	25	12
DNRL25-2	25	25	10	19	6
DNRS25-2	21	16	8.93	13	8
Total	482	454	9.99	358	124

[a] N = number of isolates; [b] MLG = number of multilocus genotypes; [c] eMLG = genotypic richness (expected number of multilocus genotypes in a rarefied sample of 10 isolates); [d] L1 = abundance of Lineage 1; [e] L2 = abundance of Lineage 2.

2.2. Isolation and Culturing

Needles with mature pseudothecia of *P. gaeumannii* were selected for ascospore isolations. Groups of six needles from each sample were attached to the lids of 100 mm styrene Petri dishes with double-sided tape and suspended above the agar surface to allow ascospore discharge. After 48–72 h, individual germinating ascospores were excised from the agar surface with the aid of flame-sterilized forceps and isolated onto 2% malt agar (MA) (Difco Laboratories, Detroit, MI, USA). Site information, tree number, and a unique isolate number were recorded for each spore. Cultures were incubated at 17 °C for 2–6 months to allow sufficient growth for DNA extraction and permanent storage.

2.3. DNA Extractions

Total genomic DNA was extracted from vegetative mycelium using the DNeasy Plant Mini Kit 250 (Qiagen, Hilden, Germany). The protocol followed the manufacturer's instructions with the addition of an initial maceration procedure. Agar plugs extracted from *P. gaeumannii* cultures were added to cryogenic vials with sterile 2 mm glass beads. The vials were briefly submerged in liquid nitrogen to freeze the agar plugs prior to the addition of the DNeasy extraction buffer AP1. A Mini-Beadbeater-1 (BioSpec Products, Bartlesville, OK, USA) was then used to agitate each of the vials at 5000 rpm for 60 s.

2.4. Microsatellite PCR

For each isolate, ten microsatellite loci [9] were amplified in three multiplexed PCR reactions. The multiplexed reactions contained between two and five primer sets, each with a fluorescent dye label on the reverse primer. The sequences of the primers were identical to those described in [9] but without the 18 bp M13 universal tails, resulting in shorter PCR products. The PCR reactions were performed using the Qiagen Type-It Microsatellite PCR kit, and the protocol was employed according to the manufacturer's instructions, but with reaction volumes of 12.5 µL. The amplification was performed with a PTC-200 thermal cycler (MJ Research, Inc. Waltham, MA, USA) programmed according to [9].

2.5. Genotyping and Allele Scoring

Each of the multiplexed PCR reactions was diluted by a factor of 10 in deionized water, and 1 µL of the diluted product was submitted to the Center for Genome Research and Biocomputing (CGRB, Oregon State University, Corvallis, OR, USA) for genotyping via capillary electrophoresis on an ABI 3730 DNA Analyzer (Applied Biosystems-ThermoFisher Scientific Corporation, Waltham, MA, USA) with the GS-500ROX size standard. Allele sizes and genotypes were assigned with the aid of the ABI GeneMapper 4.0 software (Applied Biosystems-ThermoFisher Scientific Corporation) Bins were set such that samples could be identified based on their sizes and fluorescent labels, and panels were set to recognize previously reported allele size ranges [9] adjusted to account for the absence of the M13 primer tails. Microsatellite alleles were called using the standard algorithm in the GeneMapper software, and were also validated visually at each locus for each isolate.

2.6. Data Analysis

Multilocus genotypes from a total of 482 *P. gaeumannii* isolates were included in this study. Data formatting and analyses were performed with R version 3.2.1 [10] and GenAlEx 6.5 [11,12]. The formatted genotypes were imported to R for use with *Poppr* 2.0.2 [13]. For all analyses described here, the mutlilocus genotype data were stratified in a population hierarchy, as described in [14]. Lineages were considered as the most inclusive level of this hierarchy, sampling sites were considered subpopulations within lineages, and trees were considered subpopulations within sites.

Shannon-Weiner diversity (H), Stoddart and Taylor's index (G) [15], Simpson's Index (λ) [16], expected heterozygosity (H_e, Nei's gene diversity) [17], and genotypic richness, were compared at two levels of the population hierarchy, site and lineage. Genotypic richness was estimated as the

number of expected multilocus genotypes (eMLG) in a rarefied sample size (n). These diversity parameters were chosen based on their descriptive power and utility as outlined by [18]. Because these analyses are sensitive to differences in sample sizes between the populations, diversity was assessed on rarefied sub-samples of the data. For a comparison of diversity between lineages, 128 isolates were included in the analysis. For a comparison of diversity across sites, the sample sizes were rarefied to 10 isolates.

Analysis of molecular variance (AMOVA) was used to compare the genetic variation within and between the levels of the population hierarchy. Estimates of $\boldsymbol{\phi}$ were used to infer gene flow and population differentiation [19]. For these analyses, clone-correction was used to remove repeated MLGs. Statistical significance was assessed with randomization tests with 999 permutations.

The unweighted pair group method with arithmetic means (UPGMA) algorithm was used to construct dendrograms. Their associated bootstrap statistics were calculated using *Poppr* 2.0.2 and dendrograms were visualized with FigTree version 1.4.2 [20]. UPGMA method groups organisms together based on genetic distance determined by the similarity of their multilocus genotypes. An analysis of branching patterns and clustering allowed for the inference of population structure. For the assessments of population structure and lineage membership, all of the 482 isolates were used to construct a bootstrapped UPGMA dendrogram. For analyses of genetic clustering among isolates at smaller spatial scales, dendrograms were constructed with random samples of 100 isolates from a clone-corrected data set. For bootstrapping, 1000 replicate trees were sampled. Rogers' distance [21], a Euclidean measure of genetic distance, was chosen for this analysis due to the fact that it does not rely upon assumptions that the microsatellite loci evolve by the stepwise mutation model.

Mantel's test, an estimate of spatial autocorrelation, was performed to test for correlations between geographic distance and genetic distance. A matrix of genetic distances between populations, calculated according to [21], was compared to a matrix of Euclidean distances between the geographic coordinates of each of the sampling sites. A randomization test was performed in which the data were permuted 999 times to obtain a p-value.

3. Results and Discussion

3.1. Richness and Diversity

All 10 of the microsatellite loci employed in this study were polymorphic. The number of alleles at each locus ranged from 13 to 53. Of the 482 isolates included in the analyses, a total of 454 unique MLGs were identified (Table 1). A total of 354 multilocus genotypes (MLGs) were consistent with those previously described as Lineage 1, and 128 were consistent with previous descriptions of Lineage 2 [9]. Genotypic diversity indices, including Shannon-Wiener, Stoddart and Taylor's, and Simpson's, were significantly greater for Lineage 1 than Lineage 2 (Table 2). Comparisons of genotypic diversity in rarefied samples of 10 isolates from each site revealed a general geographic trend of diversity increasing from west to east at the latitude of Tillamook, Oregon (Figure 2A). The site with the least genotypic diversity was the westernmost site, T-02, while the greatest occurred at site T25-2, approximately 50 km east of T-02. This increase in genetic diversity coincided with an increasing proportion of Lineage 1 isolates in sites east of Tillamook (Table 1, Figures 2A and 3). The high genetic diversity within Lineage 1 suggests that it is native to the eastern Coast Range, where it is most abundant and diverse, as suggested in [8]. A comparison of genotypic diversity between 10 isolates of each lineage revealed that Lineage 1 is significantly more diverse than Lineage 2 (Table 2, Figure 2B).

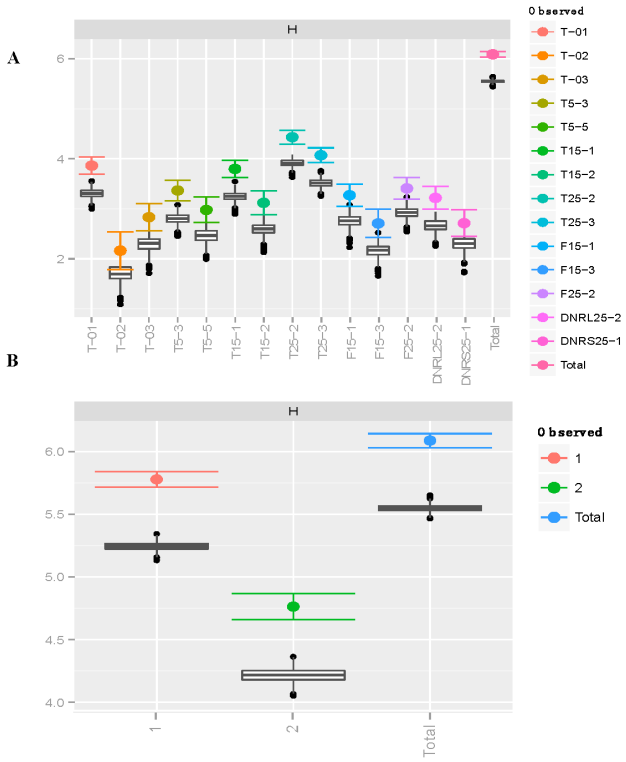

Figure 2. (**A**) Comparisons of *P. gaeumannii* genotypic diversity by sampling site. N = 10; (**B**) Comparisons of *P. gaeumannii* genotypic diversity by lineage. 1 = Lineage 1, 2 = Lineage 2. N = 128. H = Shannon-Weiner diversity. The colored dots with error bars represent the observed statistics and their associated 95% confidence intervals. The black and white box and whisker plots represent the values estimated via bootstrapping with 1000 replicates.

Table 2. Diversity and heterozygosity of multilocus *P. gaeumannii* genotypes from two levels of the population hierarchy. (**A**) Diversity and heterozygosity measured for each sampling site (N = 10 isolates). (**B**) Diversity and heterozygosity values for each lineage (N = 128 isolates).

A				
Site	**H** [a]	**G** [b]	**λ** [c]	**H_e** [d]
T-01	3.864 (3.69, 4.04)	47.08 (42.0, 52.1)	0.979 (0.97, 0.99)	0.821
T-02	2.164 (1.79, 2.54)	8.333 (6.30, 10.37)	0.880 (0.79, 0.97)	0.749
T-03	2.833 (2.56, 3.11)	17.00 (14.3, 19.8)	0.941 (0.90, 0.98)	0.806
T5-3	3.367 (3.16, 3.57)	29.00 (25.5, 32.5)	0.966 (0.95, 0.98)	0.781
T5-5	2.979 (2.72, 3.23)	19.17 (16.0, 22.3)	0.948 (0.92, 0.98)	0.726
T15-1	3.799 (3.62, 3.97)	44.08 (39.3, 48.9)	0.977 (0.97, 0.99)	0.778
T15-2	3.120 (2.88, 3.36)	22.15 (18.8, 25.6)	0.955 (0.93, 0.98)	0.804
T25-2	4.433 (4.30, 4.57)	73.69 (65.1, 82.3)	0.986 (0.98, 0.99)	0.630
T25-3	4.071 (3.92, 4.22)	58.07 (52.8, 63.3)	0.983 (0.98, 0.99)	0.717
F15-1	3.272 (3.05, 3.50)	25.49 (21.8, 29.2)	0.961 (0.94, 0.98)	0.751
F15-3	2.708 (2.43, 2.99)	15.00 (12.5, 17.5)	0.933 (0.89, 0.98)	0.810
F25-2	3.409 (3.20, 3.62)	27.94 (23.6, 32.3)	0.964 (0.95, 0.98)	0.815
DNRL25-2	3.219 (2.99, 3.45)	25.00 (21.7, 28.3)	0.960 (0.94, 0.98)	0.787
DNRS25-1	2.714 (2.45, 2.98)	14.23 (11.5, 17.0)	0.930 (0.89, 0.97)	0.759
Total	6.089 (6.03, 6.14)	417.8 (401, 435)	0.998 (0.997, 0.998)	0.820
B				
Lineage	**H**	**G**	**λ**	**H_e**
1	5.780 (5.71, 5.85)	303.7 (289, 318)	0.997 (0.996, 0.997)	0.728
2	4.764 (4.66, 4.87)	114.7 (107, 122)	0.991 (0.989, 0.993)	0.745
Total	6.089 (6.03, 6.15)	417.8 (400, 435)	0.998 (0.997, 0.998)	0.820

[a] H = Shannon-Weiner diversity index; [b] G = Stoddart and Taylor's index; [c] λ = Simpson's index; [d] H_e = Nei's expected heterozygosity. Numbers in parentheses are 95% confidence intervals calculated by bootstrapping.

3.2. Phylogeography

The two lineages were recovered in varying proportions across the 14 study sites (Figure 3). Lineage 1 was recovered from all sites and comprised 26%–100% of total isolates at any given site; Lineage 2 comprised 0%–74% of isolates at the site level (Table 1). Lineage 2 was most abundant at sites within 16 km inland near Tillamook, Oregon, with decreasing abundance along this latitudinal transect to the east. All but one of the 158 isolates analyzed from sites T25-2 and T25-3 (~50 km inland from Tillamook, OR, USA) were determined to belong to Lineage 1 (Figure 3, Table 1). The same geographic trend did not occur further south, as the F25-2 site (~50 km inland from Florence, OR, USA) comprised approximately 32% Lineage 2. The two sites in southwestern Washington, DNRL25-2 and DNRS25-2 (~50 km inland), comprised 24% and 21% Lineage 2, respectively.

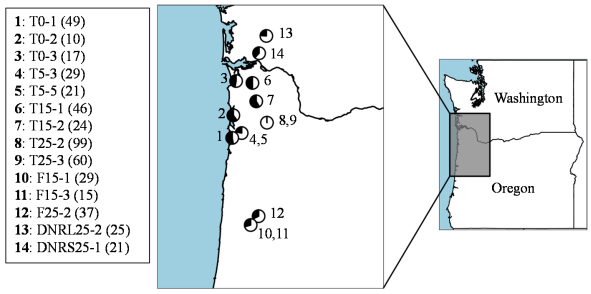

Figure 3. Map showing the relative distributions of two lineages of *P. gaeumannii* across the 14 sites sampled for this study. Lineage 1 is represented by empty (white) circles, while Lineage 2 is represented by filled (black) circles. The numbers next to each pie chart correspond to the site names in the legend at left, and the numbers in parentheses indicate sample sizes. Lineage proportions from sites 4 and 5, 8 and 9, 10 and 11, respectively, were pooled and displayed as single pie charts to avoid overlap.

The primary focus of this investigation was to correlate lineage phylogeography with disease distribution. In this case, climate (*i.e.*, temperature and precipitation gradients) may be an important factor influencing the different distribution patterns of the two lineages across the landscape. There is strong evidence that climatic variables such as winter temperature and precipitation in the spring and early summer influence the abundance of *P. gaeumannii*, and thus disease [22–26]. The western Oregon Coast Range is particularly suited to support abundant populations of *P. gaeumannii* because it receives greater spring precipitation, and has generally milder winter, and cooler summer, temperatures than the rest of the region. The observed distribution of the lineages observed in this study and others [8,22], may be strongly influenced by seasonal temperatures. Trends in phylogeography also suggest that environmental conditions may limit the distribution of Lineage 2 relative to Lineage 1. One explanation may be that Lineage 2 is better adapted to warmer winter temperatures and thus is limited by colder winter temperatures to the east. Conditions in the northern Oregon Coast Range may have become particularly suitable for the growth and proliferation of *P. gaeumannii* and SNC in recent decades due to the effects of climate change [22,24] as well as forest practices favoring increased abundance of Douglas-fir relative to other species [2]. Both favorable environmental conditions and abundance of a susceptible host may have contributed to a recent expansion or migration of Lineage 2 into this region from coastal areas in southern Oregon where it appears to be more dominant.

It is important to note that there does not appear to be a particularly high incidence or severity of SNC at sites near the southern coast of Oregon [8] where Lineage 2 was most abundant in the analysis in [5]. Furthermore, where Lineage 1 dominates in Douglas-fir forests further inland, SNC severity is generally low or moderate. These trends, and the findings of the present study in which sites in the region known to have the greatest severity of SNC disease were found to have a combination of the two lineages, suggest that some synergistic effect or competitive interaction may be occurring between the two lineages. While the occurrence of hybridization between the two lineages may

be possible (a lack of somatic compatibility has yet to be demonstrated) it is considered unlikely, given the strong differentiation and low rates of gene flow between the lineages found in this study. Phylogenetic studies that utilized nucleotide sequence data [7] also suggested that the lineages might be reproductively isolated from one another, thus making interbreeding and hybridization improbable. An alternative explanation for the relationship between disease severity and lineage coincidence may be that a recent emergence of more aggressive races of *P. gaeumannii* has occurred in this region. While this has been proposed as a potential explanation for the recent disease outbreak, direct assessments of aggressiveness among strains collected from sites varying in disease severity have proven inconclusive [8]

3.3. Population Structure and Differentiation

The existence of two lineages of *P. gaeumannii* was first posited by Winton [8] on the basis of SSCP genotypes. Their differentiation was also supported by mutlilocus gene genealogies of highly conserved nuclear housekeeping genes [7]. While it appears that the two lineages are distinct subpopulations that coexist in relatively close spatial proximity, reproductive isolation between them has yet to be definitively demonstrated. A comparison of genetic variation within and between two levels of the population hierarchy, lineage and site, revealed significant subpopulation differentiation. Most of the genetic variance in the total sample population could be attributed to within-tree variation (61.8%, Table 3). Between-lineage variation accounted for 22.7% of the total, sampling site accounted for 4.7%, and the remaining variation (10.8%) occurred due to variation among trees within sites (Table 3). The ϕ statistic provides an estimate of population differentiation and gene flow among the various levels of the population hierarchy. Values of ϕ in the range of 0.15 to 0.25 reflect a high degree of differentiation, and are generally the result of low gene flow [27]. While the two lineages were highly differentiated (ϕ_{LT} = 0.227, p = 0.001), sites were only slightly differentiated from one another within lineages (ϕ_{SL} = 0.061, p = 0.001). Subpopulations of *P. gaeumannii* within individual trees also appear to be significantly differentiated from one another, suggesting a local establishment of infection from inoculum within the same tree (ϕ_{TS} = 0.148, p = 0.001) (Table 3). The fact that lineages are highly differentiated suggests that they may be reproductively isolated due to behavioral differences or genetic incompatibilities. While ϕ_{LT} theoretically should be close to 1 if there is complete reproductive isolation, it is quite rare to observe F-statistics or their analogs approaching 1, even among populations that are thought to be reproductively isolated [27]. Whether the observed within-lineage variance reflects the actual rate of gene flow and admixture, or is an artifact of a recent divergence of the lineages, is not entirely clear. Since microsatellites have very high rates of mutation, it is also possible that the apparent admixture between lineages may be due to the convergence of isolates from each lineage upon the same alleles at some microsatellite loci through random mutation (homoplasy).

When all samples were displayed on a UPGMA dendrogram based on Rogers'genetic distance [21] the basal branches split the 482 isolates into two discrete sub-population groupings that corresponded to previously identified lineages [9] (Figure 4). The divergence between these groups was statistically supported by a bootstrap value of 100% for 1000 replicate trees. The grouping of isolates was used to infer relatedness at various levels of the population hierarchy. For example, isolates from the same tree within a site clustered together with relatively high bootstrap support in many cases. In a UPGMA dendrogram produced from a random subsample of 100 individuals, single-spore isolates 5 and 6, isolated from tree 701 at site T-03, clustered together in 99.5% of replicate trees (Figure 5A). On an adjacent branch, isolates from two different trees, 1744 and 1752 at site T5-5, clustered together in 69.4% of replicate trees (Figure 5B). There is little statistical support for genotypic similarity between isolates from trees at different sites. For example, isolates from sites that are 15 miles (24 km) apart, T-01 and T15-1, only clustered together in 53.7% of replicate trees (Figure 5C). From the UPGMA analyses, it is clear that individuals from the same trees generally have very similar genotypes, suggesting a high level of relatedness and local dispersal. As the spatial distance between samples increases, the

genetic similarity of corresponding isolates decreases. For instance, isolates that clustered together in the UPGMA analyses that came from the same trees had greater bootstrap support for their close genetic similarity than those that came from different trees within the same site, while there was little statistical support for clustering among isolates from more distant sites. This suggests that some degree of isolation by distance (IBD) exists, even though the Mantel test did not indicate a significant relationship between geographic distance and genetic distance (R^2 = 0.088, p = 0.271).

Table 3. Table summarizing the results of the analysis of molecular variance (AMOVA) performed with the 454 *P. gaeumannii* isolates possessing unique MLGs. The relative genetic variances explained by each of the levels of the population hierarchy are shown, and ϕ *(Phi)* statistics are shown as estimates of subpopulation differentiation and gene flow.

Hierarchical Level	Variance (%)	ϕ	p *
ϕ_{LT} (between lineages)	22.671	0.227	0.001
ϕ_{SL} (among sites within lineages)	4.719	0.061	0.001
ϕ_{TS} (among trees within sites)	10.772	0.148	0.001
ϕ_{TT} (within trees)	61.838	0.382	0.001

* p-Value was obtained for the ϕ statistic using a randomization test with 999 permutations.

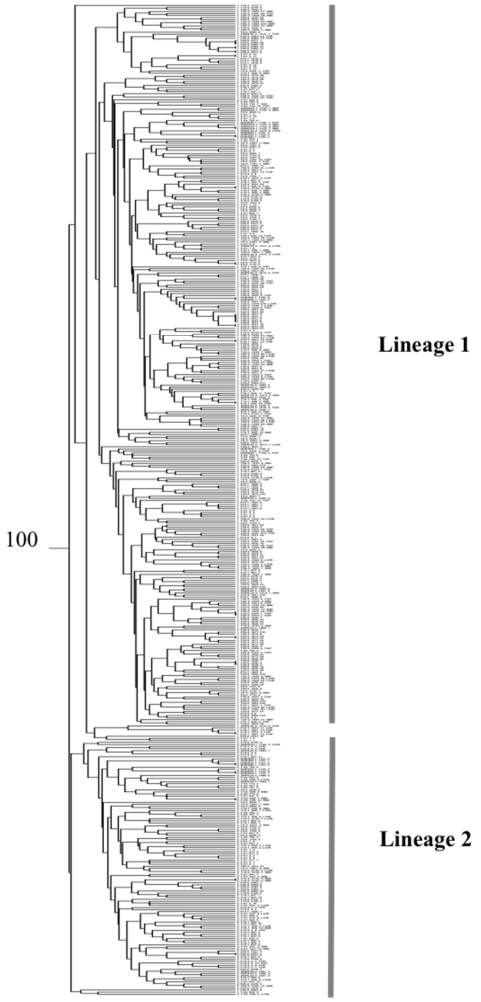

Figure 4. Unweighted pair-group method using arithmetic means (UPGMA) dendrogram showing clustering among the 482 *P. gaeumannii* isolates due to genotypic similarity. The basal node label represents the bootstrap statistic from 1000 replicate trees. Genetic distance was calculated according to Rogers (1972).

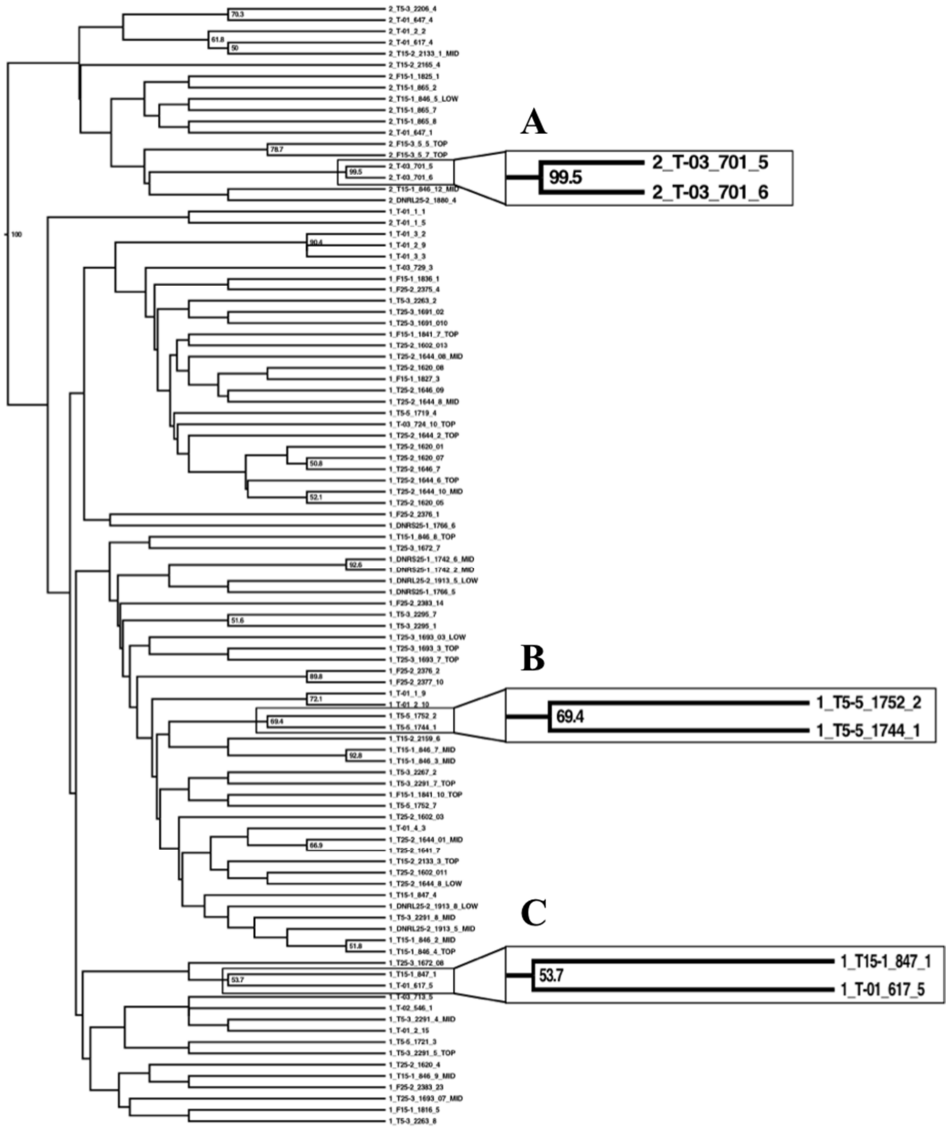

Figure 5. Unweighted pair-group method using arithmetic means (UPGMA) dendrogram constructed using 100 randomly selected *P. gaeumannii* isolates from the clone-censored data set. Node labels represent bootstrap statistics from 1000 replicate trees. Genetic distance was calculated according to Rogers (1972). (**A**) An example of clustering between two isolates from the same tree (701) at site T-03; (**B**) An example of clustering between two isolates from different trees (1752, 1744) at the same site (T5-5); (**C**) Clustering between two isolates from trees at two different sites (T15-1 and T-01).

4. Conclusion

While the relative aggressiveness of the two lineages is not known, the results of this study seem to support previous findings that suggest that *P. gaeumannii* lineage abundance and distribution is determined by winter temperature and precipitation. These findings are significant due to the fact that disease severity is determined primarily by pathogen abundance. The distribution of Lineage 2 is restricted to the western Coast Range in northern Oregon, and is virtually absent from Douglas-fir forests and plantations in the northeastern Coast Range. This distribution appears to be correlated with SNC disease severity assessed by annual aerial surveys. Sites where the two lineages occur in sympatric local populations are located within 50 km of the coast and exhibit the most severe SNC symptoms. The genetic structure of the *P. gaeumannii* populations included in this study supports reproductive isolation, as there is strong differentiation between lineages. Populations of this fungus

are not structured geographically, and genetic differentiation among sites is weak suggesting high rates of gene flow. Information about the population structure of this fungus should be used to improve predictive models and management strategies used in the control of this disease and the mitigation of its impacts in Douglas-fir silviculture.

Future studies in this pathosystem should focus on direct assessments of aggressiveness among isolates from the two lineages, and also among isolates collected from sites with varying degrees of disease severity, through inoculation trials. It is also of interest to further pursue molecular and genomic studies to learn more about the phylogenetic relationship between the two lineages. Whether they could be considered separate species cannot be determined using markers such as microsatellites. Finer resolution population genomic studies as well as comparative genomics could potentially provide answers to these questions. These investigations could provide insight into the evolutionary implications of sympatric speciation in fungi.

Acknowledgments: We would like to thank P. Reeser and W. Sutton for providing support, assistance, and advice on the laboratory techniques and protocols used in this study. Z. Kamvar and J. Tabima provided assistance in *Poppr* troubleshooting and also helped to interpret figures and statistics used for population genetics inference. Funding from the Swiss Needle Cast Cooperative at Oregon State University, The Portland Garden Club, Cascade Mycological Society, and the US Forest Service is gratefully acknowledged. We would also like to acknowledge the Department of Botany and Plant Pathology as well as the Graduate School at Oregon State University for their generous contributions to student travel. We thank two anonymous reviewers for their constructive comments on an earlier draft.

Author Contributions: P.B. performed all sample processing, molecular work, and data analysis. J.S. and P.B. performed isolations and culture maintenance. P.B. originally wrote all text in this article with later additions and corrections by J.S. P.B. produced all figures and tables presented here.

Conflicts of Interest: The authors declare no conflict of interest.

References

1. Boyce, J.S. A needle-cast of Douglas Fir associated with *Adelopus gaeumannii*. *Phytopathology* **1940**, *30*, 649–659.
2. Hansen, E.M.; Stone, J.K.; Capitano, B.R.; Rosso, P.; Sutton, W.; Winton, L.; Kanaskie, A.; McWilliams, M.G. Incidence and impact of Swiss needle cast in forest plantations of Douglas-fir in coastal Oregon. *Plant Dis.* **2000**, *84*, 773–778. [CrossRef]
3. Manter, D.K.; Kavanagh, K.L.; Filip, G.M. Pseudothecia of Swiss needle cast fungus, *Phaeocryptopus gaeumannii*, physically block stomata of Douglas fir, reducing CO_2 assimilation. *New Phytol.* **2000**, *148*, 481–491. [CrossRef]
4. Manter, D.K.; Winton, L.M.; Filip, G.M.; Stone, J.K. Assessment of Swiss needle cast disease: Temporal and spatial investigations of fungal colonization and symptom severity. *J. Phytopathol.* **2003**, *151*, 344–351. [CrossRef]
5. Oregon Department of Forestry. Swiss Needle Cast (SNC) Aerial Survey, 1996–2015. Avaliable online: http://www.oregon.gov/odf (accessed on 28 September 2015).
6. Stone, J.K.; Capitano, B.R.; Kerrigan, J.L. The histopathology of *Phaeocryptopus gaeumannii* on Douglas-fir needles. *Mycologia* **2008**, *100*, 431–444. [CrossRef] [PubMed]
7. Winton, L.M.; Hansen, E.M.; Stone, J.K. Population structure suggests reproductively isolated lineages of *Phaeocryptopus gaeumannii*. *Mycologia* **2006**, *98*, 781–791. [CrossRef] [PubMed]
8. Winton, L.M. Phylogenetics, Population Genetics, Molecular Epidemiology, and Pathogenicity of the Douglas-Fir Swiss Needle Cast Pathogen Phaeocryptopus gaeumannii. Ph.D. Thesis, Oregon State University, Corvallis, OR, USA, 2001.
9. Winton, L.M.; Stone, J.K.; Hansen, E.M. Polymorphic microsatellite markers for the Douglas-fir pathogen *Phaeocryptopus gaeumannii*, causal agent of Swiss Needle Cast disease. *Mol. Ecol. Notes* **2007**, *7*, 1125–1128. [CrossRef]
10. R Core Team. R: A Language and Environment for Statistical Computing. R Foundation for Statistical Computing, Vienna, Austria. Available online: http://www.R-project.org (accessed on 6 June 2013).
11. Peakall, R.; Smouse, P.E. Genalex 6: Genetic analysis in Excel. Population genetic software for teaching and research. *Mol. Ecol. Notes* **2006**, *6*, 288–295. [CrossRef]

12. Peakall, R.; Smouse, P.E. Genalex 6.5: Genetic analysis in Excel. Population genetic software for teaching and research—An update. *Bioinformatics* **2012**, *28*, 2537–2539. [CrossRef] [PubMed]
13. Kamvar, Z.N.; Tabima, J.F.; Grünwald, N.J. Poppr: An R package for genetic analysis of populations with clonal, partially clonal, and/or sexual reproduction. *PeerJ* **2014**, *2*. [CrossRef] [PubMed]
14. Grünwald, N.J.; Hoheisel, G.A. Hierarchical analysis of diversity, selfing, and genetic differentiation in populations of the oomycete *Aphanomyces euteiches*. *Phytopathology* **2006**, *96*, 1134–1141. [CrossRef] [PubMed]
15. Stoddart, J.A.; Taylor, J.F. Genotypic diversity: Estimation and prediction in samples. *Genetics* **1988**, *118*, 705–711. [PubMed]
16. Simpson, E.H. Measurement of diversity. *Nature* **1949**, *163*. [CrossRef]
17. Nei, M. Estimation of average heterozygosity and genetic distance from a small number of individuals. *Genetics* **1978**, *89*, 583–590. [PubMed]
18. Grünwald, N.J.; Goodwin, S.B.; Milgroom, M.G.; Fry, W.E. Analysis of genotypic diversity data for populations of microorganisms. *Phytopathology* **2003**, *93*, 738–746. [CrossRef] [PubMed]
19. Excoffier, L.; Smouse, P.E.; Quattro, J.M. Analysis of molecular variance inferred from metric distances among DNA haplotypes: Application to human mitochondrial DNA restriction data. *Genetics* **1992**, *131*, 479–491. [PubMed]
20. Rambaut, A. FigTree Version 1.4.2. Available online: http://tree.bio.ed.ac.uk/software/figtree/ (accessed on 10 June 2014).
21. Rogers, J.S. Studies in Genetics. In *Measures of Genetic Similarity and Genetic Distances*; University of Texas Publication: Texas, TX, USA, 1972; pp. 145–153.
22. Manter, D.K.; Reeser, P.W.; Stone, J.K. A climate-based model for predicting geographic variation in Swiss needle cast severity in the Oregon Coast Range. *Phytopathology* **2005**, *95*, 1256–1265. [CrossRef] [PubMed]
23. Stone, J.K.; Hood, I.A.; Watt, M.S.; Kerrigan, J.L. Distribution of Swiss needle cast in New Zealand in relation to winter temperature. *Australas. Plant Pathol.* **2007**, *36*, 445–454. [CrossRef]
24. Stone, J.K.; Coop, L.B.; Manter, D.K. Predicting effects of climate change on Swiss needle cast disease severity in Pacific Northwest forests. *Can. J. Plant Pathol.* **2008**, *30*, 169–176. [CrossRef]
25. Watt, M.S.; Stone, J.K.; Hood, I.A.; Palmer, D.J. Predicting the severity of Swiss needle cast on Douglas-fir under current and future climate in New Zealand. *For. Ecol. Manag.* **2010**, *260*, 2232–2240. [CrossRef]
26. Watt, M.S.; Stone, J.K.; Hood, I.A.; Manning, L.K. Using a climatic niche model to predict the direct and indirect impacts of climate change on the distribution of Douglas-fir in New Zealand. *Glob. Chang. Biol.* **2011**, *17*, 3608–3619. [CrossRef]
27. Balloux, F.; Lugon Moulin, N. The estimation of population differentiation with microsatellite markers. *Mol. Ecol.* **2002**, *11*, 155–165. [CrossRef] [PubMed]

List of Refereed Publications

Disease Distribution, Severity and Epidemiology

Hansen, E. M., Stone, J. K., Capitano, B. R., Rosso, P., Sutton, W., Winton, L., Kanaskie, A. and M. G. McWilliams. 2000. Incidence and impact of Swiss needle cast in forest plantations of Douglas-fir in coastal Oregon. Plant Disease. 84: 773-779.

Manter, D. K., Reeser, P. W., and J. K. Stone. 2005. A climate-based model for predicting geographic variation in Swiss needle cast severity in the Oregon coast range. Phytopathology. 95: 1256-1265.

Rosso, P. H. and E. M. Hansen. 2003. Predicting Swiss needle cast disease distribution and severity in young Douglas-fir plantations in coastal Oregon. Phytopathology. 93: 790-798.

Stone, J. K., Hood, I. A., Watt, M. S. and J. L. Kerrigan. 2007. Distribution of Swiss needle cast in New Zealand in relation to winter temperature. Australasian Plant Pathology. 36: 445-454.

Stone, J. K., Capitano, B. R. and J. L. Kerrigan. 2008. The histopathology of *Phaeocryptopus gaeumannii* on Douglas-fir needles. Mycologia. 100: 431-444.

Stone, J. K., Coop, L. B. and D. K. Manter. 2008. Predicting the effects of climate change on Swiss needle cast disease severity in Pacific Northwest forests. Canadian Journal of Plant Pathology. 30: 169-176.

Watt, M. S., Stone, J. K., Hood, I. A. and D. J. Palmer. 2010. Predicting the severity of Swiss needle cast on Douglas-fir under current and future climate in New Zealand. Forest Ecology and Management (*in press*).

Forest Protection Issues

Kelsey, R. G. and D. K. Manter. 2004. Effect of Swiss needle cast on Douglas-fir stem ethanol and monoterpene concentrations, oleoresin flow, and host selection by the Douglas-fir beetle. Forest Ecology and Management. 190: 241-253.

Shaw, D. C., Filip, G. M., Kanaskie, A., Maguire, D. A. and W. Littke. 2011. Managing an epidemic of Swiss needle cast in the Douglas-fir region of Oregon: The Swiss Needle Cast Cooperative. Journal of Forestry (*in press*).

Genetic Resistance/Tolerance in Douglas-fir

Kastner, W., Dutton, S. and D. Roche. 2001. Effects of Swiss needle cast on three Douglas-fir seed sources on a low-elevation site in the northern Oregon Coast Range: Results after five growing seasons. Western Journal of Applied Forestry. 16 (1): 31-34.

Jayawickrama, K.J.S., D. Shaw, and T.Z. Ye. 2012. Genetic Selection in Coastal Douglas-fir for tolerance to Swiss Needle Cast Disease. Proceedings of the fourth international workshop on the genetics of host-parasite interactions in forestry: Disease and insect resistance in forest trees. Gen. Tech. Rep. PSW-GTR-240. Albany, CA: Pacific Southwest Research Station, Forest Service, U.S. Department of Agriculture. 372 p.

Johnson, G. R. 2002. Genetic variation in tolerance of Douglas-fir to Swiss needle cast as assessed by symptom expression. Silvae Genetica. 51: 80-86.

Temel, F., Johnson, G. R. and J. K. Stone. 2004. The relationship between Swiss needle cast symptom severity and level of *Phaeocryptopus gaeumannii* colonization in coastal Douglas-fir (*Pseudotsuga menziesii var. menziesii*). Forest Pathology. 34: 383-394.

Temel, F., Johnson, G. R. and W. T. Adams. 2005. Early genetic testing of coastal Douglas-fir for Swiss needle cast tolerance. Canadian Journal of Forest Research. 35: 521-529.

Genetics of Phaeocryptopus gaeumannii

Winton, L. M., Hansen, E. M. and J. K. Stone. 2006. Population structure suggests reproductively isolated lineages of *Phaeocryptopus gaeumannii*. Mycologia. 98 (5): 781-791.

Winton. L. M., Stone, J. K. and E. M. Hansen. 2007. The systematic position of *Phaeocryptopus gaeumannnii*. Mycologia. 99: 240-252.

Mensuration and growth effects

Maguire D. A., Kanaskie, A., Voelker, W., Johnson, R. and G. Johnson. 2002. Growth of young Douglas-fir plantations across a gradient in Swiss needle cast severity. Western Journal of Applied Forestry. 17: 86-95.

Maguire, D. A. and A. Kanaskie. 2002. The ratio of live crown length to sapwood area as a measure of crown sparseness. Forest Science. 48: 93-100.

Maguire, D. A., Mainwaring, D. B. and Kanaskie A. 2011. Ten-year growth and mortality in young Douglas-fir stands experiencing a range in Swiss needle cast severity. Can. J. For. Res. 41: 2064-2076.

Weiskittel, A. R., Garber, S. M., Johnson, G. P., Maguire, D. A. and R.A. Monserud. 2007. Annualized diameter and height growth equations for Pacific Northwest plantation-grown Douglas-fir, western hemlock, and red alder. Forest Ecology and Management. 250: 266-278.

Weiskittel, A. R., Maguire, D. A., Garber, S. M. and A. Kanaskie. 2006. Influence of Swiss needle cast on foliage age class structure and vertical distribution in Douglas-fir plantations of north coastal Oregon. Canadian Journal of Forest Research. 36: 1497-1508.

Weiskittel, A. R., Maguire, D. A. and R. A. Monserud. 2007. Modeling crown structural responses to competing vegetation control, thinning, fertilization, and Swiss needle cast in coastal Douglas-fir of the Pacific Northwest, USA. Forest Ecology and Management. 245: 96-109.

Weiskittel, A. R., Maguire, D. A. and R. A. Monserud. 2007. Response of branch growth and mortality to silvicultural treatments in coastal Douglas-fir plantations: Implications for predicting tree growth. Forest Ecology and Management. 251: 182-194.

Weiskittel, A. R. and D. A. Maguire. 2007. Response of Douglas-fir leaf area index and litterfall dynamics to Swiss needle cast in north coastal Oregon, USA. Annals of Forest Science. 64: 121-132.

Weiskittel, A. R. and D. A. Maguire. 2006. Branch surface area and its vertical distribution in coastal Douglas-fir. Trees. 20: 657-667.

Weiskittel, A. R., Temesgen, H., Wilson, D. S. and D. A. Maguire. 2008. Sources of within and between-stand variability in specific leaf area of three ecologically distinct conifer species. Annals of Forest Science. 65: 103-112.

Zhao, J., Maguire, D. A., Mainwaring, D. B., Kanaskie, A. 2012. Climatic influences on needle cohort survival mediated by Swiss needle cast in coastal Douglas-fir. Trees 26: 1361-1371

Zhao, J., Mainwaring, D. B., Maguire, D. A., Kanaskie, A. 2011. Regional and annual trends in Douglas-fir foliage retention: Correlations with climatic variables. For. Ecol. And Management 262: 1872-1886

Zhao, J, Maguire DA, Mainwaring DB, Kanaskie A. 2015. The effect of within-stand variation in Swiss needle cast intensity on Douglas-fir stand dynamics. Forest Ecology and Management. 347:75-82.

Zhao, J., Maguire, D. A., Mainwaring, D. B., Wehage, J., Kanaskie, A. 2013. Thinning Mixed Species Stands of Douglas-Fir and Western Hemlcok in the Presence of Swiss Needle Cast: Guidelines Based on Relative Basal Area Growth of Individual Trees. For. Sci. 60 (1): 191-199.

Nutrition and soil interactions

Waring, R. H., Boyle, J., Cromack, K. Jr., Maguire, D. and A. Kanaskie. 2000. Researchers offer new insights into Swiss needle cast. Western Forester. 45 (6): 10-11.

El-Hajj, Z., Kavanagh, K., Rose, C., and Z. Kanaan-Atallah. 2004. Nitrogen and carbon dynamics of a foliar biotrophic fungal parasite in fertilized Douglas-fir. New Phytologist. 163: 139-147.

Mulvey, R.L., Shaw, D.C., Maguire, D.A. 2013. Fertilization impacts on Swiss needle cast disease severity in Western Oregon. Forest Ecology and Management 287: 147-158.

Perakis, S. S., Maguire, D. A., Bullen, T. D., Cromack, K., Waring, R. H. and J. R. Boyle. 2005. Coupled nitrogen and calcium cycles in forests of the Oregon Coast Range. Ecosystems. 8: 1-12.

Pathology and physiological host effects

Bennett, P., Stone, J. 2016. Assessments of Population Structure, Diversity, and Phylogeography of the Swiss Needle Cast Fungus (*Phaeocryptopus gaeumannii*) in the U.S. Pacific Northwest. Forests: 7, 14.

Black, B. A., Shaw, D. C. and J. K. Stone. 2010. Impacts of Swiss needle cast on overstory Douglas-fir forests of western Oregon Coast Range. Forest Ecology and Management. 259: 1673-1680.

Lee, H.E., Beedlow, P.A., Waschamnn, R.S., Burdick, C.A., Shaw, D.C. 2013. Tree-ring analysis of the fungal disease Swiss needle cast in western Oregon coastal forests. Can Journal of For. 43(8):677-690.

Manter, D. K., Bond, B. J., Kavanagh, K. L., Rosso, P. H. and G. M. Filip. 2000. Pseudothecia of Swiss needle cast fungus, *Phaeocryptopus gaeumannii*, physically block stomata of Douglas-fir, reducing CO_2 assimilation. New Phytologist. 148 (3): 481-491.

Manter, D. K. 2002. Energy dissipation and photoinhibition in Douglas-fir needles with a fungal-mediated reduction in photosynthetic rates. Phytopathology. 150: 674-679.

Manter, D. K., Bond, B. J., Kavanagh, K. L., Stone, J. K. and G. M. Filip. 2003. Modeling the impacts of the foliar pathogen, *Phaeocryptopus gaeumannii*, on Douglas-fir physiology: net canopy carbon assimilation, needle abscission and growth. Ecological Modeling. 164: 211-226.

Manter, D. K. and Kavanagh, K. L. 2003. Stomatal regulation in Douglas-fir following a fungal-mediated chronic reduction in leaf area. Trees. 17: 485-491.

Manter, D. K., Kelsey, R. G., and J. K. Stone. 2001. Quantification of *Phaeocryptopus gaeumannii* colonization in Douglas-fir needles by ergosterol analysis. Forest Pathology. 31: 229-240.

Manter, D. K., Winton, L. M., Filip, G. M. and J. K. Stone. 2003. Assessment of Swiss needle cast disease: temporal and spatial investigations of fungal colonization and symptom severity. Phytopathology. 151: 344-351.

Saffell, B.J., Meinzer, R.C., Voelker, S.L., Shaw, D.C., Brooks, R.J., Lachenbruch, B, McKay, J. 2014. Tree-ring stable isotopes record the impact of a foliar fungal pathogen on CO_2 assimilation and growth in Douglas-fir. Plant, Cell & Environment. doi: 10.1111/pce.12256

Winton, L. M., Manter, D. K., Stone, J. K. and E. M. Hansen. 2003. Comparison of biochemical, molecular and visual methods to quantify *Phaeocryptopus gaeumannii* in Douglas-fir foliage. Phytopathology. 93: 121-126.

Winton, L. M., Stone, J. K., Watrud, L. S. and E. M. Hansen. 2002. Simultaneous one-tube quantification of host and pathogen DNA with real-time polymerase chain reaction. Phytopathology. 92: 112-116.

Winton, L. M., Stone, J. K. and E. M. Hansen. 2007. Polymorphic microsatellite markers for the Douglas-fir pathogen *Phaeocryptopus gaeumannii*, causal agent of Swiss needle cast disease. Molecular Ecology. 7: 1125-1128.

Silviculture and Control

Filip, G., Kanaskie, A., Kavanagh, K., Johnson, G., Johnson, R. and D. Maguire. 2000. Research Contribution 30, Forest Research Laboratory, College of Forestry, Oregon State University, Corvallis, Oregon.

Mainwaring, D. B., Maguire, D. A., Kanaskie, A. and J. Brandt. 2005. Growth responses to commercial thinning in Douglas-fir stands with varying intensity of Swiss needle cast. Canadian Journal of Forest Research. 35: 2394-2402.

Stone, J. K., Reeser, P. W. and A. Kanaskie. 2007. Fungicidal suppression of Swiss needle cast and pathogen reinvasion in a 20-year-old Douglas-fir stand. Western Journal of Applied Forestry. 22: 248-252.

Wood Quality

Johnson, G. R., Gartner, B. L., Maguire, D. and A. Kanaskie. 2003. Influence of Bravo fungicide applications on wood density and moisture content of Swiss needle cast affected Douglas-fir trees. Forest Ecology and Management. 186: 339-348.

Grotta, A. T., Leichti, R. J., Gartner, B. L. and G. R. Johnson. 2004. Effect of growth ring orientation and placement of earlywood and latewood on MOE and MOR of very-small clear Douglas-fir beams. Wood and Fiber Science. 37: 207-212.

Johnson, G. R., Grotta, A. T., Gartner, B. L. and G. Downes. 2005. Impact of the foliar pathogen Swiss needle cast on wood quality of Douglas-fir. Canadian Journal of Forest Research. 35: 331-339.